



University of Kentucky
UKnowledge

Theses and Dissertations--Plant and Soil
Sciences

Plant and Soil Sciences

2015

UNVEILING NOVEL ASPECTS OF D-AMINO ACID METABOLISM IN THE MODEL BACTERIUM PSEUDOMONAS PUTIDA KT2440

Atanas D. Radkov
University of Kentucky, a.radkov@gmail.com

[Right click to open a feedback form in a new tab to let us know how this document benefits you.](#)

Recommended Citation

Radkov, Atanas D., "UNVEILING NOVEL ASPECTS OF D-AMINO ACID METABOLISM IN THE MODEL BACTERIUM PSEUDOMONAS PUTIDA KT2440" (2015). *Theses and Dissertations--Plant and Soil Sciences*. 67.

https://uknowledge.uky.edu/pss_etds/67

This Doctoral Dissertation is brought to you for free and open access by the Plant and Soil Sciences at UKnowledge. It has been accepted for inclusion in Theses and Dissertations--Plant and Soil Sciences by an authorized administrator of UKnowledge. For more information, please contact UKnowledge@lsv.uky.edu.

STUDENT AGREEMENT:

I represent that my thesis or dissertation and abstract are my original work. Proper attribution has been given to all outside sources. I understand that I am solely responsible for obtaining any needed copyright permissions. I have obtained needed written permission statement(s) from the owner(s) of each third-party copyrighted matter to be included in my work, allowing electronic distribution (if such use is not permitted by the fair use doctrine) which will be submitted to UKnowledge as Additional File.

I hereby grant to The University of Kentucky and its agents the irrevocable, non-exclusive, and royalty-free license to archive and make accessible my work in whole or in part in all forms of media, now or hereafter known. I agree that the document mentioned above may be made available immediately for worldwide access unless an embargo applies.

I retain all other ownership rights to the copyright of my work. I also retain the right to use in future works (such as articles or books) all or part of my work. I understand that I am free to register the copyright to my work.

REVIEW, APPROVAL AND ACCEPTANCE

The document mentioned above has been reviewed and accepted by the student's advisor, on behalf of the advisory committee, and by the Director of Graduate Studies (DGS), on behalf of the program; we verify that this is the final, approved version of the student's thesis including all changes required by the advisory committee. The undersigned agree to abide by the statements above.

Atanas D. Radkov, Student

Dr. Luke A. Moe, Major Professor

Dr. Arthur Hunt, Director of Graduate Studies

UNVEILING NOVEL ASPECTS OF D-AMINO ACID METABOLISM IN
THE MODEL BACTERIUM *PSEUDOMONAS PUTIDA* KT2440

DISSERTATION

A dissertation submitted in partial fulfillment of the requirements for the degree of
Doctor of Philosophy in the College of Agriculture, Food, and Environment
at the University of Kentucky

By
Atanas D Radkov

Lexington, Kentucky

Director: Dr. Luke A Moe, Associate Professor of Plant Physiology

Lexington, Kentucky

2015

Copyright © Atanas D Radkov 2015

ABSTRACT OF DISSERTATION

UNVEILING NOVEL ASPECTS OF D-AMINO ACID METABOLISM IN THE MODEL BACTERIUM *PSEUDOMONAS PUTIDA* KT2440

D-amino acids (D-AAs) are the α -carbon enantiomers of L-amino acids (L-AAs), the building blocks of proteins in known organisms. It was largely believed that D-AAs are unnatural and must be toxic to most organisms, as they would compete with the L-counterparts for protein synthesis. Recently, new methods have been developed that allow scientists to chromatographically separate the two AA stereoisomers. Since that time, it has been discovered that D-AAs are vital molecules and they have been detected in many organisms. The work of this dissertation focuses on their place in bacterial metabolism. This specific area was selected due to the abundance of D-AAs in bacteria-rich environments and the knowledge of their part in several processes, such as peptidoglycan synthesis, biofilm disassembly, and sporulation. We focused on the bacterium *Pseudomonas putida* KT2440 which inhabits the densely populated plant rhizosphere. Due to its versatility and cosmopolitan character, this bacterium has provided an excellent system to study D-AA metabolism.

In the first chapter, we have developed a new approach to identify specific genes encoding enzymes acting on D-AAs, collectively known as amino acid racemases. Using this novel method, we identified three amino acid racemases encoded by the genome of *P. putida* KT2440. All of the enzymes were subsequently cloned and purified to homogeneity, followed by a complete biochemical characterization. The aim of the second chapter was to understand the specific role of the peculiar broad-spectrum amino acid racemase Alr identified in chapter one. After constructing a markerless deletion of the cognate gene, we conducted a variety of phenotypic assays that led to a model for a novel catabolic pathway that involves D-ornithine as an intermediate. The work in chapter three identifies for the first time numerous rhizosphere-dwelling bacteria capable of catabolizing D-AAs. Overall, the work in this dissertation contributes a novel understanding of D-AA catabolism in bacteria and aims to stimulate future efforts in this research area.

KEYWORDS: D-amino acids, rhizosphere, *Pseudomonas putida* KT2440, catabolism

Atanas D Radkov

Student's signature

9-21-2015

Date

UNVEILING NOVEL ASPECTS OF D-AMINO ACID METABOLISM IN THE
MODEL BACTERIUM *PSEUDOMONAS PUTIDA* KT2440

By

Atanas D Radkov

Dr Luke A Moe

Co-Director of Dissertation

Dr Arthur Hunt

Co-Director of Dissertation

Dr Arthur Hunt

Director of Graduate Studies

9-21-2015

Date

ACKNOWLEDGMENTS

Although a doctoral dissertation must reflect the work of a single person, I think this is rarely the case. Based on my experience, it requires an entire laboratory, and more, in order to address and develop every aspect of a dissertation. With that in mind, I would like to first thank my adviser, professor Luke A Moe, for his constant support and continuous help. Over the course of my graduate career, I have learnt a tremendous amount about science and about academic behavior from him. As I am the first PhD student graduating from his laboratory, I witnessed not only my own growth as an independent scientist but also his growth as an independent investigator. This combination led to a unique and enriching experience for me.

As I mentioned in the beginning, there are many people to thank. First, I am grateful to my committee members, Dr Arthur Hunt, Dr Mark Coyne, and Dr Seth DeBolt, as well as my outside examiner Dr Daniel Potter, for being part of my journey and providing constructive advice. Due to the close proximity of the Hunt to the Moe laboratory, I have been in contact with Dr Arthur Hunt on multiple occasions and I would like to specifically express my gratitude for his help on several major projects part of my dissertation. Additionally, I would like to thank all of the graduate students and staff part of the Moe laboratory for their understanding and for answering my questions. I am forever grateful to Dr Audrey Law, the manager of Moe laboratory, for her patience and understanding during the early phases of my research. She taught me practical skills that were extremely important and helped me develop my projects quickly that, in turn, led to publishable results. In addition, I would like to thank two undergraduate students that I had the honor to work with, Katlyn McNeill and Kory Brinker. Collaborating with them on several projects contributed to the development of my communication skills, as well as my ability to coordinate multiple lines of research. Most recently, I had the chance to work with two visiting scholars, Dr Qingxiang Yang and Dr Koji Uda, who spent time in Moe laboratory with the desire to learn new techniques and create new contacts. I had the privilege to conduct research alongside with them and learn from their diverse scientific experiences.

Last but not least, there are also many people to thank who are part of my personal life and without whom none of my work, starting with my arrival to the United States, would have been possible. I would like to begin with my family in Bulgaria who gave me the opportunity to attend a university, learn, and become a responsible and independent individual. My mother has constantly encouraged me throughout the past nine years of university studies and has always supported my initiative to attend graduate school. Lastly, I am particularly grateful to my wife who has been patient and calm in the face of some lengthy days necessary to complete my experiments. She has been my closest companion during my time at the University of Kentucky and without her I would not have had a similarly fruitful, but also peaceful, path to my PhD.

TABLE OF CONTENTS

ACKNOWLEDGMENTS	iii
LIST OF TABLES	vi
LIST OF FIGURES	vii
Chapter One: Background and Introduction	1
Part One: Amino acids and <i>Pseudomonas putida</i> KT2440	1
Part Two: Presence and synthesis of D-AAs in bacteria	4
Part Three: Physiological roles of D-AAs in bacteria	9
Aims of dissertation.....	10
Chapter Two: Amino acid racemization in <i>Pseudomonas putida</i> KT2440	12
Background and Introduction	12
Results.....	13
Growth profile: AAs as the sole carbon and nitrogen source.....	13
Recovered genes with a potential role in AA racemization.....	15
Substrate specificity of <i>Pseudomonas putida</i> KT2440 amino acid racemases	18
Kinetic parameters of amino acid racemases.....	20
Bioinformatic analysis of <i>P. putida</i> KT2440 racemase genes.....	22
Discussion.....	26
Methods.....	29
Growth studies using D- and L-AAs as the sole source of carbon and nitrogen	29
Genomic library construction and screening.....	30
Preparation of constructs and protein purification	31
<i>In vitro</i> enzyme assays.....	31
Phylogenetic analysis.....	34
Chapter Three: A broad-spectrum AA racemase indirectly affects the synthesis of L-proline in <i>Pseudomonas putida</i> KT2440	35
Background and Introduction	35
Results.....	36
Alr localization and specific activity in LB media.....	36
Lys racemization <i>in vivo</i>	39
Gene expression analysis between wild-type and Δalr	42
Alr deletion had an effect on AA catabolism	46
Minimal media experiment comparing the growth of wild-type and Δalr	48
AAs that rescue the bradytrophic phenotype of the Δalr strain.....	50
Total cellular AA concentration.....	52
Discussion.....	54
Methods.....	58
Construction of markerless mutation via Short Overlap Extension PCR (SOE PCR).....	58
Periplasmic protein isolation and enzyme assays	59

Peptidoglycan isolation and composition analysis.....	60
Gene expression analysis	60
Growth assays.....	61
Phenotype rescue assays	61
Analysis of total cellular AA concentration.....	62
Chapter Four: Abundance and diversity of rhizosphere-dwelling bacteria	
catabolizing D-amino acids	63
Background and Introduction	63
Results	63
Enumeration of rhizobacteria catabolizing D-AAs.....	63
Phylogenetic identification of bacterial isolates	66
Methods	70
Culture-dependent enumeration of bacteria	70
Identification of bacterial isolates based on 16S rRNA gene sequencing....	70
Chapter Five: Conclusion	72
Appendix A: Genes involved in D-arg catabolism by <i>P. putida</i> KT2440.....	74
Background and Introduction	74
Results	74
Selection of positive clones	74
Confirmation of positive clones via sequencing.....	74
Identification of relevant regions.....	77
Methods	81
Construction of genomic library	81
Transformation into <i>E. coli</i>	81
Screening of library on D-arg	81
Selection of clones	81
Isolation of plasmids, sequencing, and data analysis.....	82
Enzyme purification and preliminary assays.....	82
Appendix B: Chemotaxis towards D-AAAs by <i>P. putida</i> KT2440.....	83
Background and Introduction	83
Results	84
Methods	86
References	90
Vita	103

LIST OF TABLES

Table 2.1 Screening results from <i>P. putida</i> KT2440 genomic libraries	17
Table 2.2 Percent normalized relative activity of racemases on D- and L-AAs ...	19
Table 2.3 Kinetic parameters of racemases determined on a collection of D- and L-AAs	21
Table 2.4 Gradients used in AA enantiomer HPLC analysis	33
Table 3.1 Specific activity of BSAR	37
Table 3.2 Specific activity of wild-type and Δalr <i>P. putida</i> KT2440 protein fractions.....	38
Table 3.3 AAs detected in peptidoglycan and culture supernatant.....	41
Table 3.4 Comparison of gene expression between the wild-type and Δalr strain after 6hrs of growth in LB media.....	45
Table 3.5 Growth profile of <i>P. putida</i> KT2440, wild-type and Δalr	47
Table 3.6 Minimal media phenotype rescue after 30hrs incubation in PG medium	51
Table 3.7 Total cellular AA concentration after growth in PG medium.....	53
Table 4.1 Number of isolates at 10^{-5} soil dilution on each tested AA enantiomer.	65
Table 4.2 Phylogenetic analysis of isolates that catabolized individual L - and D-AA enantiomer pairs as the sole source of carbon and nitrogen	68

LIST OF FIGURES

Figure 1.1 The established catabolic pathways for L- and D-lys in <i>P. putida</i> KT2440.....	3
Figure 1.2 D-AAs in peptidoglycan.....	5
Figure 1.3 AA racemization mechanisms	8
Figure 2.1 Ability of <i>Pseudomonas putida</i> KT2440 to use D- and L-AAs as the sole source of carbon and nitrogen	14
Figure 2.2 Phylogenetic analysis of the alanine racemase/Alr	23
Figure 2.3 Genomic synteny analysis on the regions surrounding <i>dadX</i> and the proline racemase (<i>proR</i>) from <i>Pseudomonas putida</i> KT2440.....	25
Figure 3.1 LB growth profile and lys racemization in vivo.....	40
Figure 3.2 Genome coverage achieved after RNA-Seq data analysis.....	44
Figure 3.3 Minimal media growth profile.....	49
Figure 3.4 The role of the Alr BSAR in L-lys, L-arg, and L-ornithine catabolism and L-pro synthesis.....	57
Figure A.1 <i>P. putida</i> KT2440 genome. The location of each identified region is labeled.....	76
Figure A.2 Four of the identified regions from D-arg screens, labeled A, B, C, D	79
Figure B.1 Chemotaxis assays – positive and negative controls.....	84
Figure B.2 Representative agar plates used in the colony counting after the chemotaxis assays	85
Figure B.3 Chemotaxis setup - plate with inserted capillaries after sealing over the flame.....	88
Figure B.4 Chemotaxis setup – complete.....	89

Chapter One: Background and Introduction

Part One: Amino acids and *Pseudomonas putida* KT2440

Rhizosphere soil differs from bulk soil by the presence of plant roots. They are responsible for the release of carbon rich root exudates, serving as an energy source for rhizosphere-dwelling organisms. Further, these compounds have roles in plant pathogen resistance, as well as plant competition (10). A variety of soil-dwelling organisms are attracted by sugars, amino acids (AAs), and phenolics, leading to diverse inhabitants and an intricate communication network.

Pseudomonas putida KT2440 (Class γ -Proteobacteria; Gram-negative) is a model rhizosphere-dwelling bacterium and one of the most versatile rhizosphere inhabitants – its genome has characteristics of terrestrial, rhizosphere, and aquatic bacteria (83). Typical of generalist soil bacteria, the genome of *P. putida* KT2440 contains 894 paralogous gene domain families, suggesting a capability for diverse functions rather than niche specialization. *P. putida* KT2440 is one of the best-studied representatives of the genus, partly because of its potential as a biocontrol agent and for the production of fine chemicals (90, 96). This organism is specifically known for its metabolic versatility, being able to catabolize a large array of organic compounds, including aliphatic and aromatic hydrocarbons (83). About 12% of the *P. putida* KT2440 genome (370 cytoplasmic membrane transport systems) is dedicated to nutrient transport. Based on bioinformatic analysis, the largest family of transporters (94 paralogous members) is likely involved in AA uptake. This is also in accordance with the finding that the genome portion dedicated to AA metabolism and transport is much larger relative to that used for carbohydrates (83). Considering the abundance of AAs in the plant rhizosphere, AA uptake and metabolism are considered an advantageous trait for successful rhizosphere colonization (85). In fact, *in vivo* expression technology (IVET) studies have identified DNA regulatory elements involved in the transport and metabolism of L-pro and L-lys, as well as chemotaxis in *P. putida* KT2440, activated upon exposure to maize root exudates and contributed to colonizing the plant roots (81, 105, 128). Although the plant rhizosphere is complex and the community structure, as well as the plant-microbe symbioses, are not well understood, *P. putida* KT2440 has been established as a model organism to study rhizobacteria, including root colonization and plant-microbe communication (85, 90, 91).

The L-enantiomer of the 19 chiral AAs predominates in biological systems. However, it has been established that many organisms have the ability to convert an L-AA into its mirror image D-enantiomer, via a process known as racemization, or epimerization when AAs contain more than one chiral center (e.g. ile) (102, 142). L- and D-AAs differ in the spatial orientation of the atoms attached to their α -carbon. With the exception of glycine, the remaining 19 of 20 proteinogenic AAs are chiral at the α -carbon. The inversion of the stereochemistry about the α -

carbon is normally accomplished by enzymes known as racemases or epimerases (for epimerization), and aminotransferases.

Despite that D-AAAs are not used for protein synthesis, bacteria are known to synthesize them using the above mechanisms. D-AAAs are mainly produced due to their integral role in macromolecules (e.g. peptidoglycan) and a variety of antibiotics (102, 130). In addition, the pathways for D-AA metabolism in bacteria have evolved to serve not only a biosynthetic purpose but also a catabolic role. In particular, *P. putida* KT2440 likely encodes racemase/epimerase enzymes because it has been demonstrated to catabolize D-AAAs, specifically D-lys (26, 109). L-Lys is catabolized via the aminovalerate pathway. However, the piperolate pathway has also been described in *P. putida* KT2440 in which a putative racemase converts L-lys to D-lys, which in turn is transformed to an α -ketoacid and can be used by the bacterium as a sole carbon and nitrogen source (Fig. 1.1). The two pathways are interconnected and important for proper cell development (108, 109). Furthermore, Molina-Henares et al. isolated *P. putida* KT2440 auxotrophic mutants for 13 of the 20 proteinogenic AAs. The authors demonstrated that arg, leu, pro, and cys auxotrophy was rescued when the corresponding D-AAAs were added to a minimal growth media (91). The study demonstrates the racemization ability of *P. putida* KT2440 towards four AAs. Lastly, it is important to note that the genome of *P. putida* KT2440 has been sequenced and annotated (96).

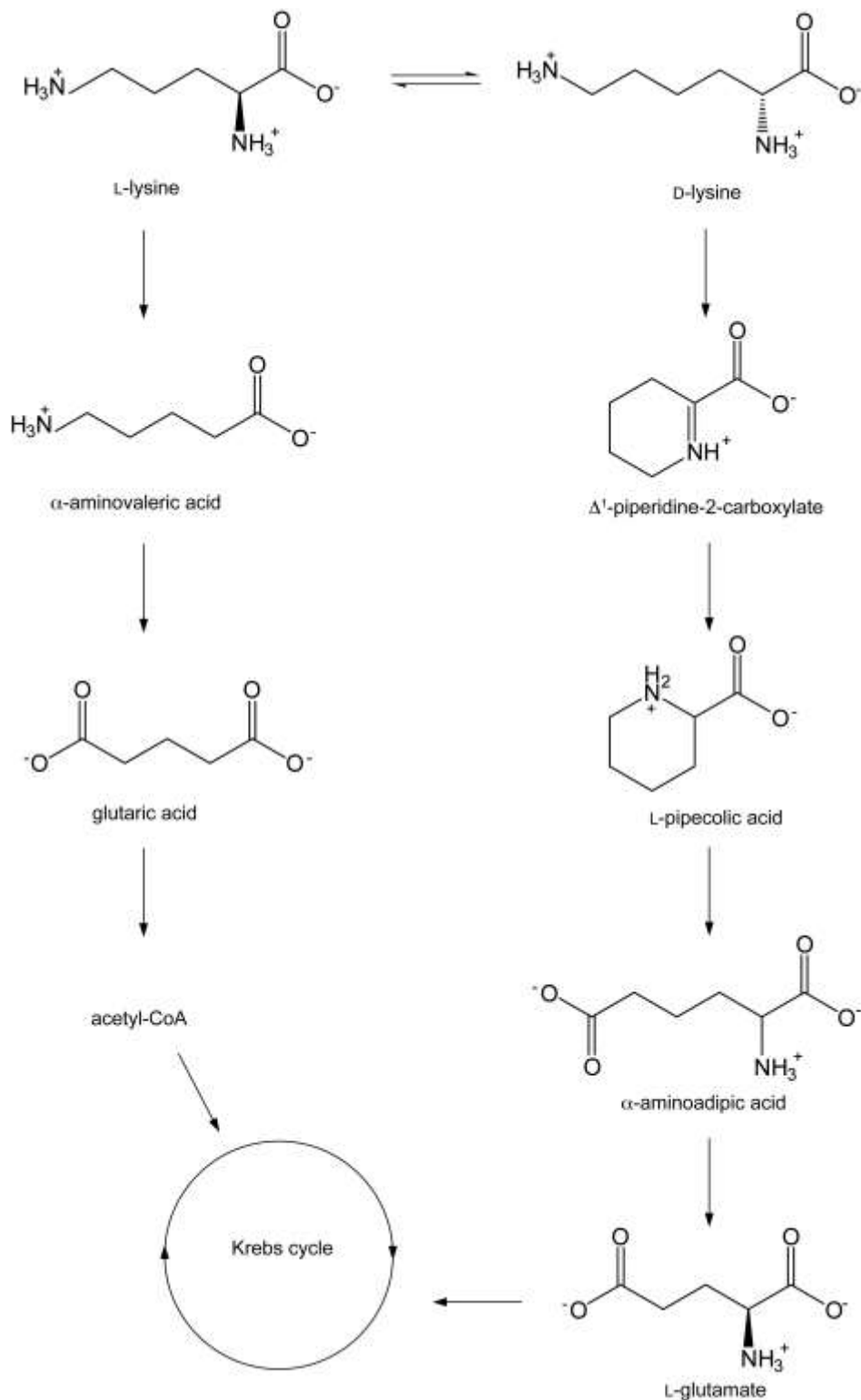


Figure 1.1 The established catabolic pathways for L- and D-lys in *P. putida* KT2440. The L-lys pathway is named after the intermediate α-aminovaleric acid (AMV), while the D-lys pathway – after the α-aminoadipic acid intermediate (AMA).

Part Two: Presence and synthesis of D-AAs in bacteria

The appearance of D-AAs in alkali-treated proteins was realized in the first decade of the 20th century. By the middle of the century, scientists began studying D-AAs in the bacterial cell envelope (110). A few decades later, the integrity of the peptidoglycan (PG) layer was shown to be maintained by peptide cross-links, interconnected by D-AAs (132). PG is a well-studied macromolecule due to its potential to serve as a target for numerous antibiotics (130). Recently it has been established that a number of different D-AAs can be incorporated into PG. In addition to the required D-glu at the second position and D-ala at the fourth position of the peptide stem connecting the two glycan chains, D-enantiomers of lys, ser, isoglutamine, gln, pro, phe, tyr, val, ile, leu, and met have been detected at the third or fourth position (5, 12, 25, 130) (Fig. 1.2). Furthermore, some D-AAs (ala, glu, ser, asp, asn, lys, ornithine) can be incorporated in the interpeptide bridge found between the peptide stems (130).

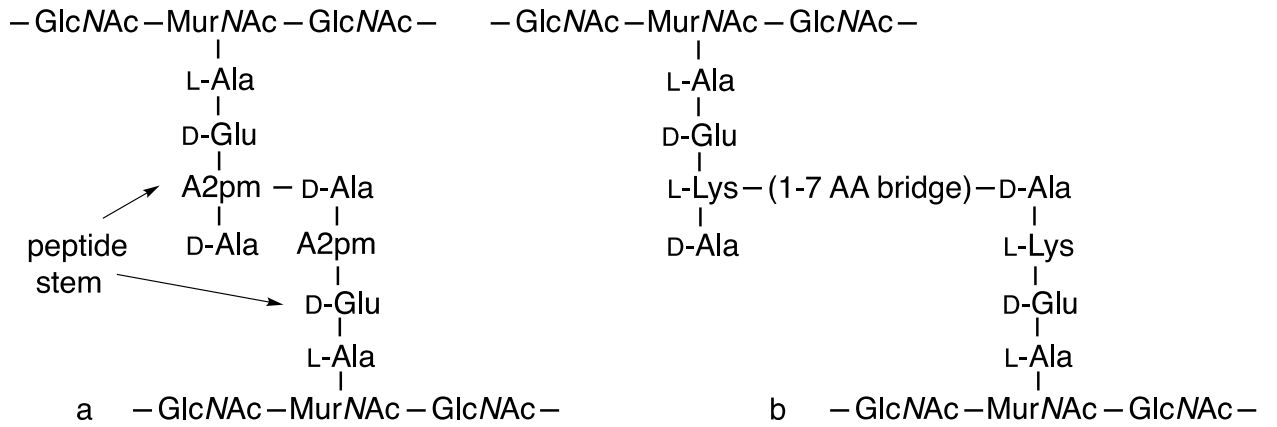


Figure 1.2 D-AAc in peptidoglycan (GlcNAc *N*-acetylglucosamine; MurNAc *N*-acetylmuramic acid; A2pm 2,6-diaminopimelic acid). a Direct cross-linkage of PG peptide stems. b Linkage of peptide stems through an interpeptide bridge.

In addition to PG, other macromolecules from bacterial origin that contain high amounts of D-AAs are poly- γ -glutamate (PGA) and teichoic acids (TAs) (102). PGA is a viscous polymeric extracellular molecule that is found primarily in Gram-positive bacteria and imparts on the cell an ability to evade the immune system (23). Depending on the species, PGA could be comprised of only L-glu, only D-glu, or a combination of the two. The pathogen *Bacillus anthracis*, for example, has a PGA layer that consists solely of D-glu residues (23). In addition to PGA, Gram-positive bacteria are also known to contain TAs, the extracellular anionic molecules comprised of polymeric glycerol phosphate moieties. D-Ala is abundant in TAs but the degree of D-alanylation varies from species to species (97). The degree of D-alanylation is known to regulate physiological responses in bacteria such as autolytic activity and cellular defense (106, 129). In addition, the lack of D-ala in TAs could render cells more susceptible to antimicrobials as well as an attack by the host immune system (30, 68). Lastly, D-AAs are commonly found in peptide antibiotics produced not only by bacteria but other organisms (22). The most common mechanism for the synthesis of such antibiotics is through non-ribosomal peptide synthetase enzymes. After searching the NORINE non-ribosomal peptide database (includes 1164 curated peptides of prokaryotic as well as eukaryotic origin) using individual D-AAs as the query term, it was found that the D-enantiomers of ala, ser, leu, and glu are the most prevalent, each present in over 100 curated peptides (22).

Most D-AAs used in the synthesis of PG, TAs, and PGA are produced as free AAs and are subsequently incorporated into these macromolecules. Bacteria synthesize D-AAs using two separate, but related, mechanisms. The first mechanism relies on a proton exchange reaction, leading to the inversion of stereochemistry about the α -carbon of a particular chiral L-AA (Fig. 1.3). This is a reversible reaction that involves a single substrate and it is accomplished by racemase or epimerase enzymes. Although racemization and epimerization are very similar, the former is reserved for reactions that involve compounds with only one chiral center (ala racemization), while the latter – compounds with more than one chiral center (ile epimerization). Racemase/epimerase enzymes are subdivided into two classes based on their use of a cofactor-dependent or cofactor-independent reaction. Cofactor-dependent enzymes use a pyridoxal-5'-phosphate (PLP) cofactor. The PLP cofactor aids the enzyme by stabilizing the planar carbanion intermediate via an external aldimine, thus lowering the pK_a of the α -proton. In addition to the PLP cofactor, it is proposed that there are two active site bases involved in deprotonation and reprotonation of the α -carbon as part of the stereochemistry inversion (124). The cofactor-independent racemase/epimerase enzymes also use a two-base mechanism which, however, lacks the stabilization effect of the PLP cofactor. Two cys residues function as the active site residues among enzymes for which these residues have been determined (21, 43, 76, 123).

The second known mechanism is also reversible and involves a stereospecific amination of a particular α -ketoacid (Fig. 1.3). The major difference with the first mechanism is that a second amino group-donor molecule is

required. The amino group is transferred stereospecifically to the α -ketoacid by an aminotransferase enzyme. This mechanism is common among bacteria for L-AA synthesis (84, 127). D-AA aminotransferases follow the same biosynthetic pathway whereby an amino-group donor (typically D-ala) and an α -ketoacid are used for the production of a new α -ketoacid (pyruvate from D-ala) and a D-AA product (e.g. D-glu from α -ketoglutarate). Although this mechanism is similar to the one described for racemase/epimerase enzymes in that they both employ a PLP cofactor, the specific underlying steps vary considerably. Lastly, D-AA aminotransferases show high specificity for the amino group acceptor (typically α -ketoglutarate) (133). Interestingly, there are also characterized such enzymes that can donate an amino group to a wide range of α -ketoacid acceptors, leading to the synthesis of a large variety of D-AAs (66).

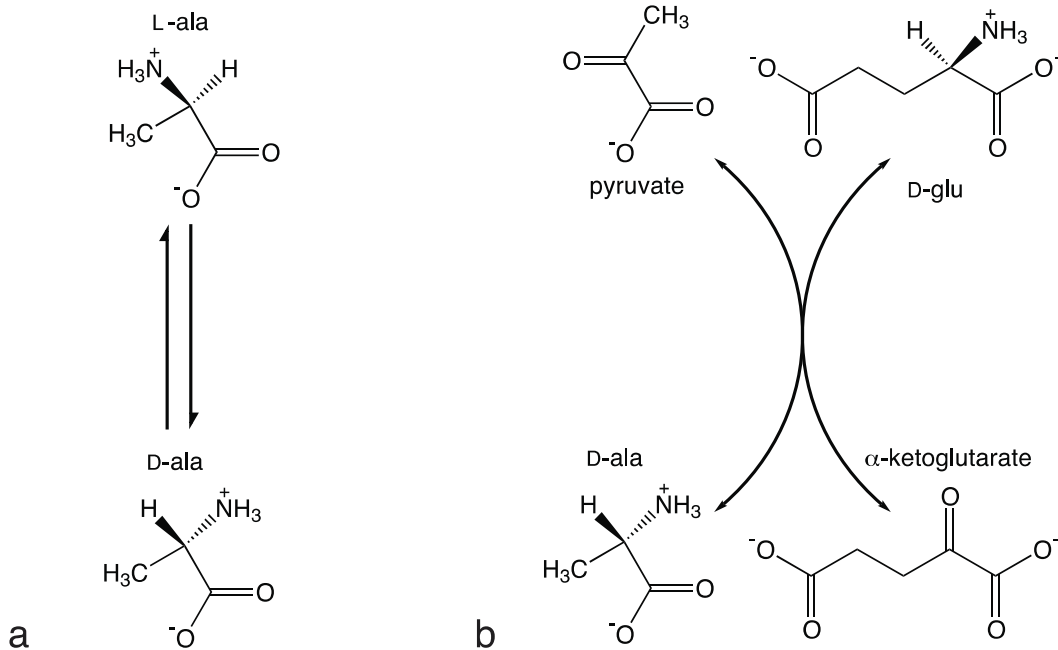


Figure 1.3 AA racemization mechanisms. a Reaction that proceeds via deprotonation and reprotonation conducted by AA racemase and epimerase enzymes. b Reaction that involves two substrates and two products conducted by AA aminotransferase enzymes. Amino group is transferred from a donor molecule (D-ala or D-glu) to an α -ketoacid (pyruvate or α -ketoglutarate).

In contrast to the synthesis mechanisms already described for free D-AAs, most D-AAs incorporated into peptide antibiotics are produced concurrently with antibiotic synthesis (116). In the case of the algal toxin microcystin-LR (99), the non-ribosomal peptide synthetase operon contains an ORF encoding a Glutamate racemase. The racemase produces D-glu which is directly loaded onto the non-ribosomal peptide synthetase enzyme and incorporated into the antibiotic. Generally, however, non-ribosomal peptide synthetases include an epimerization domain (E domain) responsible for the change in AA stereochemistry (116). An example here is the well-known cyclodecapeptide Gramicidin S. During its synthesis, the GrsA enzyme adenylates L-phe using ATP which is followed by formation of a covalent phosphopantetheinylated L-phe thioester adduct. The L-phe moiety is epimerized by the E domain and the D-phe thioester adduct is subsequently processed by the GrsB enzyme to produce Gramicidin S. Although E domains are considered the most common method for D-AA incorporation by non-ribosomal peptide synthetase enzymes, it should be noted that certain enzymes directly load free D-AAs rather relying on E domains (122).

Part Three: Physiological roles of D-AAs in bacteria

Recent advances in the field of D-AA metabolism and their effect on bacterial physiology are relevant to the biochemistry of D-enantiomers in rhizosphere bacteria. First, an AA racemase enzyme was identified using novel functional soil metagenomics (27). The authors identified a Lysine racemase and characterized the ability of the enzyme to interconvert the L and D stereoisomers under different conditions and in the presence of inhibitory substances. Second, a report by Hubert Lam and co-workers described the ability of D-AAs to control bacterial cell morphology during different growth phases (70). The authors were able to show that D-AAs regulate PG synthesis during stationary phase, are directly incorporated into the PG, and could act on Penicillin-binding proteins, involved in PG remodeling and synthesis. Furthermore, it was demonstrated that D-AAs may act on several bacterial strains, including *Vibrio cholera* and *Bacillus subtilis* as well as other strains that do not synthesize D-AAs themselves. The significance of these results is that D-AAs may serve as an interspecies signal to modify cell morphology and metabolism in the face of harsh environmental conditions. In addition to molding PG structure, D-AAs are also known to affect bacterial biofilms. Kolodkin-Gal et al. found that a mixture of D-AAs, namely D-met, D-leu, D-tyr, and D-trp, found in *Bacillus subtilis* culture supernatant can act on biofilms and trigger their disassembly. Additionally, *Staphylococcus aureus* as well as *Pseudomonas aeruginosa* were two other species shown to lose their ability to aggregate in a biofilm in the presence of D-AAs (67). In a later study, Leiman et al. found that D-AAs may inhibit protein synthesis in *B. subtilis*, and consequently they would act as an antibiotic rather than a signal to disassemble biofilms (72). Sporulation is a complex physiological process that involves the regulation and integration of multiple metabolic pathways (35). It has been discovered that D-ala and D-his can prevent spore germination in many *Bacillus*

species (51, 52). Specifically, D-ala has been demonstrated to antagonize the spore germination response, normally initiated by L-ala. Consequently, D-ala may function as an auto-inhibitory molecule, prohibiting spore germination under low nutrient availability and high population density (25). Finally, it should be noted that even though an enhancement of the knowledge of D-AA metabolism in bacteria has been achieved, little information is based on rhizosphere research.

Aims of dissertation

The goal of the dissertation is to further our understanding of D-AA metabolism in bacteria. Taken together, the experiments help unravel a putative L-ornithine catabolic pathway that proceeds through D-ornithine and leads to L-pro synthesis in our model organism *P. putida* KT2440. Additionally, more information is contributed on the abundance and identity of rhizosphere-dwelling bacteria able to catabolize D-AAs.

In chapter one, the aim was to identify and characterize enzymes acting on D-AAs in *P. putida* KT2440. Our approach involved the use of *E. coli* AA auxotrophic strains incapable of surviving in the absence of a particular L-AA. Leu, lys, pro, and phe auxotrophs were used to construct *P. putida* KT2440 genomic libraries. These libraries were subsequently screened on minimal media containing the corresponding D-enantiomer in place of the necessary L-AA. The rationale was that if a particular clone contained a gene encoding an enzyme that can act on a D-AA and produce the corresponding L-counterpart, the auxotrophic strain would survive and grow. Our focus was on AA racemase enzymes. Several clones were identified that contained open reading frames (ORFs) encoding three such enzymes, annotated as DadX alanine racemase, Alr alanine racemase, and Proline racemase. The enzymes were biochemically characterized to determine their substrate specificities and elucidate the Michaelis-Menten kinetics for the best substrate. Interestingly, DadX was the only true Alanine racemase, while the Alr enzyme displayed broad substrate specificity with the highest activity on both stereoisomers of lys and arg. Furthermore, the annotated Proline racemase did not have any activity with either enantiomer of pro or most other tested AAs. However, it showed activity only towards the four epimers of hypro. Lastly, phylogenetic analysis was conducted to emphasize the unique nature of the Alr enzyme, suggestive of an interesting and complex role in AA metabolism by *P. putida* KT2440.

The Alr enzyme and its specific part in the physiology of *P. putida* KT2440 is the topic of the second chapter. A markerless deletion mutant of the *alr* gene was constructed via homologous recombination using an established method. A number of phenotypic assays, including enzyme assays, AA catabolism and synthesis, as well as biofilm assays, were conducted in order to understand the effect of the mutation. Our conclusion was that the enzyme is involved in the catabolism of L-lys, L-arg, and L-ornithine as the sole source of carbon and nitrogen. We further explored the inability of the *alr* mutant to catabolize L-ornithine as well as the wild-type. After conducting a growth assay in minimal media, we noticed that the *alr* mutant displayed bradytrophic growth, its growth lagged far behind that of the wild-type but eventually the mutant reached similar

levels. The same growth experiment was repeated as before only this time a collection of L- and D-AAs were added individually to pinpoint the specific AAs able to alleviate the bradytrophic phenotype. Interestingly, several L-AAs, including L-pro, as well as D-ornithine, rescued the mutant phenotype. Our results led us to propose a model whereby the Alr broad-spectrum AA racemase is involved in the synthesis of D-ornithine from the L-enantiomer, which subsequently leads to the production of L-pro, an essential AA for proper cell growth. This set of experiments uncovers for the first time a potential central place of D-ornithine in AA metabolism of *P. putida* KT2440.

The third chapter aims to enhance our general knowledge of D-AA catabolism by bacteria. A culture-dependent approach was taken in order to identify novel D-AA catabolizing bacteria inhabiting the plant rhizosphere. Each stereoisomer from a collection of 21 L- and 21 D-AAs was added to a minimal medium agar as the sole source of carbon and nitrogen, after which sweet corn rhizosphere soil was plated at different dilutions. Bacterial isolates were observed on every tested D-AA. A collection of these bacteria were preserved as glycerol stocks and were classified down to the species level after conducting 16S rRNA amplicon sequencing. Most of our environmental isolates were part of three major phylogenetic Classes, *Actinobacteria*, *α -Proteobacteria*, and *β -Proteobacteria*. An intriguing finding was the presence of several *Arthrobacter* species (class *Actinobacteria*) that were isolated from 18 of the 21 tested D-AAs. The message here is that there is an abundance of bacteria having the ability to utilize D-AAs for growth. We hope that our research will incite scientific interest to study D-AAs and further understand their place in biology.

Copyright statement: Portions of this chapter were published in Applied Microbiology and Biotechnology published by Springer International Publishing AG (Radkov, A D and Moe, L A. 2014. Bacterial synthesis of D-amino acids. Appl. Microbiol. Biotechnol. vol. 98 no. 12 p. 5363-74).

Chapter Two: Amino acid racemization in *Pseudomonas putida* KT2440

Background and Introduction

Of the 20 canonical proteinogenic amino acids (AAs), 19 are chiral about their α -carbon and therefore exist in one of two spatial arrangements, referred to as the L- and D-stereoisomers. Nature has effectively selected for L-AAs to serve as the building blocks of ribosomally synthesized peptides and as important metabolic intermediaries in the cell. Their corresponding D-enantiomers are far less prevalent in most biological systems. Nonetheless the D-enantiomer of each of the 19 proteinogenic AAs has been detected in biological systems (11, 17, 19, 67, 70, 98), and in certain environments D-amino acids are abundant. This includes microbe-rich environments such as topsoil (16), fermented foods (41) and the rumen (113). Where free D-AA content was measured in bacterial culture supernatant or ethanolic extracts of freeze-dried bacterial samples, the most abundant free D-AA was typically D-ala, but high concentrations of D-asp, D-glu, D-leu and D-met were also noted in some species (70, 113). The D-stereoisomer of ala comprises up to 65% of the free ala in some samples (113), and millimolar D-ala concentrations have been measured in culture supernatant (70). Consequently, when D-AAs are detected in environmental samples their presence is typically attributed to bacteria.

Because certain D-AAs are essential components in bacterial peptidoglycan (PG) (e.g. D-ala and D-glu) their abundance in bacterial culture is not surprising (130). Nonetheless, the D-AA distribution in culture does not necessarily match that expected simply for synthesis of PG (70). Recent work has shown that complex physiological processes such as biofilm formation, PG remodeling, and sporulation are influenced by the presence of certain D-AAs (67, 70, 114). For example, the D-stereoisomers of leu, met, trp, and tyr were shown to disassemble mature biofilms of *B. subtilis* at concentrations as low as 10nM (67). The corresponding L-enantiomer did not have the same effect. In this case, the bacterium is shown to synthesize the specific D-AA of note, but little is known about how this is accomplished. Further, bacterial catabolism of D-AAs has been noted and may be important for colonization of D-AA rich environments (95, 109). Bacterial synthesis of D-AAs proceeds via enzymatic racemization of the corresponding L-enantiomer. Amino acid racemases catalyze the interconversion of the L- and D-enantiomers using either a PLP-dependent or -independent mechanism. The PLP-dependent alanine racemase enzyme class has been studied extensively, owing to its potential as a target for antimicrobials (32). These enzymes are known to be necessary for D-ala synthesis for PG, as targeted disruption results in D-ala auxotrophy (135). However, many bacteria encode more than one annotated alanine racemase in their genome. Catabolism of D-AAs can also be initiated through enzymatic racemization to form the corresponding L-AA, although racemase-independent catabolic mechanisms also exist.

Pseudomonads are noted as models in ecological genomics (83, 138), pathogenesis (7, 31), and host-microbe interactions (79, 86). They may also be considered as models in D-AA biology. Recent work in *Pseudomonas*

aeruginosa PAO1 and *Pseudomonas putida* KT2440 has revealed unique mechanisms by which D-AAs are catabolized (73, 95, 109). Here we build on this work by assessing the D- and L-AA catabolic capacity of *P. putida* KT2440, employing a functional screen to identify genes involved in D-AA metabolism, characterizing enzymes involved in AA racemization, and identifying key differences in the genomics of D-AA metabolism between related pseudomonads.

Results

Growth profile: AAs as the sole carbon and nitrogen source

Other studies have described the catabolic versatility of *P. putida* KT2440, yet a comprehensive analysis of growth on D- and L-AAs as a sole carbon and nitrogen source has not been reported (91, 109, 136). To assess the potential for racemization of D-AAs, we performed a series of growth studies on *P. putida* KT2440 in which D- and L-AAs were provided as the sole carbon and nitrogen source (Fig. 2.1). No growth was recorded on either stereoisomer of met, thr, leu, or trp. In instances where only the L-stereoisomer was catabolized, asp, asn, his, gln, glu, and pro were the most rapidly catabolized. Among those AAs where both enantiomers were catabolized the two enantiomers of 4-hydroxyproline, *cis*-D- and *trans*-L-hydroxyproline (hereafter *cis*-D-hypro and *trans*-L-hypro), as well as those of ala conferred the most rapid growth, while the lys and arg enantiomers were catabolized more slowly. Marginal growth was recorded on D- and L-phe after 24 hours. However, after 72 hours, these cultures reached growth levels similar to those of the other AA enantiomer pairs that were more rapidly catabolized. While previous growth experiments have established that *P. putida* KT2440 catabolizes both D- and L-lys (95, 108), *P. putida* KT2440 has not been shown previously to catabolize as sole carbon and nitrogen sources D-phe, the epimers of hypro (*cis*-D- and *trans*-L-), or D-arg. Nonetheless, *P. putida* KT2440 can use both enantiomers of phe, of arg, and of hypro as a sole nitrogen source (91, 136).

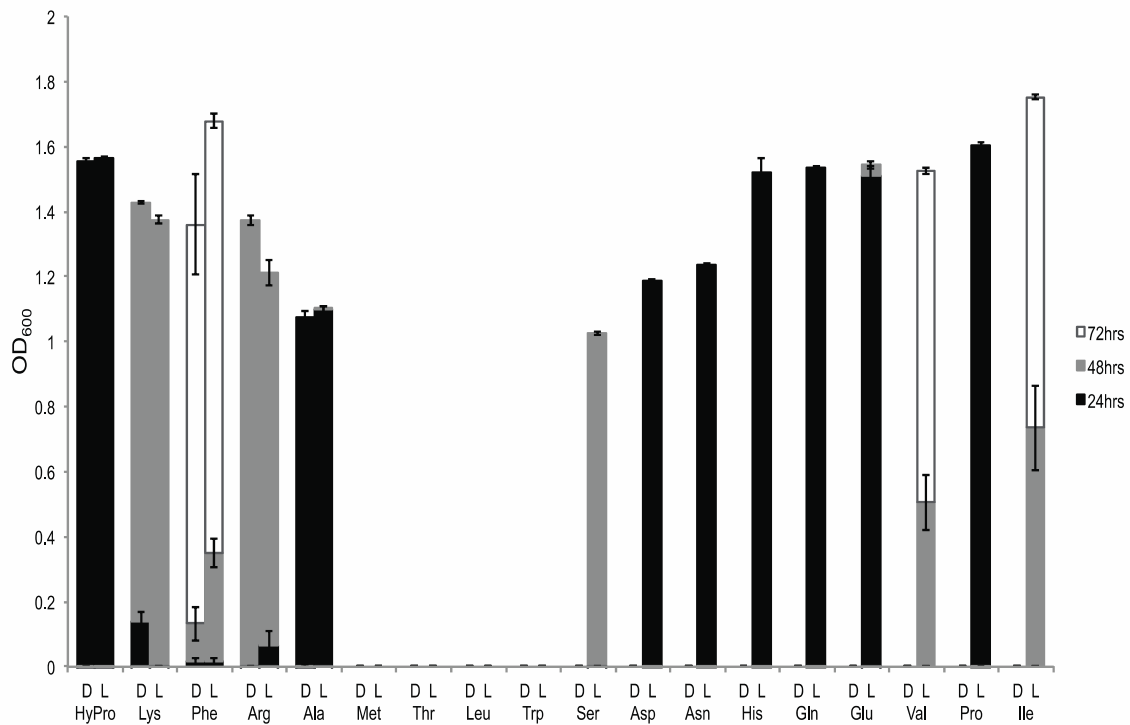


Figure 2.1 Ability of *Pseudomonas putida* KT2440 to use D- and L-AAs as the sole source of carbon and nitrogen. Each color bar represents the net increase in growth during the designated time period. The absence of a particular color bar signifies lack of growth during the corresponding time period. Cultures were grown in PG liquid minimal medium. Average values are the result of three replicates. SD included on graph.

Recovered genes with a potential role in AA racemization

Screens were conducted in *E. coli* auxotrophs to identify mechanisms for racemization of lys, pro, phe, and leu. Lys and phe auxotrophs were chosen due to the D-AA growth profiles of *P. putida* KT2440 (Fig. 2.1). The pro auxotroph was chosen due to the presence of an annotated proline racemase in the *P. putida* KT2440 genome. The leu auxotroph was chosen for two reasons. First, no ala auxotroph was available from the CGSC and leu exhibits reasonable structural similarity to ala, suggesting that a racemase that uses ala as a substrate may also use leu. Second, it is possible that *P. putida* KT2440 may also racemize AAs that it cannot use as a sole carbon and nitrogen source. Figure 2.1 shows the four AAs from this table that are not catabolized as a sole carbon and nitrogen source by *P. putida* KT2440, leu is a representative from this group. A screen on D-arg was not conducted because of the high activity of the recovered Alr enzyme in conversion of D-arg to L-arg.

From the recovered positive clones, DNA sequences were compared against the *P. putida* KT2440 genome using the Pseudomonas genome database (137) to identify ORFs encoded within each region. Because of the magnitude of the screen, identified genomic regions were typically recovered more than once, allowing us to estimate a minimal genomic region necessary for recovering the phenotype. These regions (Table 2.1) vary in size and in many cases include more than one gene that could be responsible for the observed phenotype. The genes from each region are designated according to their genomic locus tag, and the range of genes indicates the minimal unit identified for each region. Genes of interest from these regions include those whose predicted products belong to enzyme families known to catalyze reactions characteristic of AA metabolism. The minimal genomic region does not imply that more than one gene from this region is required for recovery of the phenotype. Among genomic regions in which an annotated racemase was identified, a subclone containing the racemase gene by itself conferred the same phenotype as the insert from which it originated. We concluded that the racemase genes were responsible for the observed phenotype in these cases and did not further assess other genes from these regions. In some cases, the same genes were recovered in different screens. A subset of genes from genomic region 3 identified in the D-pro screen also enabled growth in the D-leu screen, and the *alr* gene enabled growth in both the D-lys and D-leu screens. Metabolism of AAs is known to involve enzymes such as dehydrogenases, oxidoreductases, and aminotransferases (73, 95, 140), and genes annotated as such were recovered in a number of cases. The current study focuses on mechanisms for AA racemization, further work beyond the scope of this article will be necessary to establish a role for these genes in D-AA metabolism in *P. putida* KT2440. Only one recombinant clone recovered growth in screens performed on D-phe, the insert encodes a FAD-dependent oxidoreductase (PP2246) that was not recovered in any of the other screens. Interestingly, the Pseudomonas Genome Database reports this gene to be an ortholog of the *dauA* gene (catabolic D-arginine dehydrogenase) of *P. aeruginosa* PAO1, yet *P. putida* KT2440 does not

encode the other genes from the *dauBAR* operon previously shown to be involved in a two-step conversion of D-arg to L-arg in *P. aeruginosa* PAO1 (14). The genomic regions do not share any apparent similarity otherwise.

Table 2.1 Screening results from *P. putida* KT2440 genomic libraries

Supplemented amino acid	Genome region	Gene range	Annotated function of genes of interest
D-Pro	1	PP1251-PP1256	PP1255: FAD-dependent oxidoreductase
	2	PP1257-PP1259	PP1258: proline racemase
	3	PP3588-PP3597	PP3590: aromatic amino acid aminotransferase PP3591: Δ^1 -piperideine-2-carboxylate reductase PP3596: FAD-dependent oxidoreductase
D-Lys	1	PP1162-PP1165	PP1163: FAD-binding oxidoreductase
	2	PP3719-PP3727	PP3721: aspartate aminotransferase PP3722: alanine racemase/Alr
D-Leu	1	PP3589-PP3593	PP3590: aromatic amino acid aminotransferase PP3591: Δ^1 -piperideine-2-carboxylate reductase
	2	PP3593-PP3598	PP3596: FAD-dependent oxidoreductase
	3	PP3717-PP3724	PP3721: aspartate aminotransferase PP3722: alanine racemase/Alr
	4	PP5264-PP5271	PP5269: alanine racemase/DadX PP5270: D-amino acid dehydrogenase/DadA
D-Phe	1	PP2244-PP2253	PP2246: FAD-dependent oxidoreductase

^aThe coverage for the entire screening with each AA exceeded 500× genome coverage.

^bORFs in bold are the focus of the current study.

Substrate specificity of *Pseudomonas putida* KT2440 amino acid racemases

Genes encoding putative racemase activity (proline racemase PP1258, alanine racemase/Alr PP3722, alanine racemase/DadX PP5269) were subcloned into pET28b for *in vitro* characterization. Each enzyme was purified to homogeneity and analyzed for its relative activity on both stereoisomers of each of the 19 chiral, proteinogenic AAs (Table 2.2). The protein product of the gene annotated as *alanine racemase/alr* (Alr) demonstrated the broadest substrate specificity of the recovered racemases. Despite its annotation as a putative alanine racemase, substrates that conferred the highest activity (Table 2.2) were lys (normalized to 100% for both D- and L-) and arg. The protein product of the gene annotated as *alanine racemase/dadX* (DadX) demonstrated activity with both ala stereoisomers, showed negligible activity with D-cys and L-ser, and exhibited no activity with the remaining AAs. The putative proline racemase did not exhibit measurable racemase activity with any of the 19 chiral proteinogenic L-AAs or their corresponding D-enantiomers. Nonetheless, the gene did rescue the phenotype of the *E. coli* pro auxotroph strain in the presence of D-pro, which is indicative of at least minimal racemization *in vivo*. Because previous work identified hydroxyproline epimerase activity in cell-free extract of the related *Pseudomonas putida* KT2442 (32), we assessed the activity of the putative proline racemase with four epimers of hypro. The different epimers arise from chirality about the α -carbon and the γ -carbon in the AA. Isomerization about the α -carbon, typical of AA racemization, results in interconversion of the *cis*-D-hypro and *trans*-L-hypro epimers. The conversion of either L-hypro epimer appears not to be affected by the chirality about the γ -carbon atom, described by the *cis*- and *trans*- notations (Table 2.2). However, *cis*-D-hypro confers a much higher activity compared to *trans*-D-hypro suggesting a potential influence of γ -carbon chirality in the racemization of the D-hypro epimers.

Table 2.2 Percent normalized relative activity of racemases on D- and L-AAs^a

Purified enzyme	D-AAs ^b	Normalized percent activity (\pm SD)	L-AAs ^b	Normalized percent activity (\pm SD)
alanine racemase (Alr)	Lys	100 \pm 6.6E-9	Lys	100 \pm 8.1E-7
	Arg	87 \pm 1.64	Arg	11 \pm 0.79
	Met	12 \pm 0.2	Met	6 \pm 0.22
	Gln	7 \pm 0.09	Gln	3 \pm 0.1
	Ala	3 \pm 0.15	Ser	2 \pm 0.09
	Ser	3 \pm 0.09	Ala	1 \pm 0.03
	Leu	1 \pm 0.08	Asn	1 \pm 0.08
	His	1 \pm 0.03	Leu	1 \pm 0.02
	Asn	1 \pm 0.07	His	1 \pm 0.02
	Others	ND ^d	Others	ND ^d
alanine racemase (DadX)	Ala	100 \pm 2.2E-7	Ala	100 \pm 2.4E-6
	Cys	8 \pm 0.2	Ser	1 \pm 0.04
	Others ^c	ND ^d	Others ^c	ND ^d
proline racemase	<i>cis</i> -D-HyPro		100 \pm 1.2E-6	
	<i>trans</i> -L-HyPro		32 \pm 0.82	
	<i>cis</i> -L-HyPro		32 \pm 1.82	
	<i>trans</i> -D-HyPro		23 \pm 0.62	
	Others		ND ^d	

^aPercent activity values were normalized for difference in derivatization between each D- and L-enantiomer (44).

^bFinal assay concentration for each AA was 50mM, except Tyr (2.21mM) and Asp (25mM). Assays were performed in triplicate only for those AAs that showed activity greater than zero.

^cOthers category comprises all remaining chiral proteinogenic L-AAs.

^dND – Not Detected.

Kinetic parameters of amino acid racemases

The alanine racemase Alr demonstrated a K_M in the μM range for D-lys while the K_M for L-lys was significantly higher (Table 2.3). However, the V_{max} values suggest a more rapid racemization in the direction of D-lys formation. Nonetheless, the V_{max}/K_M values indicate a 4-fold higher overall enzymatic efficiency in the D \rightarrow L direction.

Considering that both Alr and DadX catalyze racemization of ala (Table 2.2), we established the kinetic parameters of both enzymes with each ala enantiomer (Table 2.3). For the conversion of D-ala to L-ala, the K_M value of Alr was approximately twice that of DadX, while the V_{max} value for the DadX reaction was $\sim 5\times$ greater than Alr, contributing to a $\sim 10\times$ higher V_{max}/K_M value for the DadX reaction for the conversion of D-ala to L-ala. In the direction of L-ala to D-ala, Alr showed a $\sim 2\times$ lower K_M value and a $\sim 15\times$ lower V_{max} value, which contributes to $\sim 10\times$ higher V_{max}/K_M values for DadX. There is significant variability in reported enzyme parameters for racemases; this can likely be attributed to differences in reaction conditions. Owing to the reversible nature of the reaction, the lack of a depleting co-substrate, and the reasonably similar catalytic efficiencies in either direction, it is necessary to limit the overall reaction time and minimize substrate turnover or the reverse reaction will confound the data. The assay conditions utilized in this work were optimized for an amino acid racemase reaction, using low (below two μM) enzyme concentrations with one minute reaction times, ensuring that less than 10% of the total substrate from each reaction was turned over. The literature on ala racemization and the responsible enzymes is fairly extensive, and the kinetic parameters have been established for racemases from a number of bacterial species, including *P. aeruginosa* PAO1 (118), two *P. fluorescens* strains (61), *S. typhimurium* (36, 134), *E. coli* (59), and *Staphylococcus aureus* (112). Recorded K_M values in the direction of D- to L-ala vary from 4.2 to 8.7mM while V_{max} values in the same direction range from 6.5 to 770 U mg^{-1} . Similar disparities exist for kinetic analysis in the opposite direction: K_M values from 4.1 to 18.4mM and V_{max} values from 11 to 1500 U mg^{-1} (60).

Consistent with previous reports of hydroxyproline epimerase activity in *Pseudomonas putida* extracts (33, 39), the putative proline racemase only exhibited activity with hypro as a substrate. Kinetic values for the isomerization of *cis*-D-hypro and *trans*-L-hypro (epimers about the α -carbon) are shown in Table 2.3. The enzyme exhibited a lower K_M value for *cis*-D-hypro as well as a higher maximum velocity in the D \rightarrow L direction, resulting in a $27\times$ greater V_{max}/K_M value in the conversion of *cis*-D-hypro to *trans*-L-hypro than in the opposite direction.

Table 2.3 Kinetic parameters of racemases determined on a collection of D- and L-AAAs^a

Enzyme	Substrate	K _M ^b (mM)		V _{max} ^b (mM min ⁻¹ μg enz ⁻¹)		V _{max} K _M ⁻¹	
		D → L	L → D	D → L	L → D	D → L	L → D
alanine racemase (Alr)	Lys	0.359±0.06	8.96±1.52	1.647±0.04	10.09±0.97	4.588	1.126
alanine racemase (DadX)	Ala	15.71±2.79	12.62±0.74	0.053±0.00	0.044±0.00	0.003	0.003
	Ala	7.726±0.63	24.57±2.64	0.281±0.02	0.69±0.087	0.036	0.028
proline racemase	HyPro (cis-D- and trans-L-)	5.26±1.12	15.04±4.19	0.567±0.07	0.063±0.00	0.108	0.004

^aThe substrates with the highest normalized percent activity were chosen for kinetic analysis, as well as D-/L-ala for Alr and *trans*-L-hypro for proline racemase.

^bParameters were determined via non-linear regression according to the Michaelis-Menten equation.

Bioinformatic analysis of *P. putida* KT2440 racemase genes

The genome of *P. putida* KT2440 possesses 894 paralogous gene domain families, which is the highest number known relative to other sequenced bacterial genomes (117). Only the genome of *P. aeruginosa* PAO1 approaches that number with 809, while other genomes possess 50% of that or fewer (83). Consequently, we assessed whether the genetic loci characterized in this study demonstrate identity and genomic synteny to those found in the genomes of other bacteria. We performed a BLASTp analysis using the deduced protein sequence of alanine racemase/Alr (Fig. 2.2A). The displayed branches of the constructed tree have high support values (≥ 0.8), suggesting a confirmation of the tree topology. We found that the *P. putida* KT2440 Alr clusters only with similar proteins from *P. putida* strains and is quite different from those found in other *Pseudomonas* species and other bacteria (Fig. 2.2A).

Because of differences in substrate specificity between the Alr and DadX enzymes, we considered the relationship between substrate specificity, gene class, and genomic neighborhood among the *alr* and *dadX* gene families. Figure 2.2B shows a phylogenetic tree of all annotated *alr* and *dadX* gene entries in the *Pseudomonas* genome database (accessed 6/20/2013). While this is not a complete assessment of alanine racemase genes among pseudomonads, a clear delineation, with strong branch support, can be made between *alr* genes from *P. putida* entries and the remaining *alr* and *dadX* genes from these pseudomonads. Figure 2.2B also indicates strong conservation among pseudomonad *dadX* genes, but significant divergence among the remaining *alr* genes.

Analysis of *alr* genomic synteny among pseudomonads revealed a strong conservation of the selected genetic loci between the two *Pseudomonas putida* strains, KT2440 and GB-1 (Fig. 2.2C), as well as a similarly high synteny between *P. aeruginosa* and *P. protegens* Pf-5 (formerly *P. fluorescens* Pf-5). The notable difference is the lack of the *alr* gene in this region in the latter two species. This difference was previously noted by Yang and Lu (141) when describing the L-arginine transaminase pathway (initiated by the *aruH* and *arul* genes from Fig. 2.2C) in *P. aeruginosa* PAO1. The genomic synteny of the regions surrounding *dadX* and the proline racemase (*proR*) was also explored (Fig. 2.3A). We observed high synteny for the regions bordering *dadX* among each of the tested pseudomonads (same species as for the *alr* analysis), similar to that reported by He et al. (49). Some conservation was noted among these species with regards to the *proR* gene (Fig. 2.3B). Conservation of genes involved in hypro metabolism between *P. putida* and *P. aeruginosa* was previously noted by Watanabe, et al. (136).

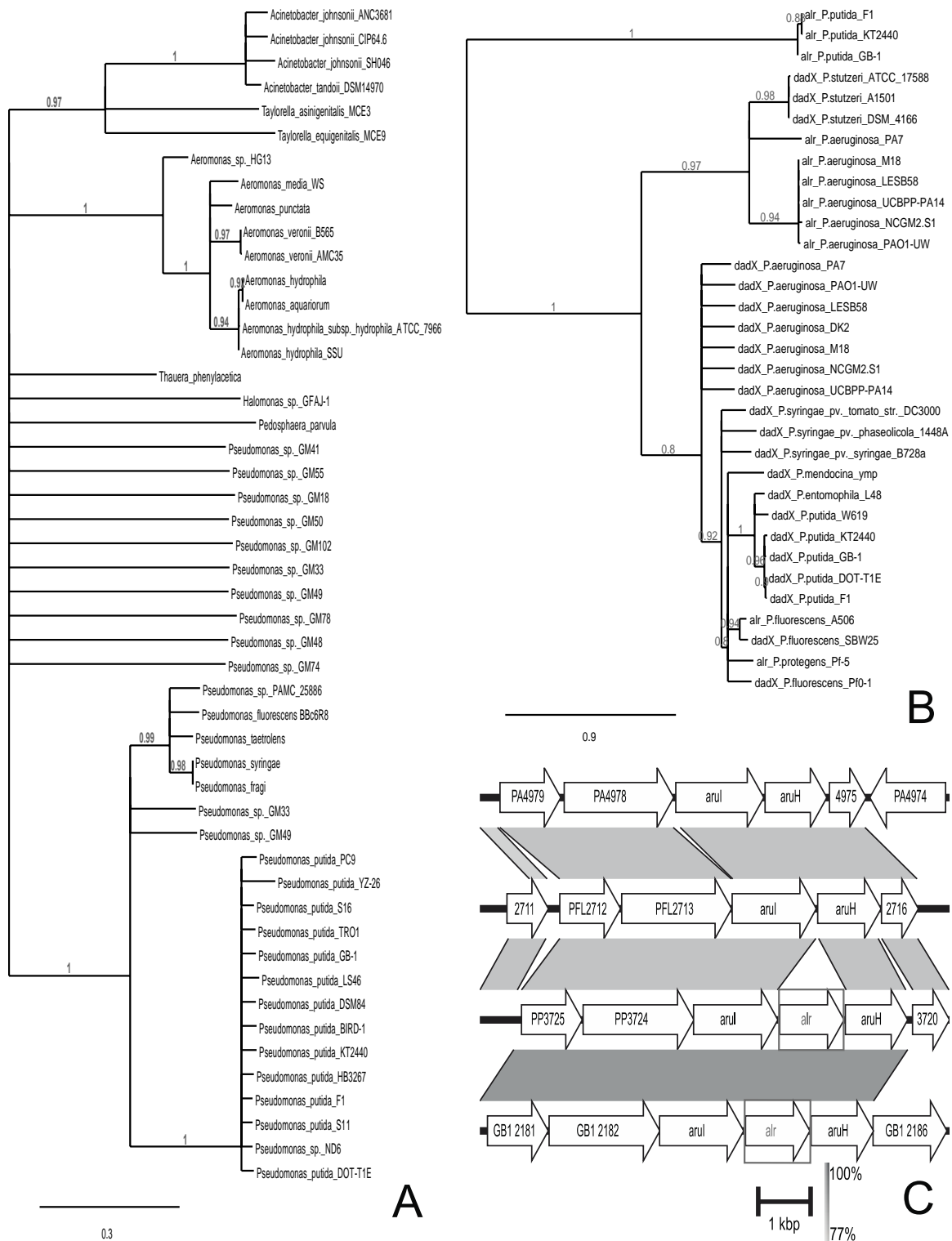


Figure 2.2 Phylogenetic analysis of the alanine racemase/Alr. (A) Tree of the 50 non-redundant protein sequences most identical to alanine racemase/Alr. (B) Tree of the annotated DadX and Alr from the sequenced genomes in the *Pseudomonas* Genome Database. Distance bars represent expected proportion of substitutions per amino acid site. (C) Genomic synteny analysis on regions

bordering the *alr* gene from *Pseudomonas putida* KT2440 (included are three additional genomic regions from *P. aeruginosa* PAO1, *P. protegens* Pf-5, and *P. putida* GB-1). Gene annotations based on the Pseudomonas Genome Database. The capped line represents actual DNA length. The gradient scale provides the percent identity for the genomic loci.

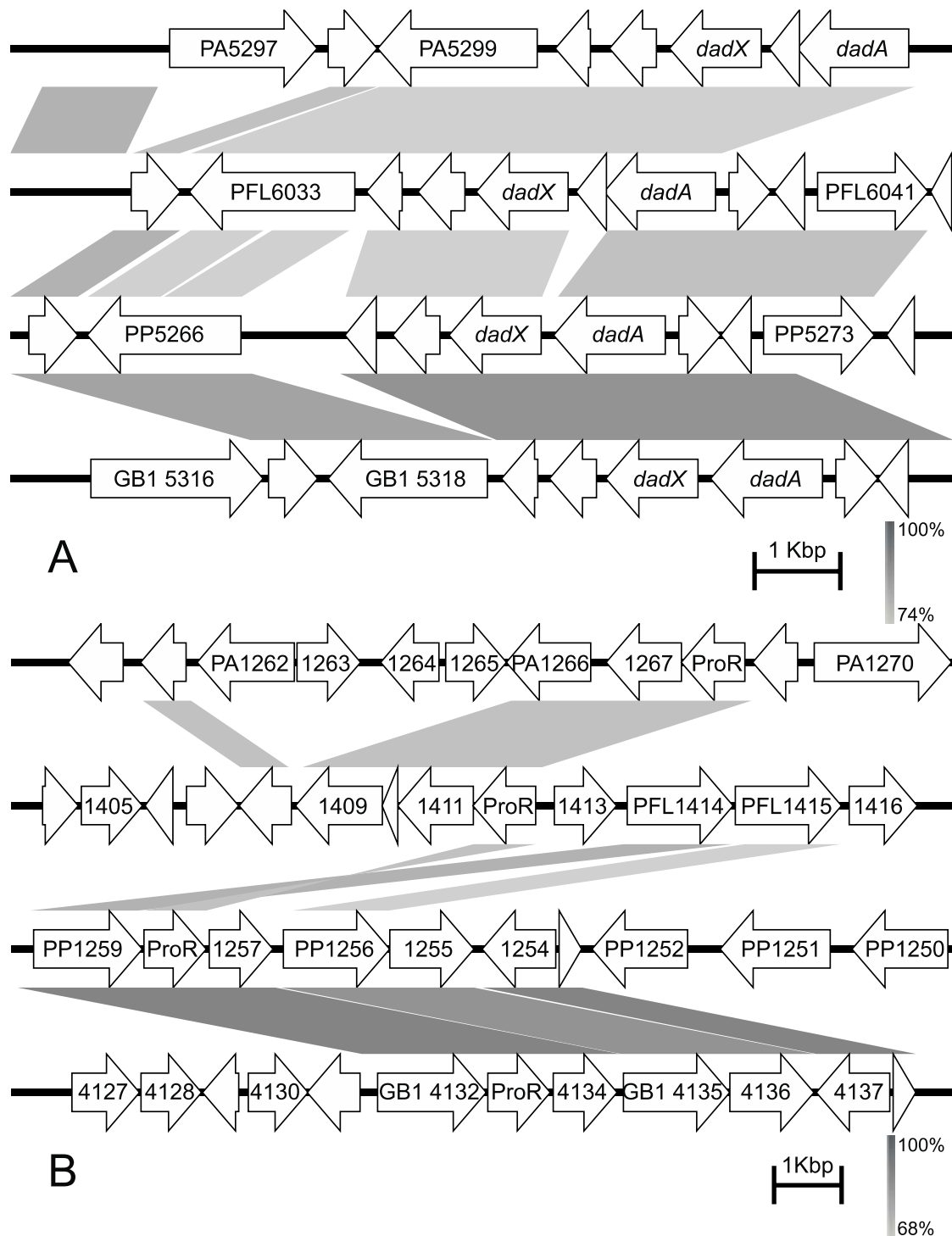


Figure 2.3 Genomic synteny analysis on the regions surrounding *dadX* (A) and the proline racemase (*proR*) (B) from *Pseudomonas putida* KT2440 (included are three additional genomic regions from *P. aeruginosa* PAO1, *P. protegens* Pf-5, and *P. putida* GB-1). Gene annotations based on the *Pseudomonas* Genome Database. The capped line represents actual DNA length. The gradient scale provides the percent identity for the genomic loci.

Discussion

Few comparative statements can be made about D-AA utilization profiles (as sole carbon and nitrogen sources), yet in observing the profiles of *P. aeruginosa* PAO1 (74) and *P. putida* KT2440, some differences are noted. *P. aeruginosa* PAO1 will not use either D-lys or D-phe as sole sources of carbon and nitrogen while *P. putida* KT2440 will. Yet *P. aeruginosa* will use four other D-AAs that are not catabolized by *P. putida* KT2440: D-asn, D-gln, and D-glu, and D-val. Incidentally, *P. putida* KT2440 will catabolize the L-stereoisomer of each of these. In addition to elaborating on the extent of D-AA utilization by *P. putida* KT2440, we reasoned that these growth profiles may give us information about AAs that undergo racemization. For those AAs in which both enantiomers are catabolized, it is plausible that our genomic screen will recover a mechanism by which the enantiomers are directly interconverted. However, more than one mechanism exists for recovering growth using this screen. This includes racemization of the D-AA to produce its corresponding L-AA by amino acid racemases. Another mechanism involves deamination of the D-AA, producing its corresponding achiral α -keto acid, followed by stereospecific amination to produce the L-AA. This two-enzyme process was shown to be involved in conversion of D-arg to L-arg via coupled catabolic and anabolic dehydrogenases encoded by the *dauBAR* operon in *P. aeruginosa* (73). While the *dauBAR* operon is not encoded by *P. putida* KT2440, a genomic clone encoding an enzyme that catalyzes only the first step of this two-step process may recover growth due to the presence of native α -keto acid transamination activity (the second step of the above process) within the *E. coli* screening host. The loci recovered from these genomic screens indicate that both racemization and deamination clones were identified. The latter includes putative FAD-dependent oxidoreductases, dehydrogenases and aminotransferases. Members of these classes of enzymes are known to catalyze deamination of AAs, but are not capable of direct enzymatic racemization (74, 95, 109, 136, 140). Multiple genomic loci were recovered from three of the four screens, as indicated in Table 2.1. Only one genomic locus was recovered from the phe screen. Based on the annotated function of the recovered genes, we chose to further study the proline racemase (*proR*, PP1258), and the two alanine racemases (*alr*, PP3722; *dadX*, PP5269). Future work will address the reactions and specificities of the other recovered genes.

The gene annotated as a proline racemase from *P. putida* KT2440 exhibited no *in vitro* racemization of pro; rather, it appears to be a 4-hydroxyproline epimerase based on its *in vitro* enzymatic activity. This enzymatic activity is widespread among bacteria that colonize animals and plants (80, 115), owing to the abundance of *trans*-L-hypro in both collagen and plant cell wall proteins (8, 24). In the catabolic pathway described by Gryder and Adams for a *P. putida* isolate (46), *trans*-L-hypro is first isomerized to *cis*-D-hypro by a (then unknown) 4-hydroxyproline epimerase. The product is then further oxidatively metabolized in several steps to produce α -ketoglutarate. We report here that the *P. putida* KT2440 proline racemase encodes the enzyme necessary to initiate this catabolic pathway via epimerization, and recommend that the current “proline

racemase” designation be changed to “4-hydroxyproline epimerase”. Interestingly, the *in vitro* reaction appears to be much more efficient in the opposite direction—that is, in conversion of the D-hydro epimer to the L-hydro epimer (Table 2.2). Despite the lack of *in vitro* proline racemase activity, the enzyme must provide sufficient reactivity *in vivo* to account for the relatively small amount of L-pro necessary to recover growth of the pro auxotroph. Nonetheless, any proline racemase activity it exhibits in *P. putida* KT2440 would be minimal as it is not sufficient to allow for growth on D-pro. Figure 2.1 shows that the bacterium grows readily on L-pro. Watanabe, et al., describe differences in the genes involved in L-hydro metabolism in *P. putida* and *P. aeruginosa* (136), where they attribute convergent evolution to differences in a key gene involved in this pathway. Nonetheless, each uses an orthologous 4-hydroxyproline epimerase to initiate the process and some conservation is seen among genes immediately surrounding this gene (Figure 2.3B and (136)).

Owing to the ubiquity of D-ala in PG, racemization of ala by bacteria is a well-known phenomenon and numerous reports describe identification and characterization of enzymes involved in ala racemization (61, 112, 118, 135). Data from Table 2.2 shows that the DadX enzyme exhibits tight substrate specificity, suggesting a single role in interconversion of ala stereoisomers. This is consistent with the activity of those DadX orthologs that have been characterized (61, 118). Often referred to as a “catabolic racemase” (134), DadX enzymes are proposed to serve a role in catabolism of L-ala whereby L-ala is converted to D-ala before catalytic dehydrogenation to form pyruvate (135). The *dadAX* genomic locus, which also encodes the D-amino acid dehydrogenase (*dadA*) used in this catabolic process in *P. aeruginosa* (49), exhibits significant synteny among closely related pseudomonads (Figure 2.3 and (49)). The *P. putida* KT2440 DadX enzyme shows overall similar V_{\max}/K_M values for both the L \rightarrow D and D \rightarrow L conversions. Incidentally, the V_{\max}/K_M values using L- and D-ala as substrates are ~10-fold lower for the *P. putida* KT2440 Alr enzyme (Table 2.3), largely stemming from lower V_{\max} values with both L- and D-ala. Nonetheless, in instances where both *alr* and *dadX* genes exist in the same organism, the Alr isozyme is considered as the “anabolic” alanine racemase and is attributed as the source for periplasmic D-ala used in PG synthesis (36). Based on the available sequences in GenBank, *alr*-encoded alanine racemases appear to be more widespread than do *dadX*-encoded alanine racemases. However, the presence of both annotated alanine racemases is not unusual, as this is seen in a large number of *Proteobacteria*. Each of the 184 bacterial *dadX* alanine racemase gene entries in GenBank is from a member of the α -, β -, or γ -*Proteobacteria*, while the 1088 bacterial *alr* alanine racemase entries are more widely distributed (accessed 6/13/13). No uniform racemase gene nomenclature exists, however, and many genes are annotated as simply “alanine racemase”. Interestingly, previous work has established that both the *alr* and *dadX* genes from *P. aeruginosa* PAO1 can rescue a D-ala auxotroph in *E. coli*, indicating that production of D-ala by either enzyme is sufficient for peptidoglycan synthesis (118).

Here we demonstrate that the *P. putida* KT2440 Alr exhibits relatively low activity with ala compared to other AAs, raising questions about its role in D-ala synthesis for peptidoglycan in *P. putida* KT2440. The V_{\max}/K_M with lys is nearly 3 orders of magnitude greater than that with ala in both reaction directions. Further, in contrast to the *dadX* genomic locus, the *alr* genomic locus exhibits a distinct variation between pseudomonad species (Figure 2.2C), and the *P. aeruginosa* PAO1 Alr enzyme appears to be more closely related to the *P. aeruginosa* DadX enzyme than to the *P. putida* KT2440 Alr (Figure 2.2B). The Alr phylogenetic tree generated from the top 50 BLASTp hits (Figure 2.2A) shows a clear grouping of *P. putida* Alr proteins. Despite an abundance of *alr* and *dadX* genes in the numerous sequenced genomes of *P. aeruginosa* and *E. coli* isolates, none of these gene products show sufficient similarity to be included in the tree.

Among the ten *P. aeruginosa* genomes and six *P. putida* genomes currently available at the Pseudomonas Genome Database (137) (accessed 6/12/13), each of these strains carries both the *alr* gene and the *dadX* gene. The *dadX* locus is conserved among all of these, yet the *alr* locus differs according to species. With the exception of *P. putida* W619, each of the *P. putida* strains shares the same *alr* locus organization depicted for *P. putida* KT2440 in Figure 2.2C. The location of the *P. putida* KT2440 *alr* gene, between the *arul* and *aruH* genes (Figure 2.2C, first noted by Yang, et al. (141)) is noteworthy. The *aruH* locus was previously shown to be necessary for the arginine transaminase pathway (ATA pathway) for catabolism of L-arg in *P. aeruginosa* PAO1 (141). Yang and Lu determined that expression of this locus in this organism was upregulated in the presence of L-arg, and characterized these enzymes as an L-arginine:pyruvate transaminase (AruH) and a 2-ketoarginine decarboxylase (AruL).

In *P. aeruginosa* PAO1, catabolism of D-arg is initiated by conversion to L-arg via the coupled dehydrogenases DauA and DauB of the *dauBAR* operon (73). DauA and DauB are both required for *P. aeruginosa* PAO1 to grow on D-arg as a sole carbon and nitrogen source, implying that D-arg is only metabolized via conversion to L-arg and that no other enzymatic arg racemization mechanism exists in *P. aeruginosa* PAO1. The DauA enzyme is a broad spectrum D-amino acid dehydrogenase but it functions best on D-arg and D-lys (74). Previous work demonstrated that D-lys cannot complement a L-lys auxotroph in *P. aeruginosa* PAO1 (74). Taken together, this indicates that no direct arg or lys racemase exists in *P. aeruginosa* PAO1, suggesting that the *alr* gene in *P. aeruginosa* PAO1 does not have the same substrate specificity as its *P. putida* KT2440 ortholog. Further, while the *dauBAR* locus is conserved among *P. aeruginosa* strains, it is not present in any of the *P. putida* strains from the Pseudomonas Genome Database.

Based on the above observations, it appears plausible that the Alr enzyme in *P. putida* KT2440 serves a role analogous to that of DauA and DauB in *P. aeruginosa* PAO1, in conversion of D-arg to L-arg for further catabolism by the ATA pathway. In the absence of the *dauBAR* operon, the *P. putida* KT2440 *alr* gene may be responsible for conversion of D-arg into L-arg, which is then catabolized by the products of the *aruH* operon in which the *alr* gene is

incorporated (Figure 2.2C). Moreover, Table 2.2 shows that D-arg is apparently the preferred substrate of the two arg stereoisomers. The *P. aeruginosa* DauA enzyme also oxidatively deaminates D-lys to produce 2-ketolysine, however, *P. aeruginosa* cannot catabolize D-lys as a sole carbon and nitrogen source while *P. putida* KT2440 can. Incidentally, both D-arg and D-lys induce the *dauBAR* operon in *P. aeruginosa* but only L-arg induces the *aruHI* operon (AruH acts on L-arg but not D-arg). In order for Alr to be functional in this proposed role, the *aruH-alr-arul* locus in *P. putida* would likely be induced by D-arg. This has yet to be determined.

Previous work on catabolism of D- and L-lys by *P. putida* KT2440 has indicated that each proceeds through an independent pathway and that racemization of D-lys to L-lys prior to degradation is not required (95). While it is possible that the Alr enzyme is involved in degradation of lys, its potential for synthesis of D-lys and any additional role that D-lys may play should be further explored. Catabolic routes for certain L-AAs, such as ala (135) and hypro (46), involve conversion from the L-stereoisomer into the D-stereoisomer. This clearly prevents the AA from being incorporated into peptides and may minimize the changes in gene regulation that accompany increased pools of free AAs in the cell (15, 93).

In environments where D-AAs are abundant, their presence is typically attributed to the associated microbial communities (48, 113), yet outside of a relatively few AAs nothing is known regarding their synthesis. Indeed the D-stereoisomer of each of the 19 chiral proteinogenic AAs has been identified in some capacity from either microbial cultures (25) or from microbe-enriched environments (70). The work here further establishes the pseudomonads as good models for comparative genomic analysis of bacterial metabolism and points to differences in D-AA metabolism between two of the most well studied members of this clade. However, despite an increased awareness of the roles that D-AAs play in bacterial ecophysiology, much remains to be discovered concerning the synthetic mechanisms and reasons for deployment of these compounds.

Methods

Growth studies using D- and L-AAs as the sole source of carbon and nitrogen

Sterile PG medium (119) was prepared without a carbon or nitrogen source and was supplemented with a sterile AA stock to a final concentration of 25mM. Three 3ml growth tests were conducted of each AA enantiomer. An overnight culture of *Pseudomonas putida* KT2440, incubated in liquid PG containing the regular carbon and nitrogen source (0.5% glucose and 25mM ammonium sulfate (119)), was washed with sterile water and 10 μ l was used to inoculate each tube. Growth controls consisted of un-inoculated culture tubes. The culture tubes were maintained at 28°C with shaking and OD₆₀₀ was measured after 24, 48, and 72 hours (BioMate 3 Spectrophotometer, Thermo Scientific). The respective growth control for each AA was used as blank.

Genomic library construction and screening

Genomic DNA from *Pseudomonas putida* KT2440 was isolated using a GenElute™ bacterial genomic DNA kit (Sigma-Aldrich) according to the supplemented instructions. Genomic DNA was fragmented by hydrodynamic shearing (GeneMachines hydroshear; speed: 19 cycles: 20). It was subsequently end-repaired (DNATerminator® end-repair kit, Lucigen) and 8kb-15kb fragments were gel extracted after performing agarose gel electrophoresis (Thermo Scientific GeneJET gel extraction kit). The purified DNA was ligated into a blunt-ended pUC19 vector using T4 DNA ligase (Thermo Scientific; 2 units) and the entire volume of all reactions was transformed into electrocompetent Epi300 *E. coli* cells (Epicentre). The library was prepared by incubating the recovery in LB medium with carbenicillin selection (100µg ml⁻¹) overnight at 37°C with shaking, harvesting the cells by centrifugation, and preparing a stock in 20% glycerol maintained at -80°C (126). DNA was isolated from the recombinant genomic library by miniprep (GeneJET plasmid miniprep kit, Thermo Scientific) and used to construct three additional libraries in *E. coli* AA auxotrophic strains obtained from the Coli Genetic Stock Center (www.cgsc.biology.yale.edu; leu (JW5807-2), lys (JW2806-2), pro (JW0233-2), phe (JW2580-1)). Auxotrophs were in-frame, single-gene knockouts from the Keio collection (6).

Recombinant auxotrophic genomic libraries were screened for recovery of growth on minimal medium supplemented with D-pro (10mM), D-lys (1mM), D-leu (10mM), or D-phe (10µM) (Sigma-Aldrich) in lieu of the corresponding L-AA. Briefly, portions of the glycerol stock were grown in LB overnight at 37°C with shaking, after which the cultures were washed with sterile water and 50µl of 1/100 dilutions were plated on minimal PG medium containing the respective D-AA. The screens were developed at 28°C. Positive clones, defined as those recombinant genomic clones that conferred growth of the auxotroph in the presence of the tested D-AA but not in its absence, were restreaked for isolation on PG+D-AA medium and cultures were started for plasmid DNA isolation (GeneJET plasmid miniprep kit, Thermo Scientific). Positive clones were retransformed into a fresh auxotrophic background and verified as above. Additionally, open reading frames of interest from recovered clones (alanine racemase/DadX, PP5269, NP_747370; alanine racemase/Alr, PP3722, NP_745855; proline racemase, PP1258, NP_743418) were cloned into pUC19 (*dadX* F: 5'-ATATGGATCCTATGCGTCCCGCCCGGCCCTGATC-3' (BamHI), *dadX* R: 5'-CCGCGAGCTCTCATTTCGCCGATGTAGTCCCGTGGT-3' (Sacl); *alr* F: 5'-ATATGGATCCTATGCCCTTTCGCCGTACCCTTCTG-3' (BamHI), *alr* R: 5'-CCGCGAATTCTCAGTTCGACGAGTATCTTCGGGTTG-3' (EcoRI); *proR* F: 5'-CGCCGGATCCTATGAAACAGATTCACGTCATCGAC-3' (BamHI), *proR* R: 5'-TAACGAATTCTCAGATGCCCCAGGCGAAAGGGTCT-3' (EcoRI)). The constructs were transformed via electroporation into pro, leu, or lys auxotrophic cells to verify that the identified open reading frame itself confers the growth on the D-AA substrate.

DNA was sequenced on an ABI 3730 instrument (Applied Biosystems) at the University of Kentucky Advanced Genetic Technology Center using a cycle

sequencing kit (BigDye® Terminator v3.1 cycle sequencing kit, Applied Biosystems) to elucidate the insert DNA from each positive clone. The genomic region harboring the DNA insert from positive clones was identified using the bioinformatics resources provided by the Pseudomonas Genome Database (137).

Preparation of constructs and protein purification

Open reading frames encoding the three putative amino acid racemases described above were cloned into pET28b using the same PCR primers. The constructs were employed for the production of *N*-terminal Histidine-tagged protein using *E. coli* Rosetta2 (DE3) (EMD4Biosciences, EMD Millipore). For gene overexpression, an overnight culture of Rosetta2 (DE3) cells containing the appropriate construct was used to inoculate 500ml LB culture, grown at 37°C with shaking until OD₆₀₀ was approximately 0.6-0.7. The culture was induced with 0.5mM IPTG and shaken vigorously (270 rpm) for three hours at 28°C. Induced cells were harvested by centrifugation and stored at -80°C.

For protein purification, the cells were resuspended in 2ml buffer A2X (50mM HEPES pH7.4, 200mM NaCl, 1.95mM TCEP, 10% glycerol) and lysed via sonication (ten 20s pulses at 60V with two minute breaks on ice) and the cell lysate was subjected to immobilized metal affinity column chromatography using HIS-Select® Nickel affinity gel (Sigma-Aldrich). Following loading, the column was washed with buffer A (50mM HEPES pH7.4, 100mM NaCl, 0.97mM TCEP, 5% glycerol) supplemented with 20mM imidazole, then eluted with buffer A containing 250 mM imidazole. Fractions containing the purified protein were identified by SDS-PAGE and were concentrated and buffer exchanged into buffer A2X using centrifugal concentration (Pierce® Concentrators, 7ml/9K MWCO, Thermo Scientific). Protein concentrations were determined via the Protein Assay Dye Reagent from Bio-Rad. Purified samples were analyzed by SDS-PAGE (Precise Tris-HEPES Gels, Thermo Scientific) to assess apparent protein purity. The concentration of the purified protein was determined as above and 50µl aliquots were snap frozen in liquid nitrogen and stored at -80°C until use.

In vitro enzyme assays

AA racemization assays were performed in 2ml Eppendorf tubes for the duration of one minute at 37°C. The total volume for each assay was 200µl and comprised the following final concentrations: 50mM HEPES (pH 7.4), 20µM Pyridoxal-5'-phosphate (PLP) (PLP was added only in the characterization of the annotated alanine racemases but was not included for the proline racemase). Reactions were initiated by the addition of purified enzyme (alanine racemase/Alr - 1µM; alanine racemase/DadX - 0.7µM; proline racemase - 1.9µM; final concentrations). To quench the enzyme reaction, 40µl of 2M HCl was added. The molar concentration of enzyme used in each reaction was 10% or less of the initial substrate concentration, and we chose a reaction duration that allowed for the conversion of 10% or less of the initial substrate to minimize the reverse reaction.

Marfey's reagent (1-fluoro-2,4-dinitrophenyl-5-L-alanine amide, FDAA; Sigma-Aldrich) was used for the derivatization of AAs and reverse-phase HPLC (Dionex Ultimate 3000; Waters Nova Pak® C18, 3.9mm x 150mm column) was employed to determine the concentration of each enantiomer (82). To avoid hydrolysis of Marfey's reagent, 40µl of 2M NaOH was added to neutralize the quenched enzyme reaction prior to derivatization, followed by 100µl Marfey's reagent (0.5% solution in acetone) and 20µl 1M NaHCO₃. The derivatization was incubated at 40°C for one hour, after which it was allowed to cool to room temperature, and diluted tenfold in 80%:20% 0.05M Triethylamine-phosphate buffer pH 3.0 (TEAP):acetonitrile (concentrated phosphoric acid was used to adjust the pH of the triethylamine solution to prepare the TEAP buffer). The resulting solution was passed through a 0.22µm filter (nonsterile hydrophobic polytetrafluoroethylene PTFE syringe filters, Tisch Scientific) and placed into an amber glass vial prior to HPLC analysis. A gradient method was used for HPLC separation of most AAs: starting at 80%:20% TEAP buffer (pH3.0):acetonitrile, ramping to 70%:30% buffer:acetonitrile over 5 minutes, followed by a ramp to 50%:50% buffer:acetonitrile over 15 minutes (see Table 2.4 for additional HPLC gradients). The injection volume was 10µl and the flow rate was 0.5ml min⁻¹. Products of the derivatization were detected at 340nm. Authentic standards of each D- and L-AA were used to establish retention time, and a standard curve was generated from known AA concentrations in the reaction buffer in the absence of enzyme.

Table 2.4 Gradients used in AA enantiomer HPLC analysis

AA (D and L)	Gradient
Thr, Pro, Lys, Phe, Cys, Leu, Tyr, Ile, Ala, Trp	Start at 80%:20% TEAP buffer (pH3.0):acetonitrile; ramp to 70%:30% buffer:acetonitrile over 5 minutes; ramp to 50%:50% buffer:acetonitrile over 15 minutes; ramp to 80%:20% buffer:acetonitrile over 10 minutes; (injection volume: 10µl; flow rate: 0.5ml; detection wavelength: 340nm)
Ser, Asp, Glu, Val, HyPro	Start at 80%:20% TEAP buffer (pH3.0):acetonitrile; ramp to 70%:30% buffer:acetonitrile over 15 minutes; ramp to 50%:50% buffer:acetonitrile over 5 minutes; ramp to 80%:20% buffer:acetonitrile over 10 minutes; (injection volume: 10µl; flow rate: 0.5ml; detection wavelength: 340nm)
Arg	Start at 90%:10% TEAP buffer (pH3.0):acetonitrile; ramp to 80%:20% buffer:acetonitrile over 15 minutes; ramp to 50%:50% buffer:acetonitrile over 5 minutes; ramp to 90%:10% buffer:acetonitrile over 10 minutes; (injection volume: 10µl; flow rate: 0.5ml; detection wavelength: 340nm)
Met	Start at 80%:20% TEAP buffer (pH3.0):acetonitrile; ramp to 70%:30% buffer:acetonitrile over 5 minutes; ramp to 60%:40% buffer:acetonitrile over 15 minutes; ramp to 80%:20% buffer:acetonitrile over 10 minutes; (injection volume: 10µl; flow rate: 0.5ml; detection wavelength: 340nm)
Asn, Gln, His	Start at 85%:15% TEAP buffer (pH3.0):acetonitrile; ramp to 75%:25% buffer:acetonitrile over 15 minutes; ramp to 50%:50% buffer:acetonitrile over 5 minutes; ramp to 85%:15% buffer:acetonitrile over 10 minutes; (injection volume: 10µl; flow rate: 0.5ml; detection wavelength: 340nm)

Phylogenetic analysis

To determine any relationships between the identified enzymes in this study and other racemases, phylogenetic trees were constructed using software provided by Phylogeny.fr (33). MUSCLE was used for multiple alignment (no alignment curation; Run mode: default; Maximum number of iterations: 16), PhyML for tree construction (Statistical test for branch support: aLERT - SH-like; Substitution model: default), and TreeDyn for tree visualization (default parameters). Easyfig (120) was used for the genomic loci comparison and visualization. The FASTA sequences used in the tree construction were obtained from the GenBank database of the National Center for Biotechnology Information (NCBI) (9).

Copyright statement: This chapter was published in its entirety in the Journal of Bacteriology published by ASM Press (Radkov, A D and Moe, L A. 2013. Amino acid racemization in *Pseudomonas putida* KT2440. J. Bacteriol. vol. 195 no. 22 p. 5016-5024).

Chapter Three: A broad-spectrum AA racemase indirectly affects the synthesis of L-proline in *Pseudomonas putida* KT2440

Background and Introduction

D-Amino acids (D-AAs) are typically less abundant than their L-amino acid (L-AA) counterparts, but they are increasingly seen as important effectors of bacterial physiology (70, 72). The key structural roles of D-ala and D-glu in peptidoglycan are well appreciated, and additional D-AAs (e.g. D-lys, D-ser, and D-met) have been identified in peptidoglycan from diverse bacteria (130). Recent work has shed light on the expanding roles of D-AAs in modulating bacterial behavior, including biofilm formation/dispersal and growth phase transition (70, 72). Nonetheless, with the exception of D-ala and D-glu, much less is known concerning mechanisms and reasons for D-AA synthesis (102).

Pseudomonads are good models for studying the biology of D-AAs, as they are proficient catabolizers and synthesizers of D-AAs and metabolic pathways have already been worked out for several (50, 73, 109, 136). Previous work from our lab established that the *alr* gene from *Pseudomonas putida* KT2440 encodes a broad-spectrum AA racemase (BSAR) that exhibits the highest activity interconverting the stereoisomers of lys and arg (103). Because *P. putida* KT2440 catabolizes both D- and L-lys using independent mechanisms, it has been suggested that the Alr enzyme may be responsible for linking the two pathways (109). Indeed, catabolism of L-AAs in some cases is accomplished by initial conversion to the corresponding D-AA (e.g. L-ala catabolism in *Salmonella typhimurium*, *Escherichia coli*, *Pseudomonas aeruginosa* PAO1 and *P. putida* KT2440 (49, 78, 135)).

In addition to its proposed role in D-lys catabolism, a possible role of the Alr enzyme in D-arg and D-ornithine catabolism has to be considered. The enzyme has strong activity *in vitro* with both enantiomers of arg (103). In addition, the gene is located in a putative operon with *aruH* and *arul* (PP3721 and PP3723) involved in the catabolism of L-arg via the transaminase pathway (140, 141). Even though the activity of Alr with D- / L-ornithine has not been demonstrated *in vitro*, several biochemically characterized BSARs show activity with both enantiomers of lys and arg, as well as ornithine (64, 75, 87). On one hand, the non-proteinogenic AA L-ornithine has a central part in various physiological processes such as peptidoglycan synthesis, lipid modification, production of antibiotics, polyamines, and siderophores, as well as L-pro and L-arg synthesis (139). In fact, it has been demonstrated that in *P. putida* KT2440 the only route for L-ornithine catabolism is via the synthesis of L-pro (107, 125). In addition, the only known route in *P. putida* KT2440 for the synthesis of L-arg involves L-ornithine as well (55). On the other hand, there is minimal literature on the role of D-ornithine in cellular physiology.

With this study on the *alr* gene using a genetic knockout strain, we attempt to enhance our understanding of D-AA metabolism in bacteria. We provide evidence to support a role of the Alr enzyme in the catabolism of L-arg, L-lys, and L-ornithine *in vivo*. Furthermore, the synthesis of the respective D-enantiomers from the latter three L-AAs appears as a major catabolic route, the absence of

which hampers the growth of the Δalr mutant strain. We propose the production of L-pro from L-ornithine as the main physiological role of the Alr enzyme in *P. putida* KT2440. The Δalr strain demonstrates a growth delay relative to the wild-type in minimal media supplemented with a C and N source but lacking any AAs. This phenotype is alleviated by the addition of D-ornithine as well as L-pro. Without the addition of the latter two AAs, the mutant strain eventually reaches a growth level similar to the wild-type likely by synthesizing L-pro through the less efficient L-glu pathway. Our results support a model whereby the Alr enzyme converts L-ornithine into D-ornithine, and D-ornithine is subsequently converted into L-pro via the achiral intermediate pyrroline-2-carboxylate (Pyr2C).

Results

Alr localization and specific activity in LB media

Based on previous work (95) we hypothesized that the Alr enzyme would be localized to the periplasmic space in *P. putida* KT2440, and Table 3.1 shows that enzymatic activity was present in the periplasmic soluble protein fraction. Alr enzyme activity was not detected in the periplasmic protein fraction obtained from the Δalr strain (Table 3.1), yet alkaline phosphatase activity was detected at levels comparable to the wild-type strain (Table 3.2). Minor amounts of glucose-6-phosphate dehydrogenase activity were found in both periplasmic protein fractions compared to the soluble protein fraction remaining following cell lysis (Table 3.2). The specific activity of Alr in the wild-type strain was approximately two-fold higher during exponential growth phase relative to stationary growth phase.

Table 3.1 Specific activity (nmoles min⁻¹ mg total protein⁻¹) of BSAR *

Medium and growth phase	WT <i>P. putida</i> KT2440 Periplasmic fraction	Δ <i>alr</i> <i>P. putida</i> KT2440 Periplasmic fraction
LB stationary (OD ₆₀₀ > 1.0, overnight growth)	134.5 ± 29.8	ND
LB exponential (OD ₆₀₀ = 0.6)	239.1 ± 19.4	ND

* tested on 12.5 mM D-lys as the substrate; 1 hr assay at 37 °C; LB – Luria-Bertani rich medium

Average values of three replicates ± standard deviation are shown

ND – no activity detected

Table 3.2 Specific activity (nmoles min⁻¹ mg total protein⁻¹) of wild-type (WT) and Δ *alr* *P. putida* KT2440 protein fractions

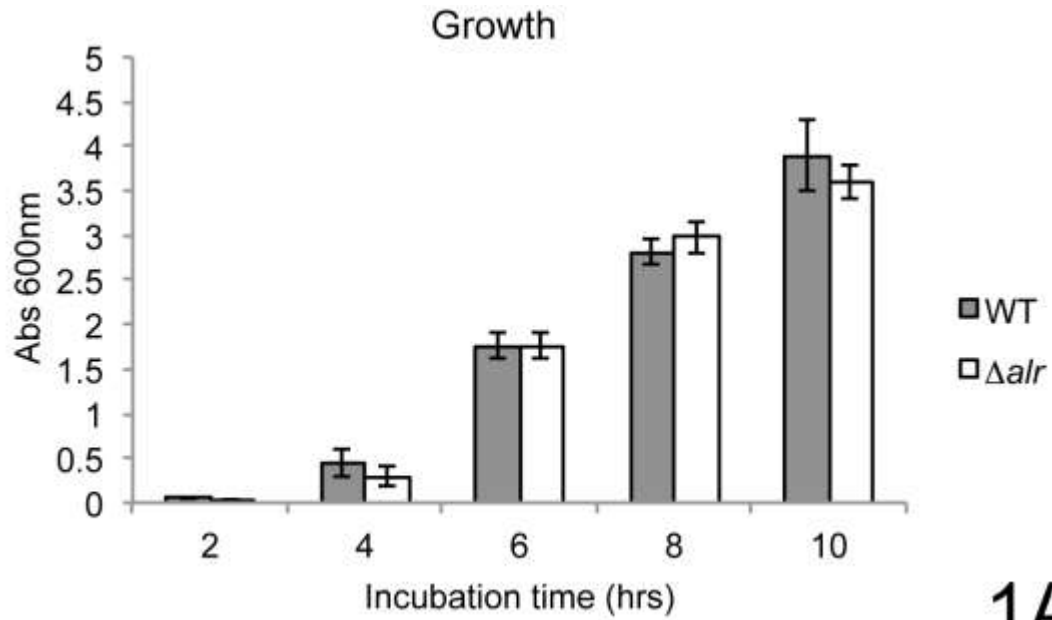
	Glucose-6-phosphate dehydrogenase (periplasmic protein fraction)	Glucose-6-phosphate dehydrogenase (remaining protein fraction)	Glucose-6-phosphate dehydrogenase (relative specific activity)	Alkaline phosphatase (periplasmic protein fraction)	Alkaline phosphatase (remaining protein fraction)	Alkaline phosphatase (relative specific activity)
WT	8.57 ± 0.68	51.32 ± 1.00	0.17 ± 0.01	1.33 ± 0.09	1.61 ± 0.06	0.83 ± 0.06
Δ <i>alr</i>	6.84 ± 1.38	46.10 ± 1.25	0.15 ± 0.05	1.16 ± 0.11	0.98 ± 0.29	1.18 ± 0.12

Average values of three replicates are reported ± standard deviation. Relative specific activity results from dividing the specific activity from the periplasmic protein fraction by the specific activity from the remaining protein fraction.

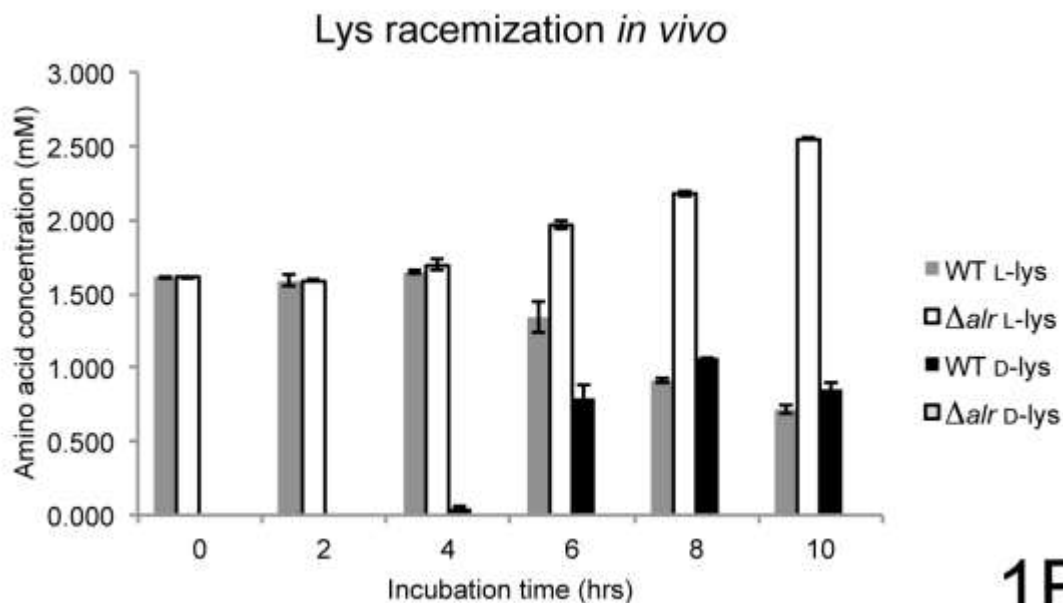
Lys racemization *in vivo*

No significant differences were observed for growth between the two strains during the course of the experiment (Fig. 3.1A). A small amount of D-lys (less than 100 μ M) was produced by the wild-type strain after 4hrs of incubation (Fig. 3.1B). The concentration of D-lys at 6hrs increased in wild-type culture supernatant, reaching almost 1mM. This occurred concomitant with a decrease in L-lys from 1.5mM to ~1.3mM. The concentration of L-lys increased to 2mM in the Δalr strain while no D-lys was detected (Fig. 3.1B). Lastly, in the case of the Δalr strain, L-lys increased to more than 2mM at 8hrs and 2.5mM at 10hrs while there was no detectable D-lys present.

Due to the presence of D-lys in the supernatant and the periplasmic localization of the Alr enzyme, the concentration of AAs in the peptidoglycan was determined. No significant differences ($p>0.05$) were observed in the stationary phase composition of peptidoglycan between the wild-type and Δalr strains (Table 3.3), precluding a role for Alr in peptidoglycan modification. Both strains had approximately equal amounts of the conventional peptidoglycan stem AAs L-ala, D-glu, and D-ala (130). The predicted crosslinking AA D,L-diaminopimelic acid was also seen, along with L-arg and L-lys. No D-lys was detected. Other as-yet-unidentified peaks were observed in the HPLC chromatogram, however none of those showed significant differences ($p>0.05$) between the two strains.



1A



1B

Figure 3.1 LB growth profile and lys racemization *in vivo*. (A) Growth measurements (OD_{600}) were performed on 5ml LB cultures grown in glass tubes. No statistically significant ($p > 0.05$) differences were found. (B) Concentration of lys enantiomers found in the culture medium (LB) removed from the glass tubes. In both panels, average values \pm SD are displayed the result of three independent experiments. Statistical analysis conducted using Student's t-test.

Table 3.3 AAs detected in peptidoglycan and culture supernatant

AA / Strain	Peptidoglycan *	
	Wild-type	Δalr
	Percent of identified AA content ^a	
L-Ala	24.2 ± 1.6	24.0 ± 2.6
D-Glu	22.9 ± 0.6	23.9 ± 3.2
D, L-Diaminopimelic acid	13.2 ± 0.3	14.0 ± 0.8
D-Ala	22.4 ± 0.0	22.3 ± 0.5
L-Lys	4.0 ± 1.5 ^b	7.2 ± 1.6 ^b
D-Lys	ND	ND
L-Arg	13.2 ± 0.8	13.1 ± 0.3
D-Arg	ND	ND
L-Ornithine	ND	ND
D-Ornithine	ND	ND

* measured during stationary phase, 50 ml culture, LB medium, 28°C, 220rpm

^a calculated as percent of the total area of the AAs shown in the table – the respective total area was the same between the two peptidoglycan fractions, as well as the same between the three supernatant fractions

^b this difference in the amount of L-lys is not statistically significant ($p > 0.05$, Student's t-test)

Average values of three replicates ± standard deviation are shown

ND – AA was not detected

Gene expression analysis between wild-type and Δalr

Using LB medium, we saw no difference in growth between the two strains but a striking difference in their ability to produce D-lys (Fig. 3.1). Consequently, we decided to perform a comprehensive gene expression analysis with the wild-type and Δalr strain in order to understand what effect the lack of D-lys synthesis may have on the bacterial physiology. More than half of the *P. putida* KT2440 genome was covered by at least one paired-end read and approximately 10% - by 10 or more paired-end reads (Fig. 3.2). When comparing the wild-type replicates and Δalr replicates using the statistical tools available in CLC Genomics Workbench, the expression of 119 genes was significantly different ($p < 0.05$), either more highly expressed in the wild-type strain or in the Δalr strain. All of the known genes involved in D-lys catabolism were significantly overexpressed ($p < 0.05$) in the wild-type relative to the mutant strain (Table 3.4). Those include the Alr BSAR PP3722, the AA dehydrogenase acting on D-lys to produce Δ^1 -piperideine-2-carboxylate (Pip2C) PP3596 (109), the Pip2C / Pyr2C reductase converting Pip2C into L-pipecolate PP3591 (95), and the downstream genes acting on L-pipecolate and converting it to L-glu, PP5257 and PP5258 (108). Moreover, these are the only genes overexpressed in the wild-type. The difference in RPKM for genes overexpressed in the wild-type varies from 100 (PP3722 and PP3596) to 1500 (PP5258), and the fold-change for every gene was above 3. The most overexpressed gene in the wild-type strain was PP3593 (fold-change 27), a putative AA transporter localized to the periplasm (Table 3.4). Although this gene has not been characterized biochemically, it is part of an operon with PP3596, also overexpressed in the wild-type strain (fold-change 6), which has been shown empirically to act on D-lys yielding Pip2C. This result suggests that PP3593 may be a novel D-AA transporter protein. A somewhat surprising finding was the gene PP3191, overexpressed in the wild-type with a fold-change value of 10 (Table 3.4). It has not been previously shown to have a role in D-AA catabolism. Although annotated as a hypothetical protein, it is part of an operon with a gene encoding a putative ornithine cyclodeaminase and it appears to contain an AA-ammonia lyase domain based on the Conserved Domain Database (CDD). This finding points to a potential connection between lys and ornithine catabolism. Lastly, the gene PP5260 has not been previously studied although it was overexpressed in the wild-type, fold-change value of 8 (Table 3.4). However, it is in close proximity with PP5257 and PP5258 genes both of which are involved in the downstream reactions following L-pipecolate and result in the synthesis of L-glu. Based on the *Pseudomonas* database (137), the gene is transcribed divergently from PP5257 and PP5258, it encodes a hypothetical protein and it does not contain any known conserved domains. At this stage, the data on this gene is scarce to allow for any speculation regarding its function. There were only four genes overexpressed in the Δalr strain relative to the wild-type (Table 3.4). It should be noted that their RPKM and fold-change values are generally lower than the genes overexpressed in the wild-type strain. Little empirical data is available regarding the function of the encoded proteins. The only available information relates to a paralog of gene PP2656 which has

been previously found to have a role in biofilm formation (34). Three of the genes overexpressed in Δalr (PP1082, PP1600, and PP2656) appear to be involved in membrane function based on bioinformatics analysis via the Pseudomonas Genome database and CDD. These genes could potentially have a role in biofilms. In fact, we found that there is a minor but statistically significant difference in the ability of the two strains to disassemble biofilms after reaching stationary phase (data not shown). This research avenue was deemed beyond the scope of this study and was not pursued any further.

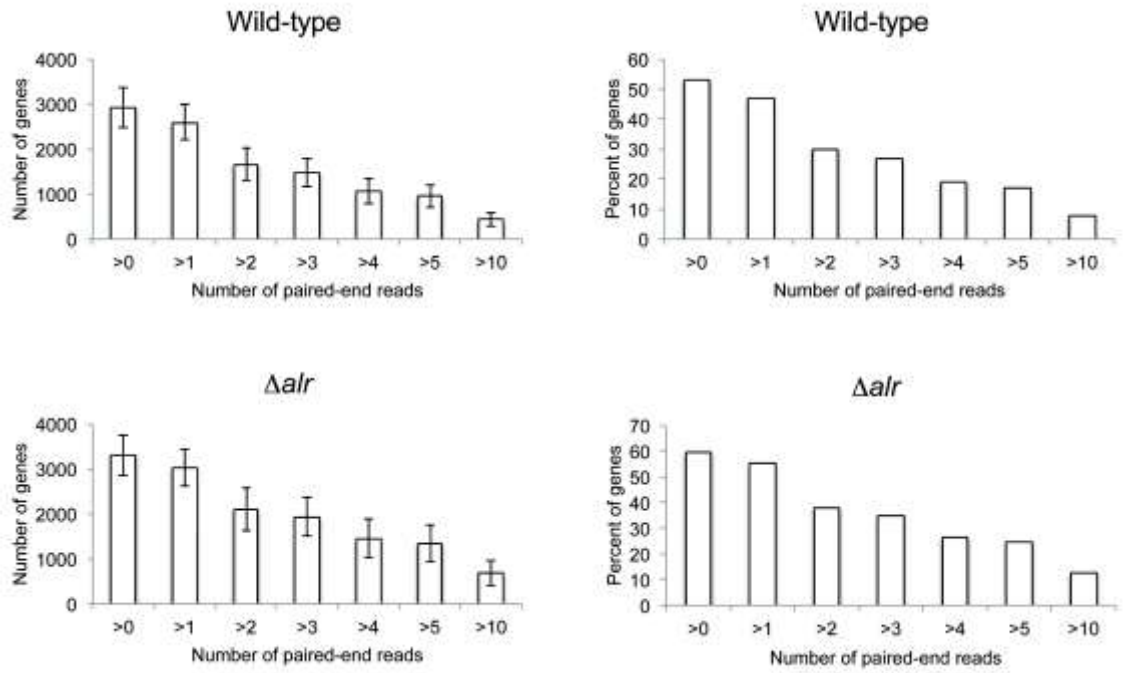


Figure 3.2 Genome coverage achieved after RNA-Seq data analysis. Average values \pm standard deviation are shown the result of three growth assays.

Table 3.4 Comparison of gene expression between the wild-type and Δ air strain after 6hrs of growth in LB media.							
Wild-type overexpressed							
Localization	Cluster of Orthologous Group (COG)	Feature ID	Conserved Domain Database	Wild-type	Δ air	Difference	Fold change
Periplasmic	Amino acid transport and metabolism; Signal transduction mechanisms	PP_3593	Part of D-lys catabolism	426.28	15.95	410.33	27
Periplasmic	Cell wall/membrane/envelope biogenesis	PP_3722	Part of D-lys catabolism	102.51	7.07	95.43	14
Cytoplasmic membrane	Energy production and conversion	PP_3591	Part of D-lys catabolism	304.20	22.82	281.37	13
Cytoplasmic	Amino acid transport and metabolism	PP_3191	CDD: AA-ammonia lyase (part of an operon with ornithine cyclodeaminase)	446.67	45.24	401.43	10
Cytoplasmic	Energy production and conversion	PP_5258	Part of D-lys catabolism	1795.84	201.07	1594.77	9
Cytoplasmic	Function unknown	PP_5260	CDD: domain of unknown function DUF1338	245.25	30.65	214.60	8
Cytoplasmic	Amino acid transport and metabolism	PP_5257	Part of D-lys catabolism	516.49	85.62	430.87	6
Cytoplasmic membrane	Amino acid transport and metabolism	PP_3596	Part of D-lys catabolism	114.49	18.81	95.69	6
Δ air overexpressed							
Localization	Cluster of Orthologous Group (COG)	Feature ID	Conserved Domain Database	Wild-type	Δ air	Difference	Fold change
Unknown	Function unknown	PP_3743	CDD: domain of unknown function DUF2388	69.99	334.68	264.69	5
Cytoplasmic	Inorganic ion transport and metabolism	PP_1082	CDD: bacterioferritin	142.78	397.85	255.07	3
Cytoplasmic membrane	Cell wall/membrane/envelope biogenesis	PP_1600	CDD: periplasmic chaperone (part of cell wall synthesis operon)	205.13	526.66	321.53	3
Periplasmic	Inorganic ion transport and metabolism	PP_2656	CDD: penicillin-binding protein-like	371.69	879.53	507.84	2

Values for wild-type and Δ air represent reads per kilobase transcript per million mapped reads (RPKM). Shown are the average values, derived from the gene expression analysis using three unique cDNA libraries for each strain. The entire gene expression analysis was conducted using CLC Genomics Workbench (CLC bio, QIAGEN). All of the included genes here have RPKM values larger than 200 and a fold-change of 3 or higher, except for the genes in bold – they have either RPKM values higher than 200 or a fold-change of 3 or higher. CDD: Conserved Domain Database.

Alr deletion had an effect on AA catabolism

The *alr* deletion did not impact whether a particular AA was used as a C and/or N source, but the rates of growth differed in some cases. Of the 21 tested D-AAAs, six were catabolized as the sole C and N source, while the remaining 15 conferred negligible growth (Table 3.5). Most of the L-AAAs (15 L-AAAs), however, were catabolized as the sole source of C and N, while six L-AAAs (cys, leu, met, thr, trp, and tyr) yielded minimal growth. When AA catabolism as the sole source of N was considered, almost every D-AA (except for D-asp, D-his, D-met, D-thr, and D-trp) and every tested L-AA were catabolized to some extent (Table 3.5). However, minimal growth ($OD_{600} \leq 0.5$ after 72hrs) was observed with L-met and L-trp. D-Pro represents a unique case because the wild-type strain utilized the AA as the only N source while the Δalr strain did not, even after 72hrs of incubation.

Table 3.5 shows clear differences between the wild-type and Δalr strains in their rates of growth using L-arg, L-lys, and L-ornithine as the sole source of carbon and nitrogen. In each case, the wild-type strain exhibited much faster growth relative to Δalr . The same trends were not observed with the corresponding D-AAAs (Table 3.5). The case of L-arg may be more complicated as there are four arg catabolic pathways characterized in both *P. putida* KT2440 and *P. aeruginosa* PAO1 (125). Incidentally, no significant growth changes were observed when the two strains were provided with these AAAs as the sole N source (Table 3.5). The main finding here is the delay in L-ornithine catabolism in the mutant strain (Table 3.5), which points to a problem with L-pro synthesis in the cell because the only known pathway for L-ornithine catabolism proceeds through L-pro (125).

Table 3.5 Growth profile of *P. putida* KT2440, wild-type (WT) and Δ *air*

	WT	Δ <i>air</i>	WT	Δ <i>air</i>	WT	Δ <i>air</i>	WT	Δ <i>air</i>
	C and N source	D-AAs	C and N source	L-AAs	N source	D-AAs	N source	L-AAs
Ala	+++	+++	+++	+++	+++	+++	+++	+++
Arg	++	++	+++	+	+++	+++	+++	+++
Asn	-	-	+++	+++	+++	+++	+++	+++
Asp	-	-	+++	+++	-	-	+++	+++
Cys	-	-	-	-	++	++	++	++
Glu	-	-	+++	+++	++	++	+++	+++
Gln	-	-	+++	+++	+++	+++	+++	+++
His	-	-	+++	+++	-	-	+++	+++
Hypro	+++	+++	+++	+++	+++	+++	+++	+++
Ile	-	-	++	++	++	++	+++	+++
Leu	-	-	-	-	++	++	++	++
Lys	++	++	+++	+	+++	+++	+++	+++
Met	-	-	-	-	-	-	+	+
Orn	++	++	+++	+	+++	+++	+++	+++
Phe	+	+	+	+	++	++	++	++
Pro	-	-	+++	+++	+	-	+++	+++
Ser	-	-	++	++	+	+	+++	+++
Thr	-	-	-	-	-	-	++	++
Trp	-	-	-	-	-	-	+	+
Tyr	-	-	-	-	++	++	+++	+++
Val	-	-	++	++	++	++	+++	+++

+++ , abs at 600nm \geq 0.5 after 24hrs of incubation; ++ , abs at 600nm \geq 0.5 after 48hrs of incubation; + , abs at 600nm \geq 0.5 after 72hrs of incubation; - , abs at 600nm $<$ 0.5 after 72hrs of incubation; Growth assay were performed in triplicate;

Minimal media experiment comparing the growth of wild-type and Δalr

The rationale for this experiment is that if a growth difference between the two strains were observed, that would indicate the mutant strain cannot synthesize a necessary nutrient, potentially L-pro. PG media was used containing glucose used as sole C source and ammonium chloride as N source. Statistically significant growth difference ($p < 0.05$) between the wild-type and the mutant strain was observed after 24, 30, and 36hrs of incubation at 28°C. The growth of the mutant strain at 48hrs was similar to that of the wild-type after 24hrs of incubation (Fig. 3.3). This phenomenon is known as bradytrophic growth. In comparison to auxotrophic growth where a genetically modified strain cannot grow without the addition of a particular nutrient, bradytrophism implies that the strain shows a delay in growth, conferred by a delay in the synthesis of a particular nutrient. The mutant strain demonstrated three-fold less growth after 24hrs, almost seven-fold less growth after 30hrs, and four-fold less growth after 36hrs. The mutant strain reached a growth level similar to the wild-type after 48hrs (Fig. 3.3).

Minimal media growth profile

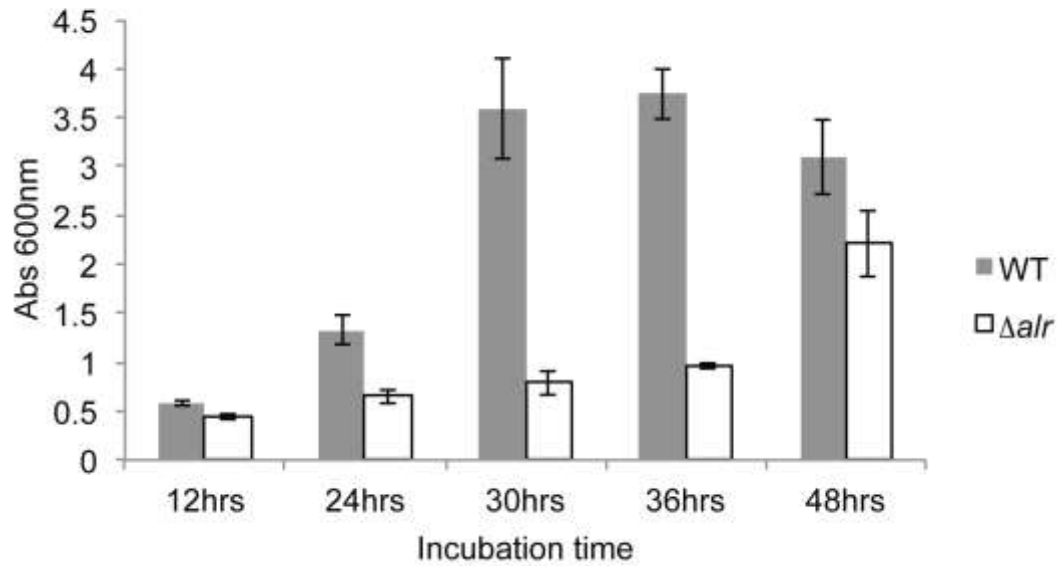


Figure 3.3 Minimal media growth profile. PG media 5ml cultures were started from individual colonies. Three separate experiments were conducted and representative average values are shown \pm SD. Significant differences between the wild-type and Δalr were observed after 24, 30, and 36hrs of incubation ($p < 0.05$, Student's t-test).

AAs that rescue the bradytrophic phenotype of the Δalr strain

Seven L-AAs, including L-pro, rescued completely the bradytrophism exhibited by the mutant strain after 30hrs of incubation in PG minimal media (the difference in growth between the wild-type and Δalr strain was less than 0.5 abs units at 600nm) (Table 3.6). This result is in line with the proposed hypothesis that L-pro synthesis is affected in the mutant strain. Two D-AAs rescued the mutant phenotype of Δalr strain when added to the PG medium already containing glucose and ammonium chloride. The mutant phenotype was completely rescued by D-ornithine as well as by *cis*-D-hypro (Table 3.6). Seven D-AAs and six L-AAs enhanced the amount of growth reached by the mutant strain relative to the growth in the absence of those AAs (PG medium with glucose and ammonium chloride only). However, those AAs did not rescue the bradytrophic phenotype of the mutant when compared to the growth of the wild-type strain in PG medium with glucose, ammonium chloride and the respective AAs (Table 3.6). When the mutant strain was grown in the presence of the remaining D- and L-AAs, the mutant phenotype of Δalr was not rescued, and the attained growth did not differ from that achieved by the mutant strain in PG medium with glucose and ammonium chloride only (Table 3.6).

Table 3.6 Minimal media phenotype rescue after 30hrs incubation in PG medium

D-AAs	Phenotype rescue	L-AAs	Phenotype rescue
Hypro	++	Pro	++
Orn	++	Phe	++
Val	+	Hypro	++
Ala	+	Ala	++
Leu	+	Asn	++
Lys	+	Asp	++
Ile	+	Glu	++
Thr	+	Gln	+
Phe	+	His	+
Trp	-	Val	+
His	-	Leu	+
Asp	-	Ile	+
Cys	-	Tyr	+
Asn	-	Trp	-
Arg	-	Orn	-
Gln	-	Arg	-
Glu	-	Met	-
Tyr	-	Thr	-
Pro	-	Cys	-
Met	-	Lys	-
Ser	-	Ser	-

++, growth difference between wild-type and $\Delta a/r$ mutant was less than 0.5 abs units (abs at 600nm)

+, growth difference between wild-type and $\Delta a/r$ mutant was more than 0.5 abs units (abs at 600nm), however, the mutant still showed higher growth relative to that observed in the absence of the supplied AA

-, wild-type exhibited normal growth but growth of the $\Delta a/r$ mutant was similar to that observed in the absence of the supplied AA

Total cellular AA concentration

In an attempt to elucidate the manner in which the AAs in Table 3.6 rescue the bradytrophic phenotype of Δalr , total cellular AA concentration was compared after both strains had reached the peak of log phase. The two strains differ significantly in their growth profile, however, the two strains would achieve similar growth stages after ~24hrs for the wild-type and ~48hrs for the Δalr based on Fig. 3.3. Using the appropriate AA standards, several AAs were identified from the HPLC chromatograms. On one hand, the concentration of L-asp, L-ornithine, L-phe, L-ala, and D-lys, D-arg was significantly higher in the wild-type relative to the mutant cultures ($p < 0.05$) (Table 3.7). The largest discrepancy was observed for the concentration of L-asp (2.6-fold higher in wild-type). Importantly, D-lys was not detected in the mutant strain confirming the absence of the Alr enzyme (D-lys was still present in the wild-type strain, 5 μ M). However, D-arg was observed in both the wild-type and the mutant strain (35 μ M and 20 μ M, respectively) (Table 3.7). Although the Alr AA racemase is not present in the mutant strain, hence a lower D-arg concentration was observed, it appears there may be a secondary route that allows for the synthesis of some D-arg. This is an interesting finding and is currently further explored in our laboratory. On the other hand, the concentration of L-glu, L-lys, and L-arg was significantly higher in the mutant strain relative to the wild-type ($p < 0.05$) (Table 3.7). The concentration of L-glu in the mutant strain reached almost 1mM while it was only slightly higher than 500 μ M in the wild-type strain. Of note is that the higher concentration of L-lys and L-arg in the mutant strain could be explained by the lack of the Alr enzyme, leading to less production of the respective D-enantiomer. The concentration of L-pro did not differ between the two strains (11 μ M) which is reasonable because of the central role occupied by L-pro in protein synthesis (Table 3.7). Although we did not detect any D-ornithine in either strain, we think this is within the norm considering the very low concentrations detected for D-lys, D-arg, as well as L-ornithine. These D-AAAs are likely converted immediately to different metabolic intermediates in order to avoid their incorporation into ribosomal proteins.

Table 3.7 Total cellular AA concentration after growth in PG medium.

WT μM	Δalr μM	WT / Δalr	t-test	AA
167 \pm 0.1	65 \pm 0.0	2.6	0.003	L-Asp
12 \pm 0.0	6 \pm 0.0	1.9	0.005	L-Orn
35 \pm 0.0	20 \pm 0.0	1.7	0.019	D-Arg
5 \pm 0.0	N.D.			D-Lys
54 \pm 0.0	37 \pm 0.0	1.5	0.001	L-Ala
13 \pm 0.0	8 \pm 0.0	1.5	0.040	L-Phe

WT μM	Δalr μM	Δalr / WT	t-test	AA
1 \pm 0.0	7 \pm 0.0	4.9	0.004	L-Arg
599 \pm 0.2	899 \pm 0.2	1.5	0.024	L-Glu
15 \pm 0.0	20 \pm 0.0	1.3	0.040	L-Lys

WT μM	Δalr μM	Δalr / WT	t-test	AA
11 \pm 0.0	11 \pm 0.0	1.0	0.924	L-Pro
N.D.	N.D.			D-Orn

Representative average values \pm SD are shown of three separate experiments. Wild-type (WT) to Δalr ratio was calculated by dividing the respective WT and Δalr AA concentration. Student's t-test was performed using Excel.

Discussion

BSARs with enzymatic properties similar to Alr have been reported for several organisms, including *Vibrio cholerae*, *Proteus mirabilis*, *Oenococcus oeni* and *Pseudomonas taetrolens* (37, 64, 69, 87). Despite available biochemical work, there is little information on the specific biological role of these enzymes. *P. putida* KT2440 encodes distinct mechanisms for catabolism of L- and D-lys, and some evidence suggests that the Alr racemase links the two pathways (108, 109). Some work, however, implicates a BSAR in synthesis of D-AAAs (D-met and D-leu) in *V. cholerae* (37, 70). In this case, the D-AAAs alter cell morphology by virtue of their incorporation into peptidoglycan. We therefore sought to explore potential roles for the Alr enzyme in AA catabolism as well as D-AA synthesis.

To better understand any further implications of the *alr* gene deletion, we compared the ability of the wild-type and mutant strains to catabolize a collection of 21 D- and L-AAAs using individual minimal media growth assays. Most of the tested D-AAAs were catabolized equally well by both strains despite the lack of the BSAR in the mutant strain. Considering the gene expression analysis results suggesting that the D-lys pathway is more active in the wild-type, this finding was a bit surprising. Moreover, the Δalr strain displayed bradytrophic growth when L-arg, L-lys, and L-ornithine were supplemented as the sole source of C and N. It appears that the *alr* gene may have a major role in the catabolism of L-lys through D-lys. This has also been confirmed by several previous studies on the D-lys pathway in which genes part of the D-lys pathway were deleted but the L-lys catabolism was subsequently negatively affected. Namely, the genes PP3596 and PP3591 (both part of the D-lys catabolic route) have been studied using genetic knockouts by two separate laboratories and in both cases the mutants showed a severe growth delay with L-lys as the sole source of C and N relative to the wild-type (95, 109). Additionally, our finding is supported by a study on *P. putida* KT2440 and the implications of catabolite repression in which the authors contribute evidence suggesting that the D-lys route is the major pathway for L-lys catabolism (93). Specifically, it was demonstrated that the global translational regulator Crc, involved in the repression of non-preferred catabolic pathways when other preferred substrates are present, guides the catabolism of L-lys mainly through the D-lys branch (known as the Amino adipate pathway) by repressing genes part of the L-lys branch (known as the Amino valerate pathway).

The most telling piece of data is that lack of the Alr enzyme in the mutant strain affects L-ornithine catabolism. The only known pathway for L-ornithine catabolism as a C and N source is through L-pro (125). In fact, this could be the main pathway for L-pro synthesis in the cell. Based on previous research, the pathway from L-glu to L-ornithine to L-pro is more favored and simple relative to the pathway from L-glu to L-pro (Fig. 3.4) (107). First, L-ornithine must be made in the cell because it is involved in the only pathway to synthesize L-arg (55). Second, the pathway from L-glu to L-pro requires ATP while useful reducing equivalents (NADH and FADH₂) are generated in the pathway from L-glu to L-ornithine to L-pro. Considering that L-ornithine must be made in the cell for proper synthesis of L-arg, it requires a single enzyme to convert L-ornithine into L-pro

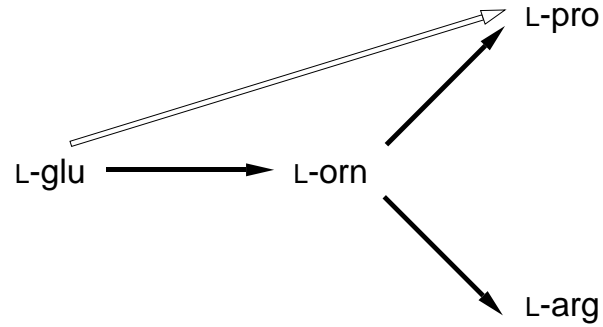
(ornithine cyclodeaminase) while there are three enzymes involved in the synthesis of L-pro from L-glu (55, 107). Lastly, the L-glu to L-pro pathway was not induced by the lack of L-pro in *Salmonella typhimurium* suggesting that the pathway may be constantly active under basal expression (14). Overall, it should be kept in mind that this pathway has not been well studied and there is likely gene redundancy preventing genetic dissection of the exact biosynthetic route.

Considering the presented evidence, two questions arise. How is L-ornithine converted to L-pro and what is the role of the BSAR in this process? The model in fig. 3.4 provides a tentative explanation for the results presented in this article, as well as previous work on D-lys catabolism. Based on current knowledge, the only known enzyme involved in the synthesis of L-pro from L-ornithine is the ornithine cyclodeaminase. *P. putida* KT2440 encodes two open reading frames annotated as such. The enzyme encoded by one of those ORFs (PP3533) has been somewhat biochemically characterized - it acts on L-ornithine but it has never been tested on other L- or D-AAAs (3, 45, 57). Additionally, Muramatsu et al. have established that one of the enzymes in the D-lys catabolic route (Pip2C/Pyr2C reductase, PP3591) can also produce L-pro in vitro from Pyr2C (95). Of note is that Pyr2C contains an achiral α -carbon and it could be synthesized from either L-ornithine or D-ornithine. Although the D-AA dehydrogenase (P3596) has been tested on L- and D-lys, it has not been tested on D-ornithine (109). Our data show that the bradytrophic growth of the *alr* mutant strain was rescued completely by D-ornithine (Table 3.6). D-Orn is needed by the cell as an essential nutrient because the *alr* mutant was able to achieve similar growth level as the wild-type strain in the presence of D-ornithine. This is a novel finding implicating a non-proteinogenic D-AA into the synthesis of L-pro. Additionally, the bradytrophic growth of the mutant was rescued by several L-AAAs. Importantly, these L-AAAs include L-pro which is in line with our proposed hypothesis that the Δalr mutant cannot synthesize L-pro. The data in table 3.7 suggest that there are several differences in the total cellular AA concentration between the wild-type and the mutant. One major difference is the significantly higher L-glu concentration in the mutant strain relative to the wild-type. Based on our proposed model (Fig. 3.4), the mutant strain would compensate for the lack of L-pro synthesis via L-ornithine by channeling more L-glu through the less efficient pathway of L-glu to L-pro. In fact, this would also explain the finding that several other L-AAAs (asp, asn, ala, phe, and hypro), as well as *cis*-D-hypro, were able to rescue the bradytrophic phenotype of the mutant strain. The underlying idea is that each of those AAAs is potentially converted to L-glu via a transaminase. There are well known enzymes that would directly deaminate the L-AA in question and transfer the amino group on α -ketoglutarate to produce L-glu (84, 127).

The model based on the data presented above (Fig. 3.4) proposes a role of Alr not only in the catabolism of L-lys and L-arg, but also a major part in the biosynthesis of L-pro via L-ornithine / D-ornithine racemization. Currently, this pathway has not been explored in any other organisms, however we suspect that D-AAAs are likely involved in other physiological processes and metabolic routes. Their role in cellular processes has largely been unexplored. However, it seems

that bacteria, and perhaps other organisms, have developed specific routes to take advantage of the unique biochemistry conferred by D-AAs.

A



B

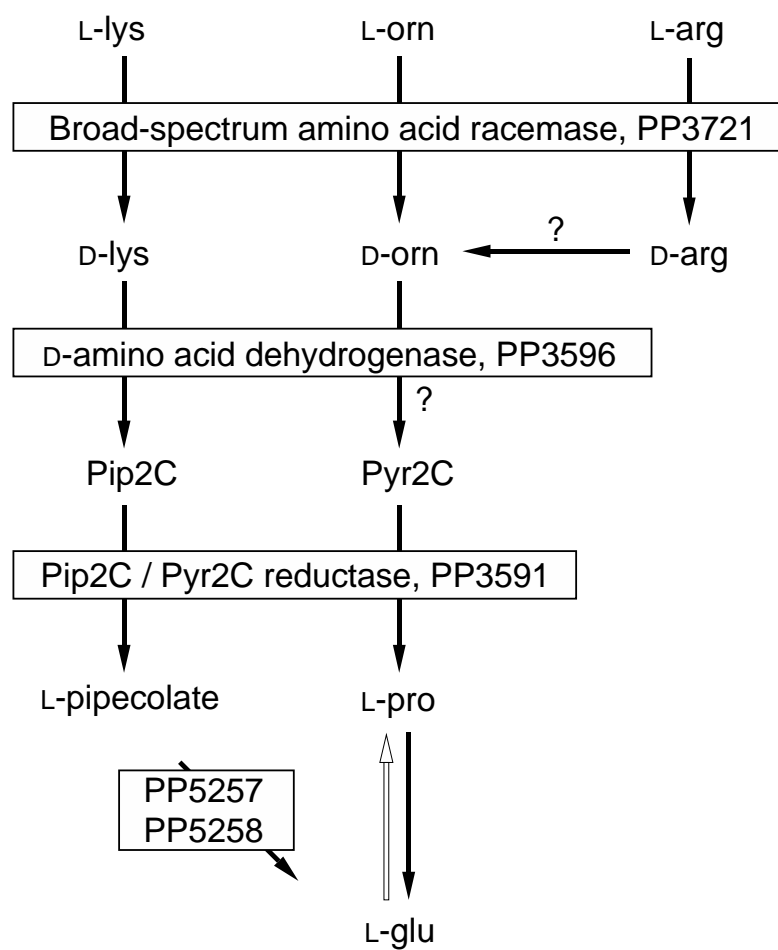


Figure 3.4 The role of the Alr BSAR in L-lys, L-arg, and L-ornithine catabolism and L-pro synthesis. The white arrow indicates a less favorable pathway than those denoted by the black arrows. The question marks signify biochemically possible reactions for which the enzymes have not been characterized. The gene numbers were obtained from the *Pseudomonas* Genome Database.

Methods

Construction of markerless mutation via Short Overlap Extension PCR (SOE PCR)

Primers down_cut (CTAGGAATTCTAATGCGCTCGGCGACGTCA, EcoRI cut site is underlined) plus down_homology (**ATGCCCTTTCGCCGTACCA**AAGATACTCGTCTGACTGA, bold type – start of *alr* gene, regular type – end of *alr* gene) and up_cut (CGTCAAGCTTCTTCATCAGCAGCGACATG, HindIII cut site is underlined) plus up_homology (TCAGTCGACGAGTATCTT**GGTACGGCGAAAGGGCAT**, regular type – end of *alr* gene, bold type – start of *alr* gene) were used in the initial round of PCR to provide fragments downstream and upstream of the *alr* gene, and also engineer an overlap sequence (primers down_homology and up_homology are the reverse complement of each other and contain 36 nucleotides of the *alr* gene). Overnight culture of *P. putida* KT2440 supplied the template DNA (2µl). Following the initial PCR, the SOE PCR was performed using ~20ng of gel purified DNA (Thermo Scientific GeneJET gel extraction kit) from each of the two above reactions, also using primers down_cut and up_cut. All reactions were completed using PrimeSTAR HS DNA Polymerase (TaKaRa) according to the provided instructions (50°C annealing temperature). The SOE PCR provided a fragment containing 500bp upstream and downstream of *alr*, including an engineered restriction enzyme cut site on each end, as well as 18 nucleotides of the start and end of the *alr* gene. The large homologous regions are needed to aid in the homologous recombination, leading to the deletion mutation. Parts of the *alr* gene (12 AAs total) were not deleted in order to achieve an in-frame deletion and also minimize any impact on the transcription of upstream and downstream genes. Vector pEX18Kan ((29); kindly provided by Virginia Stockwell, Oregon State University) and the gel purified SOE PCR fragments were digested using the appropriate restriction enzymes (Thermo Scientific FastDigest enzymes). The digested products were purified (Thermo Scientific PCR purification kit) and subsequently ligated using T4 DNA ligase (2 units Thermo Scientific ligase enzyme and 1:3 vector:insert molar ratio). The ligation reaction was kept for 2hrs at room temperature and overnight at 4°C. Prior to electroporation into *E. coli* cells (Epicentre; TransforMax EPI300 Electrocompetent *E. coli*), the ligation reactions were desalted (10mins) and heat inactivated (10mins at 65°C). Positive clones were selected on media containing Kan (30µg/ml). The pEX18Δ*alr* construct was confirmed using colony PCR (Thermo Scientific; DreamTaq Green DNA PCR Master Mix) and sequencing (Applied Biosystems; BigDye Terminator, v3.1, cycle sequencing kit), M13 -27 and M13 -20 primers (Integrated DNA Technologies). Subsequently, the purified construct (Thermo Scientific GeneJET plasmid miniprep kit) was electroporated into *P. putida* KT2440 electrocompetent cells prepared according to Choi and Schweizer (29). Briefly, two 6ml overnight LB cultures were distributed into 8 microfuge tubes and centrifuged to pellet the cells. Each pellet was washed twice with 500µl 300mM sucrose and all 8 pellets were resuspended in a total of 90µl 300mM sucrose. Between 5-10µl of purified plasmid were added (300ng-500ng),

the cells were electroporated (Bio-Rad GenePulser Xcell; Voltage - 1800V, Capacitance - 25 μ F, Resistance - 200 Ω , 1mm cuvette), followed by an immediate addition of 1ml LB and 1hr recovery in a shaker at 28°C. The entire recovery mixture was plated on a single LB/Kan plate (30 μ g/ml) and incubated at 28°C. To distinguish between single- and double-crossover events, 1ml LB aliquots, without any selection, were inoculated with individual transformants and incubated at 28°C with shaking for 2-3hrs (Virginia Stockwell, personal communication). After the incubation time, 100 μ l of 1/10 dilution were plated onto LB plates containing 5% sucrose (w/v). Several colonies were restreaked onto LB/Kan (30 μ g/ml) and LB+5% sucrose (w/v) to confirm their inability to grow in the presence of Kan selection, suggesting that they no longer carry the Kan resistance cassette. Several colonies were selected as potential deletion mutants. The markerless deletion was confirmed via colony PCR and sequencing of amplicon DNA (seq_down, GATCATGGGCAACGCACAG and seq_up, CATCCGCAATGGGCATG primers were used; expected fragment size 1.2kb for deletion mutant, while 2.4kb for wild-type revertants).

Periplasmic protein isolation and enzyme assays

Periplasmic protein was isolated according to the chloroform extraction method (4). Briefly, a 5ml culture (stationary growth phase, OD₆₀₀>1.0, and exponential growth phase, OD₆₀₀=0.6) was harvested using centrifugation. The pelleted cells were washed twice using buffer A2X (50mM HEPES pH 7.4, 200mM NaCl, 1.95mM Tris (2-carboxyethyl) phosphine hydrochloride (TCEP), 10% glycerol (v/v)). After completing the washes, the cells were resuspended in 800 μ l cold buffer A2X and 30 μ l chloroform was added. The cell mixture was vortexed briefly and maintained on ice for 15min. The treated cells were centrifuged at 11500rpm (Eppendorf Centrifuge 5424) at 4°C for 10minutes. 500 μ l of the supernatant was transferred to a new tube and kept on ice. This fraction represents periplasmic protein. The remaining, intact cell pellet was washed twice with 1ml buffer A2X and then resuspended in 1ml of the same buffer. The cells were lysed by sonication twice at 60V for 10sec with a 2min pause on ice in between. The lysate was centrifuged at 4°C at maximum speed and 500 μ l of the supernatant was transferred to a new tube and maintained on ice. This fraction represents the total protein. The identity of each protein fraction, periplasmic and total, was confirmed via enzyme assays using glucose-6-phosphate dehydrogenase (cytoplasmic localization (71)) and alkaline phosphatase (periplasmic localization (62)). The assays were performed at 37°C for 1hr in a total volume of 200 μ l. The substrates used were *para*-nitrophenyl phosphate (Sigma) for the alkaline phosphatase enzyme and glucose-6-phosphate/NADP⁺ (Sigma) for glucose-6-phosphate dehydrogenase (both substrates were in 50mM HEPES buffer, pH 7.4). The enzyme assays were quenched with 40 μ l 1M Na₂CO₃. *P. putida* wild-type as well as Δ *Alr* cultures at exponential and stationary growth phases were used to isolate periplasmic and total protein, which was subsequently used to determine Alr racemase activity according to Radkov and Moe (bio-protocol.org for a detailed protocol (104)). For

all enzyme assays, protein concentration was determined using the protein assay dye reagent from Bio-Rad.

Peptidoglycan isolation and composition analysis

Our method was adapted from Boniface, et al. (13) where it was used to demonstrate the presence of D-lys as part of the peptide stem of *Thermotoga maritima* peptidoglycan. Three 50ml LB cultures per strain (24hrs of shaking at 220rpm at 28°C) were harvested in 50ml tubes and resuspended in 5ml 20mM KH₂PO₄ (pH 7.2) with 1mM DTT. The cells were sonicated (ten cycles at 60V for 20s with 2min pause on ice in between each cycle) and Triton X-100 was added to 0.5% final concentration (v/v). The suspension was vortexed for 30s and incubated at 55°C for 30min. The treated lysate was centrifuged at 200,000 × g at 20°C for 20min (Beckman Coulter Optima L-100 XP; Type 70Ti rotor). The recovered pellet was rinsed four times with 1ml water without resuspension and then centrifuged once more using the same parameters. The pellet was resuspended in 1ml 0.1M ammonium acetate, pH 6.0. The pellet was broken using the pipette tip during resuspension, as the material becomes highly compacted after centrifugation. The resuspended pellet was incubated with 1mg/ml lysozyme (Research Product International) at 37°C with shaking (220rpm) for 2.5hrs. After incubation, the mixture was centrifuged at 18,000 × g for 10min and transferred to a new tube. Two volumes of cold acetone were added, the mixture was vortexed for 30s and then centrifuged at 18,000 × g. The entire supernatant was transferred to a glass vial and evaporated overnight under air. The remaining solid was resuspended in 900µl 6M HCl, transferred to a polypropylene 2ml microfuge tube and incubated at 95°C in a hot plate for 12-16hrs. After hydrolysis, the solution was cooled to room temperature and added to 900µl 6M NaOH. The resulting solution was derivatized using Marfey's reagent (Sigma) and analyzed via HPLC (103, 104). The elution time of each detected peak was compared to an authentic AA standard derivatized and analyzed in the same manner as the sample.

Gene expression analysis

Wild-type and $\Delta a/r$ 5ml LB cultures were started from an isolated colony on LB medium. After incubating for 24hrs, 100-fold dilution was performed to prepare fresh 1ml LB cultures of each strain. Three biological replicates were included for each strain. After incubating for 6hrs at 28°C with shaking, RNA was isolated from each culture using the RNeasy mini kit (Qiagen) according to manufacturers instructions. cDNA libraries were prepared using an established protocol (53). Briefly, 2000ng RNA was treated with DNase I (Invitrogen) in order to remove any residual genomic DNA. The samples were then treated with the rRNA RiboMinus kit (Invitrogen) according to the manufacturer's instructions to remove 16S and 23S rRNA. The treated RNA was subsequently purified using the RNeasy mini kit (Qiagen). The RNA was analyzed on a 2% agarose gel before and after each of the above treatments. SMARTSCRIBE Reverse Transcriptase (Clontech) was used for cDNA synthesis. Superase•In was used

as RNase inhibitor (LifeTechnologies). The following primers were used for the construction of each library: Reverse Transcription primer was 5'-ACACTCTTTCCCTACACGACGCTCTTCCGATCTXXXNNNNNN-3' (XXX symbolizes the space of the sample barcodes - WT1-CCA, WT2-GTG, WT3-AAT; $\Delta alr1$ -TGC, $\Delta alr2$ -CGG, $\Delta alr3$ -GAA, while NNNNNN symbolizes random hexamer) and template-switching primer was CGGTCTCGGCATTCCTGCTGAACCGCTCTTCCGATCTGG+G (the last position is occupied by a locked nucleic acid moiety). Following cDNA synthesis the samples were purified using AMPure magnetic beads (Beckman Coulter). Lastly, the cDNA was enriched using Phire Taq polymerase (Thermo-Fischer) and the following Illumina-specific PCR primers 5'-AATGATACGGCGACCGAGATCTACTCTTTCCCTACACGACGCTCTTC CGATCT-3' and 5'-CAAGCAGAAGACGGCATAACGAGATCGGTCTCGGCATTCCTGCTGAACCGCT CTTCCGATCT-3'. Each library was finally assessed on 2% agarose gel and the number of PCR cycles was varied until a smear was obtained in the 200-500 base pair size. AMPure magnetic beads (Beckman Coulter) were used to purify the enriched cDNA samples. cDNA quantification, library pooling, and the MiSeq sequencing were performed by the Advanced Genetics Technologies Center at University of Kentucky. Gene expression analysis was conducted using the CLC Genomics Workbench software (CLC bio, Qiagen).

Growth assays

A collection of 21 D-AAs and their corresponding L-stereoisomers were used to determine the growth profile for *P. putida* KT2440 and Δalr strains. Each AA was tested as the sole source of C and N, or as the sole source of N (in this case, 20mM glucose was supplied as the C source). Sterile PG minimal medium (phosphate plus glucose) was employed as the base medium (119). The final AA concentration was 25mM except for Tyr, used at 2.5mM due to limited solubility. The assays were performed in 96-well microplates (CytoOne; Flat bottom, polystyrene) in 200 μ l volume maintained at 28°C with shaking (220rpm). For each AA, three replicates were prepared and an uninoculated well was included as a growth control. Each replicate was inoculated using 1 μ l of an overnight culture in LB washed twice with sterile PG containing no N or C source. Absorbance measurements at 600nm were performed using a plate reader (Biotek Synergy HT) after 24, 48, and 72hrs. The uninoculated wells for each AA were used as a blank. After collecting the necessary data, direct PCR using seq_down and seq_up primers verified that each culture contained the appropriate strain (Δalr or wild type *P. putida* KT2440) according to the PCR band size.

Phenotype rescue assays

This experiment was conducted to elucidate a possible indirect role of the Alr enzyme in the synthesis of any AA (D- or L-enantiomer) necessary for normal growth of *P. putida* KT2440. Using PG medium (glucose and ammonium

chloride) without any additional AAs, the growth profile of the wild-type and mutant strain was determined. 5ml PG cultures were inoculated using isolated colonies from either strain grown on LB agar and the cultures were incubated at 28°C with shaking for 12, 24, 30, 36, and 48hrs. The absorbance at 600nm was determined at the end of each incubation period using a plate reader (Biotek Synergy HT). Three biological replicates were included with three technical replicates each. Based on these results, similar growth assays were conducted with the wild-type and $\Delta a/r$ strain to test which AA would rescue the growth discrepancy observed after 30hrs of incubation. The same PG medium was used (glucose and ammonium chloride), however each of the available 21 AAs was also supplemented at 1mM final concentration.

Analysis of total cellular AA concentration

The wild-type and $\Delta a/r$ strain were grown as above in liquid PG medium with glucose and ammonium chloride as C and N sources. Total cellular AAs were extracted at the peak of log phase for the wild-type and $\Delta a/r$ strain. The absorbance at 600nm was ~2.5 for each strain which would allow for proper comparison of the total cellular AA concentration. The entirety of each 5ml PG culture was pelleted and washed twice with 0.9% NaCl before resuspending with 200 μ l MeOH and incubating at 70°C for 30min (108). Following that, the cell debris was pelleted via centrifugation and the supernatant was stored at -20°C. The AA content of the MeOH supernatant was analyzed via HPLC according to Radkov and Moe (bio-protocol.org for a detailed protocol (104)).

Chapter Four: Abundance and diversity of rhizosphere-dwelling bacteria catabolizing D-amino acids

Background and Introduction

Each of the 19 chiral L-amino acids (L-AAs) used in protein synthesis has a mirror image counterpart which is inverted about the α -carbon. These non-proteinogenic AAs are collectively known as D-amino acids (D-AAs). Recent studies have demonstrated the abundance of D-AAs in microbe-rich environments such as the animal rumen, fermented foods, and soil (18, 20, 63, 113, 131). Their origin is typically attributed to bacteria because bacteria are known to employ D-AAs in the synthesis of peptidoglycan, as well as other extracellular polymers such as poly- γ -glu and teichoic acids (102). Additionally, diverse D-AAs are synthesized by bacteria yet the reasons for this are mostly unknown. Nonetheless, D-AAs have been shown to affect certain physiological processes in bacteria such as biofilm formation, sporulation, and cell wall modification (70, 72, 114), all of which are important for survival under highly variable physicochemical conditions such as those found in soil.

The region of soil directly surrounding plant roots (rhizosphere) harbors a diverse chemical milieu owing to plant root exudation, and is known as a hotspot for microbial activity. Some of the available nutrients that lure high numbers of bacteria to this environment are L-AAs, a prominent component of plant root exudate (81). Interestingly, L-AAs not only serve as potential sources of carbon and nitrogen for rhizobacteria but also can induce chemotaxis and affect root colonization in model-rhizosphere bacteria such as *Pseudomonas fluorescens* (100) and *Pseudomonas putida* KT2440 (89). D-AAs are synthesized from their corresponding L-AA through enzymatic racemization. Racemization can be done for a number of reasons, including as part of an L-AA catabolic pathway (102). While L-AA catabolism is an appreciated trait of soil- and rhizosphere-dwelling bacteria, little is known about the bacterial capacity for D-AA catabolism.

Results

Enumeration of rhizobacteria catabolizing D-AAs

Table 4.1 shows CFU counts for both L-AAs and D-AAs from both environments. Not only were colonies obtained on all D-AA plates, in many cases the CFU counts were very similar (or greater) on D-AA plates compared to their L-AA counterparts. It is perhaps not surprising that central metabolic intermediates such as the L-enantiomers of glu and asp (as well as their amides gln and asn), and ala are the most commonly utilized substrates. Further, D-ala and D-glu are typically the most abundant D-AAs in microbe-rich environments due to their universal inclusion in peptidoglycan (130), and might be expected to be routinely catabolized. Additionally, ala, glu, gln, asn, and asp are the most abundant D-AAs in the tissues of different plant species (19, 131), including maize, and consequently may be available in the soil by virtue of exudation or decomposition. Moreover, in instances where the concentration of D-AAs has

been determined in agricultural soil samples, D-ala, D-asp, and D-glu were the most abundant D-AAAs (19).

We calculated two parameters to assess the variation in growth between AA enantiomer pairs for each soil sample. Both the difference (L - D) and ratio (L / D) between L-AAAs and D-AAAs are shown in Table 4.1 and are meant to identify those AA enantiomer pairs with both the greatest and smallest differences in CFU counts. Significant differences ($p < 0.05$) between L-AA and D-AA counts are noted by black shading in the table. For both environments, L-glu, L-asn, L-his conferred significantly higher number of CFUs and the number of isolates was from two- to four-fold higher on those L-AAAs relative to their D-AA counterparts (Table 4.1, highlighted cells). Additionally, *trans*-L-hypro, L-ile, and L-asp had the same effect only for the rhizosphere soil, while significantly more bulk soil isolates were on plates containing L-ala and L-arg. Differences in CFU counts between other AA enantiomers were not statistically significant.

Table 4.1 Number of isolates at 10⁻⁵ soil dilution on each tested AA enantiomer.

AA	Rhizosphere soil				Bulk soil			
	L	D	L - D	L / D	L	D	L - D	L / D
Ala	58 ± 12	62 ± 4	-4	1	42 ± 5	26 ± 2	17	2
Arg	50 ± 11	43 ± 7	7	1	40 ± 7	24 ± 5	16	2
Asn	75 ± 6	32 ± 10	43	2	43 ± 3	28 ± 4	15	2
Asp	80 ± 5	50 ± 10	30	2	64 ± 8	53 ± 7	11	1
Cys	28 ± 10	21 ± 2	7	1	21 ± 2	16 ± 6	5	1
Gln	62 ± 14	53 ± 6	9	1	55 ± 6	47 ± 8	8	1
Glu	80 ± 8	18 ± 9	62	4	51 ± 7	11 ± 1	40	5
His	43 ± 10	11 ± 3	32	4	28 ± 2	13 ± 3	15	2
Hypro	64 ± 9	27 ± 9	36	2	26 ± 5	19 ± 3	7	1
Ile	66 ± 5	35 ± 10	30	2	38 ± 3	22 ± 11	16	2
Leu	57 ± 5	39 ± 8	18	1	31 ± 5	26 ± 3	5	1
Lys	22 ± 4	32 ± 10	-9	1	20 ± 4	17 ± 4	3	1
Met	21 ± 9	26 ± 5	-4	1	39 ± 9	40 ± 6	-1	1
Orn	46 ± 6	27 ± 12	19	2	41 ± 3	32 ± 15	9	1
Phe	45 ± 17	39 ± 1	6	1	24 ± 7	21 ± 9	3	1
Pro	67 ± 3	71 ± 2	-3	1	30 ± 11	19 ± 4	11	2
Ser	38 ± 14	22 ± 6	16	2	36 ± 7	29 ± 5	7	1
Thr	41 ± 11	48 ± 13	-7	1	41 ± 8	27 ± 7	14	2
Trp	31 ± 3	25 ± 5	6	1	27 ± 7	20 ± 3	8	1
Tyr	42 ± 4	28 ± 9	14	2	27 ± 7	34 ± 9	-7	1
Val	24 ± 7	30 ± 6	-6	1	39 ± 11	36 ± 3	3	1

The average number of isolates is shown (L and D) with standard deviation. The highlighted cells indicate the enantiomer pairs that had significantly different average values ($p < 0.05$). The relative abundance of isolates from the rhizosphere soil, as well as bulk soil, was calculated by subtracting the number of isolates counted on D-AA plates from those on L-AA plates for each AA pair (shown in column "L - D"). The ratio of isolates counted on L-AA plates and D-AA plates is shown in column "L / D".

Phylogenetic identification of bacterial isolates

Sequences were grouped into four phyla (*Actinobacteria*, *Proteobacteria*, *Bacteroidetes*, and *Firmicutes*; Table 4.2), 7 classes, 12 orders, 27 families, and 46 genera. Most (92%) of the isolates fell within three classes: *Actinobacteria*, α -*Proteobacteria*, and β -*Proteobacteria*. The most notable result from taxonomic assignment of the cultured isolates was the abundance of *Arthrobacter* species (32% of the total isolates). Isolates within this genus were able to use 18 of the tested 21 AA enantiomer pairs as the sole source of carbon and nitrogen. Although there is little information in general on the *Arthrobacter* genus, they are metabolically versatile (121) and have been noted as common inhabitants of soils as well as extreme environments (deep subsurface, arctic ice, and sites contaminated with radioactivity or hazardous chemicals) (92). Previous work on 26 soil isolates from the genus *Arthrobacter* shows that 90% or more of them were able to catabolize D-ala in addition to other L-AAAs (58). Additionally, *Arthrobacter protophormiae* (DSM15035) catabolizes D-phe, D-leu, and D-met (42), and a D-AA oxidase enzyme from this organism was shown to exhibit the highest activity with D-met, D-lys, D-arg, and D-phe. The metabolic versatility previously noted among members of this genus appears to extend to D-AAAs.

Among the most frequently isolated genera in the α -*Proteobacteria* class, *Ensifer* and *Rhizobium* are very closely related (family *Rhizobiaceae*) and belong to the diverse group of plant-nodulating nitrogen-fixing bacteria known as rhizobia. Several of the isolated rhizobia species used both enantiomers of pro, orn, trp, and val as the sole source of carbon and nitrogen. Three genera in the α -*Proteobacteria* class used D-pro as the sole source of carbon and nitrogen (the only other genus that achieved that was *Arthrobacter*).

All of the 13 identified genera within the β -*Proteobacteria* class belong to the order *Burkholderiales*. Although most of the known plant-nodulating bacteria belong to the α -*Proteobacteria* class, recently many isolates part of the β -*Proteobacteria* class, and specifically the order *Burkholderiales*, have been identified as new symbionts of legumes (28, 94). The highest number of genera within the β -*Proteobacteria* class was identified on either enantiomer of phe, as well as gln and ala. While there were four genera in the β -*Proteobacteria* class, there was only one other genus (*Arthrobacter*) capable of using D-phe (Table 4.2).

Despite that a large proportion of the identified isolates were part of the three major taxonomic classes discussed above, we identified several genera from the γ -*Proteobacteria* class and the δ -*Proteobacteria* class, as well as class *Sphingobacteria* and class *Bacilli* (Table 4.2). Based on the data presented here, a variety of rhizosphere-dwelling bacteria have the capacity to catabolize D-AAAs as the sole source of carbon and nitrogen. Our study provides the basis for future work aiming to understand the impact of D-AAAs on the bacterial community in the rhizosphere. More specifically, it would be interesting to determine the relative

abundance in the rhizosphere of the identified bacteria and also whether they represent a significant portion of the rhizosphere community.

Table 4.2 Phylogenetic analysis of isolates that catabolized individual L - and D-AA enantiomer pairs as the sole source of carbon and nitrogen				
Phylum	Class	Genus	No of seq for that genus	Amino acids from which isolates were recovered
Actinobacteria	Actinobacteria	Arthrobacter	53 (32 % of total)	ala, arg, asn, asp, cys, glu, gln, his, hypro, ile, lys, orn, phe, pro, ser, thr, trp, tyr
Actinobacteria	Actinobacteria	Microbacterium	9 (5 % of total)	cys, his, orn, ser, trp, tyr
Actinobacteria	Actinobacteria	Terrabacter	3 (2 % of total)	asp, leu, tyr
Actinobacteria	Actinobacteria	Cellulosimicrobium	2 (1 % of total)	met, trp
Actinobacteria	Actinobacteria	Agromyces	2 (1 % of total)	his
Actinobacteria	Actinobacteria	EU019987_s_LAM22	1 (1 % of total)	ser
Actinobacteria	Actinobacteria	GQ396982_s_AK1DE1_06H	1 (1 % of total)	val
Actinobacteria	Actinobacteria	Nocardioides	1 (1 % of total)	orn
Actinobacteria	Actinobacteria	Rhodococcus	2 (1 % of total)	thr
Actinobacteria	Actinobacteria	Streptosporangium	1 (1 % of total)	cys
Actinobacteria	Actinobacteria	Streptomyces	4 (3 % of total)	met
Actinobacteria	Actinobacteria	Micromonospora	2 (1 % of total)	met
Actinobacteria	Actinobacteria	Promicromonospora	1 (1 % of total)	thr
Proteobacteria	α -Proteobacteria	Ensifer	7 (4 % of total)	ala, glu, pro, trp, tyr, val
Proteobacteria	α -Proteobacteria	Rhizobium	6 (4 % of total)	gln, lys, orn, pro, val
Proteobacteria	α -Proteobacteria	Pseudaminobacter	4 (3 % of total)	orn, ser, trp
Proteobacteria	α -Proteobacteria	Sphingopyxis	3 (2 % of total)	his, leu, lys
Proteobacteria	α -Proteobacteria	Bosea	2 (1 % of total)	his, val
Proteobacteria	α -Proteobacteria	Candidatus Rhizobium	2 (1 % of total)	glu, ile
Proteobacteria	α -Proteobacteria	Mesorhizobium	2 (1 % of total)	his, hypro
Proteobacteria	α -Proteobacteria	Ochrobactrum	2 (1 % of total)	asn, pro
Proteobacteria	α -Proteobacteria	Ancylobacter	1 (1 % of total)	cys
Proteobacteria	α -Proteobacteria	Azospirillum	1 (1 % of total)	tyr
Proteobacteria	α -Proteobacteria	Devosia	1 (1 % of total)	asp
Proteobacteria	α -Proteobacteria	Shinella	1 (1 % of total)	asn
Proteobacteria	α -Proteobacteria	Sphingobium	1 (1 % of total)	ile
Proteobacteria	α -Proteobacteria	Sphingomonas	1 (1 % of total)	orn
Proteobacteria	α -Proteobacteria	Bradyrhizobium	1 (1 % of total)	thr
Proteobacteria	β -Proteobacteria	Pseudoduganella	7 (4 % of total)	ala, arg, asn, hypro, thr
Proteobacteria	β -Proteobacteria	Mitsuaria	4 (3 % of total)	ala, his, orn, phe, val

Proteobacteria		Cupriavidus		4 (3 % of total)		ala, gln, phe	
Proteobacteria	β -Proteobacteria	Pelomonas		4 (3 % of total)		gln, met, val	
Proteobacteria	β -Proteobacteria	AJ964894_s LF4-45		2 (1 % of total)		asp, phe	
Proteobacteria	β -Proteobacteria	Rivibacter		2 (1 % of total)		asn, ser	
Proteobacteria	β -Proteobacteria	Variovorax		3 (2 % of total)		phe, trp	
Proteobacteria	β -Proteobacteria	Achromobacter		1 (1 % of total)		glu	
Proteobacteria	β -Proteobacteria	Aquincola		1 (1 % of total)		cys	
Proteobacteria	β -Proteobacteria	DQ354711_s DR550SWSAEE7		1 (1 % of total)		gln	
Proteobacteria	β -Proteobacteria	Ideonella		1 (1 % of total)		ser	
Proteobacteria	β -Proteobacteria	Leptothrix		1 (1 % of total)		leu	
Proteobacteria	β -Proteobacteria	Massilia		3 (2 % of total)		leu	
Proteobacteria	γ -Proteobacteria	Pseudomonas		3 (2 % of total)		lys, pro	
Proteobacteria	γ -Proteobacteria	Moraxella		1 (1 % of total)		cys	
Proteobacteria	δ -Proteobacteria	Polyangium		2 (1 % of total)		ile, leu	
Bacteroidetes	Sphingobacteria	Chitinophaga		1 (1 % of total)		pro	
Firmicutes	Bacilli	Bacillus		7 (4 % of total)		ala, asn, gln, pro	

Methods

Culture-dependent enumeration of bacteria

Here we have conducted a culture-dependent experiment to catalog bacteria able to catabolize either of 21 AA enantiomer pairs, which includes the D- and L-enantiomers of the 19 chiral proteinogenic AAs as well as hydroxyproline (hypro) and ornithine. Soil samples were obtained from the University of Kentucky Horticulture Research Farm (Lexington, KY, USA). Soil was taken from the roots of uprooted, mature sweet corn plants (rhizosphere soil) and from a field left fallow (bulk soil), and approximately 2g of each was used to perform serial dilutions in Basal Minimal Media (BMM) without any source of carbon and nitrogen (54). L-AAs (one of 21 AAs, 1mM final concentration) or D-AAs (one of 21 AAs, 1mM final concentration) (Sigma-Aldrich) were added as the sole carbon and nitrogen source to BMM media, and cycloheximide (250 μ g/ml) (Sigma-Aldrich) was added to prevent fungal growth. Agarose, 1.5% (GeneMate, BioExpress), was used as a gelling agent instead of agar. From the 10⁻⁵ dilution of both samples, 100 μ L was spread evenly on each of 6 plates per AA (3 plates for rhizosphere and 3 for bulk soil) as well as dilute nutrient broth (DNB) plates (0.08g Difco nutrient broth per 1L of water (56)). BMM plates without carbon and nitrogen were also prepared to estimate non-specific bacterial growth. Plates were incubated at 28°C for two weeks before colony enumeration.

Identification of bacterial isolates based on 16S rRNA gene sequencing

To assess the D- and L-AA catabolism potential of a subset of the cultured isolates, we performed a colony restreak experiment. Colonies were picked from an L-AA plate and were subsequently patched onto a D-AA plate (corresponding to the L-AA plate from which the isolate was taken), as well as onto a fresh L-AA plate. Plates were incubated at 28°C for two weeks. For each of the 21 AAs, 12 isolates that demonstrated growth on both enantiomers were randomly selected and were used to inoculate DNB liquid cultures (2 ml) grown at 28°C with shaking at 220rpm for two weeks. At the end of the incubation period, glycerol stocks were prepared (25% final glycerol concentration) and the stocks were stored at -80°C. Each of the glycerol stocks was used to conduct a PCR targeting the 16S ribosomal RNA gene. PCRs contained DreamTaq 12.5 μ l (ThermoScientific), primer 27F (0.5 μ M final concentration; 5' AGAGTTTGATCMTGGCTCAG 3'), primer 1492R (0.5 μ M final concentration; 5' GGYTACCTTGTTACGACTT 3'), DNase/RNase free water 8 μ l, and 2 μ l of material from the individual glycerol stock. Cycling conditions were 95°C for 4min, 95°C for 30s and 55°C for 30s and 72°C for 90s repeated 35 times, and finally 72°C for 10min. PCR products were purified using AMPure Magnetic beads (Beckman Coulter) and 50-100 ng of the amplicon DNA was used to perform Sanger sequencing using a cycle sequencing kit (BigDye Terminator, v3.1, cycle sequencing kit; Applied Biosystems). The sequencing reactions were purified via AgenCourt CleanSeq magnetic beads (Beckman Coulter) and submitted to the Advanced Genetic

Technologies Center at University of Kentucky. Sequencing data were analyzed through the Ez-Taxon 16S rRNA database (65) to obtain the appropriate phylogenetic classification of each environmental isolate. Overall, 65% (163 isolates) of the collection of 252 isolates was identified to the species level. Of the 12 isolates for each AA, between 5 and 11 isolates per AA provided sequencing data of sufficient quality to obtain taxonomic information.

Chapter Five: Conclusion

The general goal of this dissertation is to contribute to our understanding of D-AAs in nature. We have built upon the already established knowledge in bacteria primarily because they have been shown to synthesize and catabolize a wide range of D-AAs. The majority of my work has focused on the model rhizosphere-dwelling bacterium *P. putida* KT2440 and the involvement of D-AAs in its metabolism. The plant rhizosphere is a densely populated environment due to the high abundance of root exudates. Additionally, it has been established that high concentrations of D-AAs accumulate in such bacteria-rich habitats. As a result, it is likely that many bacteria, and in particular *P. putida* KT2440, have developed an ability to utilize D-AAs as nutrients. Surprisingly, this aspect of bacterial physiology has remained largely unexplored. Only recently have there been interesting research towards unveiling the roles of D-AAs in bacterial physiology, such as their roles as intermediates in essential biochemical pathways, as well as their role as signals in major physiological processes. We hope that our research would stimulate further advances in the area of D-AA research.

Although it has been demonstrated that *P. putida* KT2440 can catabolize several D-AAs, the underlying genes and enzymes have never been characterized. In Chapter 2, a novel method was developed to identify the involved genes and subsequently characterize the encoded enzymes. The products of the enzyme activity assays were analyzed using Marfey's reagent and HPLC – an approach that had not been previously used. Three novel AA racemase enzymes were characterized biochemically – Alanine racemase Alr (acts on arg, lys, and several other AAs), Alanine racemase DadX (acts on ala), and Proline racemase (acts on the four epimers of hypro). One of the intriguing findings was the inappropriate annotation of two enzymes. Based on our results, the Alanine racemase Alr should be renamed as a broad-spectrum AA racemase, while the Proline racemase – Hydroxyproline epimerase. Furthermore, it was established that the Alr enzyme is highly conserved among *P. putida* strains but closely related enzymes are absent from other phylogenetic clades. This peculiar result led to the work presented in Chapter 3 in which the physiological role of the Alr enzyme was elucidated. A markerless deletion of the *alr* gene was established via homologous recombination that allowed us to conduct a number of phenotypic assays with the wild-type and the *alr* knockout strain. A major discovery was that the lack of an enzyme that interconverts L- and D-AA stereoisomers impacted the growth of the mutant strain with several L-AAs as the sole carbon and nitrogen source, including L-lys, L-arg, and L-ornithine, but not the ability of the strain to catabolize the corresponding D-enantiomers. Based on the bradytrophic growth of the knockout strain with L-ornithine, we postulated that the mutant is not synthesizing sufficient L-pro because the only pathway for L-ornithine catabolism in *P. putida* KT2440 is via L-pro. In further support of this result, the knockout strain exhibited bradytrophic growth in the presence of glucose and ammonium chloride (without any other AA supplement) in comparison to the wild-type strain, suggesting the lack of an essential nutrient in

the *alr* mutant. The delay in growth by the mutant strain was rescued after the addition of L-pro, as well as D-ornithine. In addition, it was also determined via Next-Gen sequencing and RNA-seq analysis that the genes involved in the D-lys catabolic pathway were more highly expressed in the wild-type strain relative to the mutant. Considering our results as a whole, we have proposed a model whereby D-ornithine has a key role not only in L-ornithine catabolism but also in L-pro synthesis. This is a novel finding because such an interconnection between L- and D-AAAs has not been demonstrated before.

The last research portion of the dissertation, Chapter 4, focuses on the community of rhizosphere-dwelling bacteria and their capacity for D-AA catabolism. As mentioned earlier, it is known that D-AAAs are abundant in bacteria-rich environments such as the rhizosphere, however, the ability of rhizobacteria to catabolize D-AAAs has not been tested in the past, except for model species such as *P. putida* KT2440 and *Bacillus subtilis*. We established a culture-dependent approach that allowed us to cultivate bacteria from sweet corn rhizosphere soil using individual D-AAAs as the sole source of carbon and nitrogen. D-Stereoisomers conferred growth to a multitude of bacteria and in some cases, the number of isolates approached that observed with the corresponding L-AA (for example, D-thr, D-pro, D-val, and D-lys). Furthermore, several isolates from each D-AA were preserved as glycerol stocks and were identified down to the species level after 16S rRNA amplicon sequencing. The three most highly represented phylogenetic clades were *Actinobacteria*, α -*Proteobacteria*, and β -*Proteobacteria*. In fact, isolates of the genus *Arthrobacter* collectively catabolized 18 of the tested 21 D-AAAs. Although our results are preliminary, we believe it clear that D-AA catabolizers are abundant in the rhizosphere and they should be further studied in order to assign their specific ecological place.

Although the focus of my dissertation is D-AA catabolism, it is likely that most D-AAAs do not serve as a major nutrient in the rhizosphere, and probably in other comparable environments, but rather act as pathway intermediates or signals. In addition to our finding of D-ornithine as a central metabolite, other D-AAAs such as D-ala, D-hypro, and D-glu are known to have key biosynthetic and catabolic roles. Furthermore, recent evidence has established that D-AAAs trigger major processes in bacteria, including biofilm disassembly, cell wall remodeling, and sporulation. As a next step, we would like to focus on the capacity of D-AAAs to serve as chemoattractants. This is a well-studied phenomenon with regards to L-AAAs (111), however, it has not been explored before with D-AAAs despite that D-stereoisomers should have a generally longer life-time relative to their L-counterparts. Furthermore, it appears likely that D-AAAs should serve such a role based on their abundance in bacteria-rich environments. From an ecological viewpoint, it would be advantageous if a bacterium has the ability to sense D-AAAs as that would equip it with an additional response mechanism to a constantly changing environment.

Appendix A: Genes involved in D-arg catabolism by *P. putida* KT2440

Background and Introduction

While it has been established that *P. putida* KT2440 can catabolize D-AAs, (D-arg, D-lys, D-phe, D-arg, D-ala, and *cis*-D-hydroxyproline) as the sole source of carbon and nitrogen, the catabolic pathway for most of these D-AAs is not known. Furthermore, in *P. aeruginosa* PAO1, catabolism of D-arg is initiated by conversion to L-arg via the coupled dehydrogenases DauA and DauB part of DauBAR operon (73). However, the route appears to differ in *P. putida* KT2440 based on genomic comparison suggesting that *P. putida* KT2440 encodes neither DauA nor DauB (103). We planned to identify potential enzyme(s) encoded by the genome of *P. putida* KT2440 that could act on D-arg and allow the strain to catabolize this AA.

During this project, a screening methodology was developed to identify genetic determinants involved in D-arg catabolism. More specifically, eight regions of the *P. putida* KT2440 genome were identified using an arg auxotrophic strain. Four contained enzyme(s) that were obvious candidates based on their bioinformatics annotation found in the Pseudomonas Genome Database. These candidates are alanine racemase (PP_3722), short chain dehydrogenase (PP_2723), succinate dehydrogenase (PP_4191), 2-oxoglutarate dehydrogenase (PP_4189), and amino acid ABC transporter/permease (PP_0927). Although there is partial evidence suggesting that two of the genes (PP_3722 and PP_2723) act on D-AAs and are involved in processes in the rhizosphere, further work is necessary to explore the ability of the identified genes to act on D-arg and other D-AAs, as well as their potential to mediate plant-microbe interactions in the rhizosphere.

Results

Selection of positive clones

Six plates of minimal media with D-arg (1mM) were prepared. A total of 1-2 million library clones were inoculated on each plate and between 100-200 showed growth. In order to confirm the true positives (those clones that can survive only in the presence of D-arg but not in its absence) a total of 300 colonies were restreaked on plates with and without D-arg. From these 300 clones, 150 required D-arg for growth.

Confirmation of positive clones via sequencing

72 of the confirmed clones were miniprep then sequenced. The remaining 78 were maintained at -80°C but were not sequenced due to time constraints. Of the 72 sequenced, 8 came back with DNA sequences that matched part of the *P. putida* KT2440 genome. There are several reasons that could have led to the lack of sequencing data from the majority of our clones such as contamination, kit (miniprep and sequencing) malfunctions, and errors at the AGTC. Some of these issues could be addressed in future studies. In the

current study, genes contained within the 8 identified regions were explored using bioinformatics tools.

DNASTar software package was used to analyze the DNA sequences and the sequence of each genomic region was put into the Pseudomonas Genome Database to find the exact location. Figure A.1 shows the entire *P. putida* KT2440 genome and the location of the 8 regions we found.

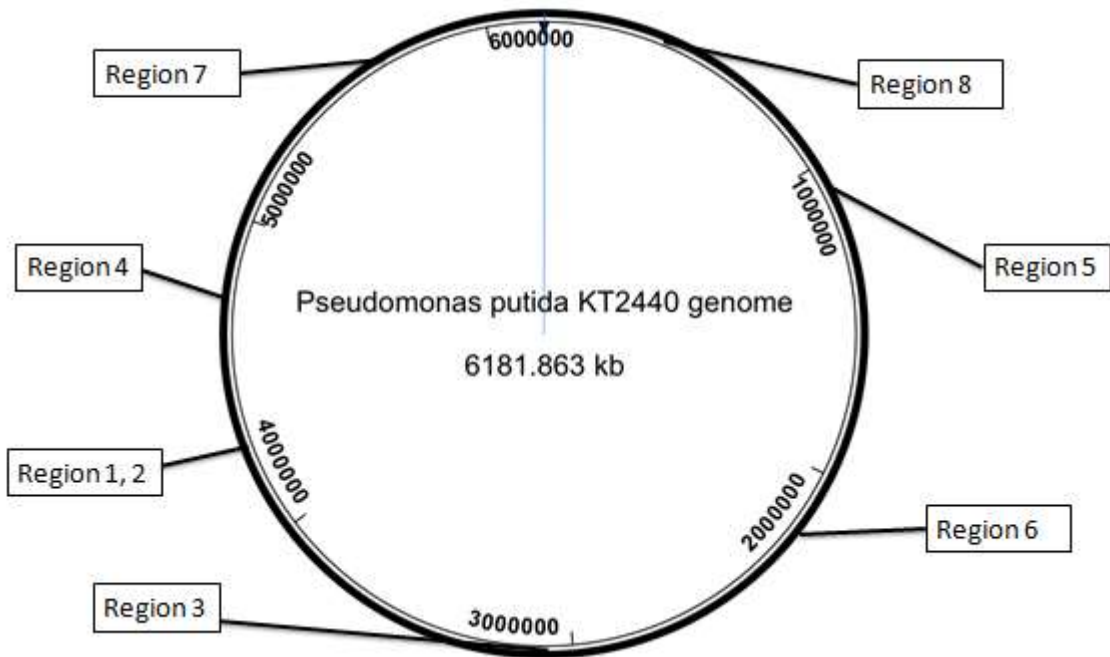


Figure A.1 *P. putida* KT2440 genome. The location of each identified region is labeled.

Identification of relevant regions

Four of the identified eight regions are shown in figure A.2. Each panel shows the location of the region on the genome and the annotated genes and corresponding proteins. The region in panel A was identified from two individual clones and the remaining three regions were not included in the figure. The reason is that we were not able to select potential gene candidates involved in D-arg catabolism simply based on bioinformatics annotation. In future studies, we plan to subclone multiple genes from these three regions and test if they have a role in D-arg catabolism.

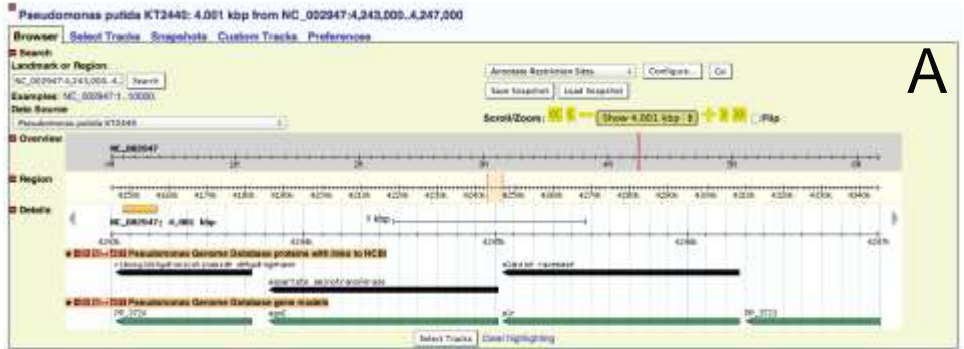
Figure A.2 panel A shows a region located between 4.2M and 4.3M bases on the *P. putida* KT2440 genome. The region is approximately 4kb in length and contains 4 ORFs (from PP_3720 to PP_3723) one of which is annotated as alanine racemase (*alr*, PP_3722). This enzyme has been identified before and tested with a collection of 21 D-AAs (103). The enzyme exhibited most activity with lys and arg but it also acted on a number of other AAs such as met, leu, ala, gln, and ser. Based on the information presented in that paper, it was concluded that the enzyme is mislabeled. It was suggested that the name were changed to broad-spectrum AA racemase. The finding of the *alr* gene in our screens and the prior evidence suggest that this broad-spectrum AA racemase is likely involved in D-arg catabolism in *P. putida* KT2440. It also establishes the credibility of our screening approach. We are planning to subclone the *alr* gene and test its ability to catabolize D-arg using the *E. coli* arg auxotrophic strain. Additionally, the function of the *alr* gene *in vivo* will be the target of future experiments.

Panel B shows a region approximately 5kb in length and located at approximately 3.1M bases on the *P. putida* KT2440 genome. Although the region contains 8 annotated ORFs, based on bioinformatics it appears that the most likely protein involved in D-arg catabolism is the short chain dehydrogenase (PP_2723). In a recent 2013 publication, this protein was induced in *P. putida* KT2440 when this organism was grown in the rhizosphere of evergreen oak (39). Consequently, this dehydrogenase may play a specific role in that environment which suggests that D-AAs may affect plant-microbe interactions. A second paper that was published on *P. putida* KT2440 has found that this gene (PP_2723), as well as a few others, show homology to typical nodule-related proteins found in other rhizosphere microorganisms (83). While there is no experimental evidence of root nodulation induced by *P. putida* KT2440, there is a need to understand the role of this gene in the rhizosphere. Although there is available research on the short chain dehydrogenase gene, little is known about the biochemical function of the encoded enzyme. We would like to subclone the gene and test its ability to rescue the arg auxotrophic phenotype of the *E. coli* strain used in our screen. As a long-term goal, the enzyme would be tested with a collection of D-AAs to determine its substrate specificity.

Panels C and D show two identified genomic regions with a potential role in D-arg catabolism. Each region contains 4 and 7 ORFs, respectively. Some of the genes encode proteins annotated as succinate dehydrogenase, 2-oxoglutarate dehydrogenase, and amino acid ABC transporter/permease. It is

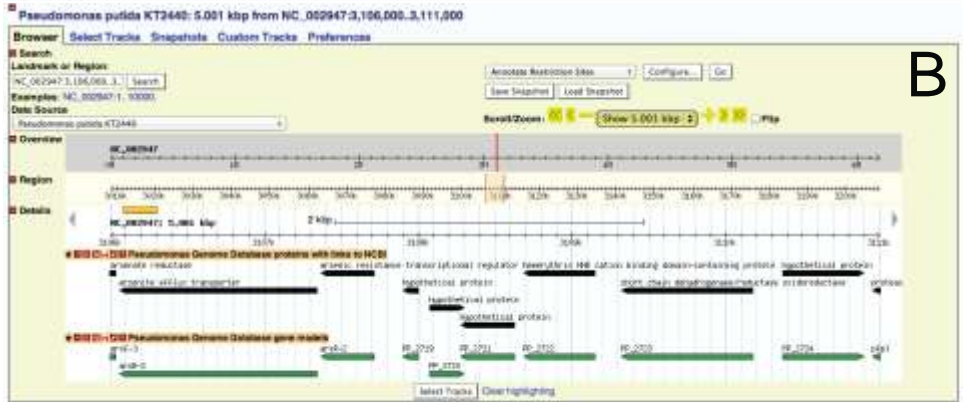
difficult to state which specific enzyme may have a role in D-arg catabolism only considering the bioinformatics annotations. Dehydrogenases are enzymes that can act AAs to produce an α -ketoacid after removing the amino group of the α -carbon. Additionally, an amino acid ABC transporter may include several domains that would allow the enzyme to act on AAs and simply transport them. Moreover, multiple genes are likely mislabeled or labeled too broadly, or too narrowly, and may have a very different function than the assigned one based on homology. In future experiments, we would subclone each of the above three genes to test their role in D-arg catabolism before targeting some of the other genes contained on the regions in panels C and D.

After conducting preliminary enzyme assays, it was determined that the dehydrogenase enzyme encoded by PP_2246 showed the highest activity with both enantiomers of tyr. A number of other AAs served as substrates. Tyr is very insoluble at physiological pH (~0.4mM) and consequently it is difficult to make comparisons between enzyme activity conferred by tyr and other AAs. The dehydrogenase enzyme encoded by PP_2723 showed the highest activity with both enantiomers of arg but it also acted on other substrates. This result confirms our previous finding that PP_2723 can rescue the mutant phenotype of an arg auxotrophic *E. coli* strain. Furthermore, it is common for dehydrogenase/oxidoreductase enzymes to act on a wide range of substrates. There are several well-characterized D-AA dehydrogenases that display a similar broad-substrate specificity as the enzymes we have described (102). Additional research will be needed, such as genetic knockout studies, to elucidate the physiological role of the identified enzymes.



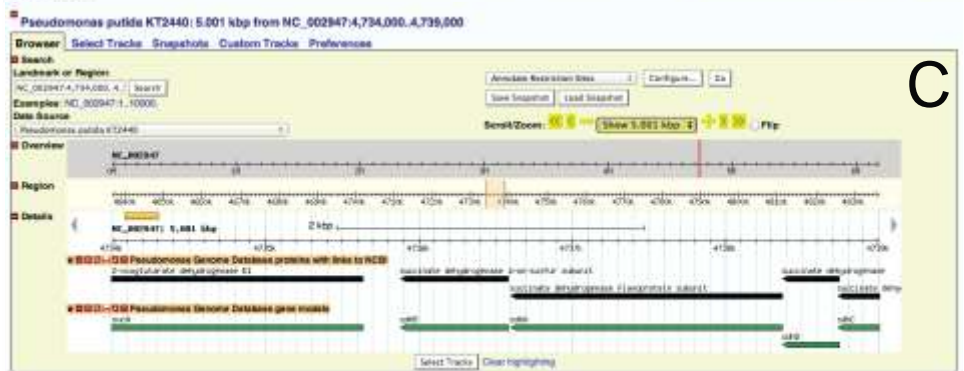
A

The Genetic Genome Browser. For questions about the data at this site, please contact its webmaster. For support of the browser software only, send email to genod-browser@lists.sourceforge.net or visit the GMOD Project web pages.



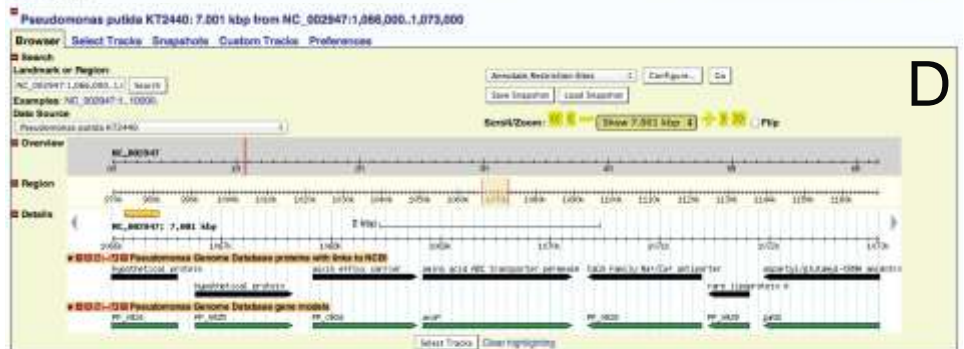
B

The Genetic Genome Browser. For questions about the data at this site, please contact its webmaster. For support of the browser software only, send email to genod-browser@lists.sourceforge.net or visit the GMOD Project web pages.



C

The Genetic Genome Browser. For questions about the data at this site, please contact its webmaster. For support of the browser software only, send email to genod-browser@lists.sourceforge.net or visit the GMOD Project web pages.



D

The Genetic Genome Browser. For questions about the data at this site, please contact its webmaster. For support of the browser software only, send email to genod-browser@lists.sourceforge.net or visit the GMOD Project web pages.

Figure A.2 Four of the identified regions from D-arg screens, labeled A, B, C, D. Each region was obtained from the Pseudomonas Genome Database and

includes four sections. The Search section contains the exact genomic location as well as the region size. The Overview section shows the entire genome and the location of the specific region (red marking). The Region section provides a detailed view of the region location on the genome. The Details section shows the entire region of question, including an appropriate metric bar, and the annotated proteins and genes contained.

Methods

Construction of genomic library

A liquid culture of *P. putida* KT2440 was grown in 5mL of Luria-Bertani (LB) medium and its genomic DNA was extracted using the commercial kit GenElute (by Sigma-Aldrich). Once the DNA was extracted, it was fragmented using a HydroShear instrument (University of Kentucky Advanced Genetic Technology Center) Gel electrophoresis was performed to specifically select the 5-10kb DNA size.

The DNA was end-repaired using an end-repair kit (Invitrogen) to produce blunt-ended fragments used in the ligation reactions. Blunt-ended pUC19 was used as the vector, and was produced via PCR amplification. The pUC19 vector and DNA were placed in a tube with the ligase enzyme (Thermo Scientific) that incubated overnight to produce a library of random segments of the *P. putida* KT2440 genomic DNA.

Transformation into *E. coli*

E. coli strain JW2768-1 was purchased from the Coli Genetic Stock Center out of Yale University. This strain is an L-arg auxotroph. An electroporator (Bio-Rad) was used to transform the *P. putida* KT2440 genomic library into electrocompetent *E. coli* JW2768-1 cells. The transformed cells were incubated overnight with carbenicillin (50µg/ml), to select for cells containing the pUC19 plasmid. After incubation, a glycerol stock was prepared and stored at -80°C in a cryotube. This represented the genomic library used for screening.

Screening of library on D-arg

The *P. putida* KT2440 library was plated on minimal media containing D-arg. The media contained glucose as the carbon source and ammonium chloride as the nitrogen source. The *E. coli* AA auxotroph could not survive in the absence of exogenously supplied L-arg. However, D-arg was provided, thus allowing us to select for clones able to survive by converting D-arg into the L-enantiomer. The appropriate D-arg concentration for screening was determined by preparing several batches of plates with different D-arg concentrations and the final decision was to use 1mM. The plates were incubated at 28°C until growth was observed. Clones were selected for restreaking to confirm their phenotype.

Selection of clones

Clones that showed growth were then restreaked on plates with and without D-arg to select those that required D-arg and eliminate the false positives (clones that had lost the auxotrophic phenotype and could synthesize L-arg using the carbon and nitrogen sources on the plate). True positive clones would only grow on the plates with D-arg.

Isolation of plasmids, sequencing, and data analysis

Plasmid DNA was isolated from positive clones using the commercial kit GeneJET (ThermoScientific). After the plasmid DNA was isolated, the genomic fragments of the plasmids were sequenced to identify open reading frames (ORFs) that play a potential role in D-arg catabolism. Nucleotide sequences were obtained by Sanger sequencing using the BigDye Terminator Cycle Sequencing product (Applied Biosystems). These sequenced reactions were purified using AgenCourt CleanSEQ (Beckman Coulter), after which the DNA solution was provided to the University of Kentucky Advanced Genetic Technology Center for sequencing. The identified regions found were mapped onto the *P. putida* KT2440 chromosome (entire genome sequence is available via the Pseudomonas Genome Database) and a BLAST search was performed to look for ORFs that encode relevant enzymes.

Enzyme purification and preliminary assays

Two genes PP_2246 (identified in Chapter 2 from a screen on D-phe) and PP_2723 (identified here from D-arg screen) were subcloned into the overexpression vector pET28. His-tag mediated protein purification was conducted as described in Chapter 1. The developed enzyme assays for FAD-dependent dehydrogenase/oxidoreductase enzymes were based on previously established methods (49). As part of the enzyme assay buffer, FAD (0.2mM), Iodonitrotetrazolium chloride (INT; 0.8mM), Phenazine methosulfate (PMS; 0.8mM), and Tris-HCl (100mM, pH 8.7) were added. All concentrations are final. Based on bioinformatics analysis it was determined that the enzymes require FAD cofactor. The assays were conducted for 10min at 37°C in 500µl total volume. The enzyme concentration in each assay was 0.1µg/µl. The assays were quenched with 40µl 4M HCl and the absorbance at 500nm was measured using Biotek plate reader.

Appendix B: Chemotaxis towards D-AAs by *P. putida* KT2440

Background and Introduction

Chemotaxis is the swimming behavior bacteria display after sensing a chemical gradient in the environment. This behavior can drive motile bacteria (all of the *Pseudomonas* species are motile) towards or away from a stimulus. The model organism that has been used to establish much of our current chemotaxis knowledge is the enteric bacterium *Escherichia coli* (38). It has four transmembrane chemoreceptors called methyl-accepting chemotaxis proteins (MCPs) that are involved in relaying a received signal to the flagellar motor. The MCPs of *E. coli* can sense numerous stimuli including AAs, sugars, and dipeptides. Although there are many similarities between the chemotaxis system of *E. coli* and that observed for *Pseudomonas* species, it appears that there are several differences. While *E. coli* has only one set of chemotaxis genes in a single gene cluster, *Pseudomonas* species have multiple gene homologs organized in several unlinked gene clusters (47). Further, genome sequence analysis has revealed that *Pseudomonas* species have numerous putative MCP genes, 26 for *P. aeruginosa* PAO1, 27 for *P. putida* KT2440, and 49 for *P. syringae* (101). So far, most of our knowledge on chemotaxis in *Pseudomonads* comes from studies on *P. aeruginosa* PAO1 – over 75 chemoattractants have been identified and 13 of the 26 MCPs have been functionally characterized (101). Although *P. putida* and *P. aeruginosa* have a similar number of MCPs, most of the protein products show low AA sequence similarity (111). While most of the MCPs share between 30% and 70% AA sequence identity, three putative *P. putida* F1 MCPs have no obvious counterparts in *P. aeruginosa* PAO1. This observation likely reflects the fact that the two organisms inhabit different environmental niches and consequently have to respond to different attractants.

Pseudomonas putida strains show chemotaxis towards carboxylic acids (succinate, malate, acetate, butyrate, citrate, indole acetic acid), AAs (ala, asn, cys, gln, ile, met, phe, ser, tyr), pyrimidines (cytosine), ethylene, and organic pollutants (toluene, benzene, naphthalene) (111). Despite that the identity of numerous chemoattractants has been revealed, there are very few studies on the ability of pseudomonads to sense and respond to the presence of D-AAs. In fact, we were able to find a single very recent study that demonstrated *P. syringae* pv *actinidiae* encodes a high-specificity chemoreceptor for the three acidic AAs L-glu, L-asp, and D-asp (locus tag Psa_14525) (88). Although D-AAs have been shown to have essential roles in the metabolism of *P. putida* KT2440, the ability of this bacterium to chemosense these compounds has not been investigated. Currently, we have developed an assay that would allow us to use a collection of 21 D- and 21 L-AA enantiomers in order to detect any chemotactic response by *P. putida* KT2440.

Results

Chemotaxis - controls

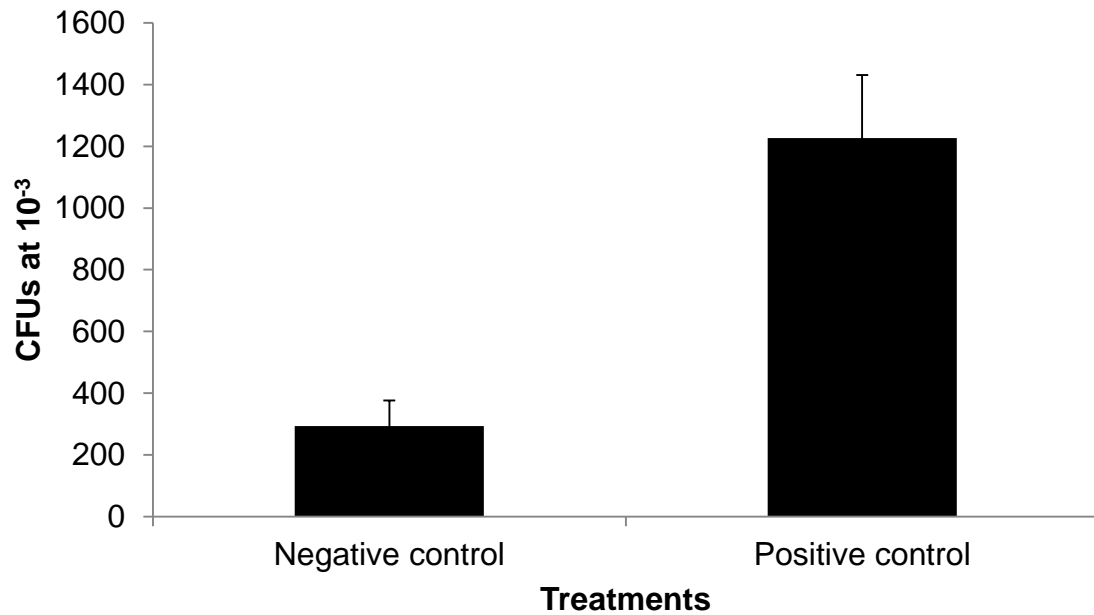
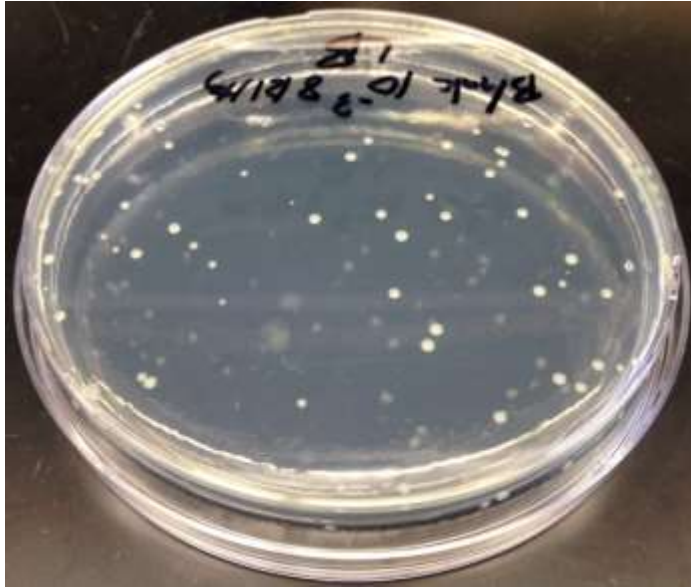
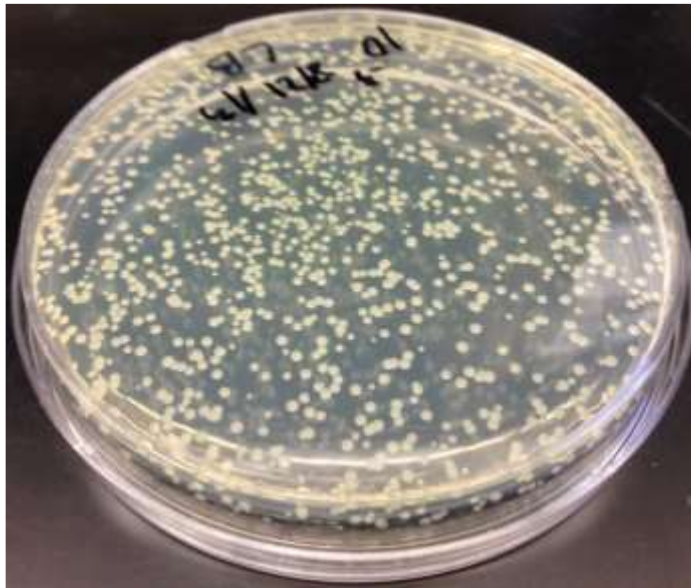


Figure B.1 Chemotaxis assays – positive and negative controls. Average values are shown \pm standard deviation. Two individual experiments were conducted with eight technical replicates. Student's t-test was conducted using Excel ($p < 0.000005$). There is a greater than four-fold difference between the two treatments.



A



B

Figure B.2 Representative agar plates used in the colony counting after the chemotaxis assays. (A) Negative control and (B) positive control.

Methods

In order to test whether a particular compound can act as a chemoattractant, an assay has been developed that uses a glass capillary filled with the compound in question that is submerged into a well containing a particular bacterial strain (2). After a certain incubation time, the contents of the capillary are plated onto a LB agar plate in order to determine CFU numbers. Positive and negative controls are included that contain a known chemoattractant solution and a solution that does not induce chemotaxis, respectively. If the tested compound induces chemotaxis, then more CFUs should be counted on the respective plates relative to those of the negative control. This chemotaxis assay has recently been adapted to use 96-well plates in order to allow a higher throughput (77).

Before conducting the chemotaxis assay, bacteria must be passaged several times on a swim plate to optimize their motility (101, 111). This was done by inoculating an LB agar swim plate (LB media diluted 1 to 10 and 0.25% agar instead of the usual 1.5%) by stabbing in the center with *P. putida* KT2440 strain picked from a glycerol stock or another agar plate. After incubating for 24 hrs at 28°C, a new swim plate is inoculated using bacteria from the outer edge growth on the initial swim plate. This process is repeated at least three times and cultures for the chemotaxis assays are started using outer edge bacteria from the most recent swim plate.

5 ml cultures of *P. putida* KT2440 were started in Minimal Saline-Succinate media (77) 24 hrs before conducting the chemotaxis experiment. After the incubation at 28°C, the OD₆₀₀ of the cultures was ~0.5 (Biotek Synergy HT plate reader). The cultures were washed twice with chemotaxis buffer (50 mM potassium phosphate, monobasic, pH 7.0, 10 μM disodium EDTA, 0.05% glycerol) (77). After washing, the cultures were combined into a single tube to reach uniformity (OD₆₀₀ was ~0.3). 350 μl of the washed cell culture was distributed into the appropriate wells of a 96-well plate. Eight replicates were used for each treatment. Only every other column of a 96-well plate could be used due to handling difficulties. The tip of each 1 μl capillary (Drummond Microcaps, Drummond Scientific) was sealed by passing it over a Bunsen burner flame for 5 s. The sealed end of each capillary was then inserted into an agar plug formed with 3% agar in water in a 96-well plate (Fig. B.1).

The plate in fig. B.1 was placed at 75°C for 30 min in order to heat the capillaries and then all of the capillaries were submerged en masse into the appropriate loading solutions for 30 min at room temperature (Fig. B.2).

After loading as depicted in fig. B.2, the capillaries were rinsed en masse in chemotaxis buffer (350 μl per well) and then immediately submerged into the plate with bacterial cells (similar setup to Fig. B.2). The current setup was incubated at room temperature for 30 min after which the capillaries were rinsed as before using chemotaxis buffer (350 μl). The contents of each capillary were expelled using the supplied rubber bulbs (Drummond Microcaps, Drummond Scientific) into 100 μl LB media. 50 μl of each replicate was plated on a single LB

agar plate in order to determine CFU counts. If necessary, further dilutions could be performed and plated after collecting the contents of each capillary.



Figure B.3 Chemotaxis setup - plate with inserted capillaries after sealing over the flame.

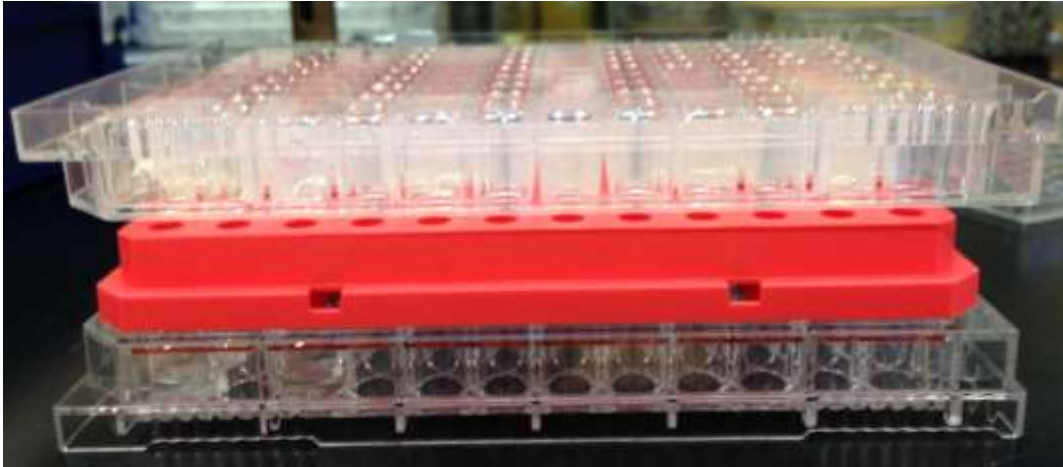


Figure B.4 Chemotaxis setup – complete. The top plate contains the capillaries and agar plugs after heating at 75°C. The middle orange plate is a pipette tip tray used as a spacer, and the bottom plate contains the appropriate chemoattractant solutions for loading the capillaries. Each well of the bottom plate contained 350µl solution. Positive control solution was 2% Casamino acids and negative control – chemotaxis buffer.

References

1. Adams E, Norton I. 1964. Purification and properties of inducible Hydroxyproline-2-epimerase from *Pseudomonas*. J. Biol. Chem. 239.
2. Adler J. 1973. A method for measuring chemotaxis and use of the method to determine optimum conditions for chemotaxis by *Escherichia coli*. J. Gen. Microbiol. 74:77–91.
3. Alam S, Wang SC, Ruzicka FJ, Frey PA, Wedekind JE. 2004. Crystallization and X-ray diffraction analysis of ornithine cyclodeaminase from *Pseudomonas putida*. Acta Crystallogr. Sect. D Biol. Crystallogr. 60:941–944.
4. Ames GF, Prody C, Kustu S. 1984. Simple, rapid, and quantitative release of periplasmic proteins by chloroform. J. Bacteriol. 160:1181–3.
5. Arias CA, Martín-Martínez M, Blundell TL, Arthur M, Courvalin P, Reynolds PE. 1999. Characterization and modelling of VanT: a novel, membrane-bound, serine racemase from vancomycin-resistant *Enterococcus gallinarum* BM4174. Mol. Microbiol. 31:1653–64.
6. Baba T, Ara T, Hasegawa M, Takai Y, Okumura Y, Baba M, Datsenko KA, Tomita M, Wanner BL, Mori H. 2006. Construction of *Escherichia coli* K-12 in-frame, single-gene knockout mutants: the Keio collection. Mol. Syst. Biol 2:2006.0008.
7. Baltrus DA, Nishimura MT, Romanchuk A, Chang JH, Mukhtar MS, Cherkis K, Roach J, Grant SR, Jones CD, Dangl JL. 2011. Dynamic evolution of pathogenicity revealed by sequencing and comparative genomics of 19 *Pseudomonas syringae* isolates. PLoS pathogens 7:e1002132.
8. Bella J, Eaton M, Brodsky B, Berman H. 1994. Crystal and molecular structure of a collagen-like peptide at 1.9Å resolution. Science 266:75–81.
9. Benson DA, Karsch-Mizrachi I, Lipman DJ, Ostell J, Sayers EW. 2011. GenBank. Nucleic Acids Res. 39:D32–7.
10. Bertin C, Yang X, Weston LA. 2003. The role of root exudates and allelochemicals in the rhizosphere. Plant Soil 256:67–83.
11. Bodanszky M, Stahl GL. 1974. The structure and synthesis of Malformin A. Proc. Natl. Acad. Sci. U. S. A. 71:2791–2794.

12. Boniface A, Bouhss A, Mengin-Lecreux D, Blanot D. 2006. The MurE synthetase from *Thermotoga maritima* is endowed with an unusual D-lysine adding activity. *J. Biol. Chem.* 281:15680–6.
13. Boniface A, Parquet C, Arthur M, Mengin-Lecreux D, Blanot D. 2009. The elucidation of the structure of *Thermotoga maritima* peptidoglycan reveals two novel types of cross-link. *J. Biol. Chem.* 284:21856–62.
14. Brady RA, Csonka LN. 1988. Transcriptional regulation of the *proC* gene of *Salmonella typhimurium*. *J. Bacteriol.* 170:2379–82.
15. Brinsmade SR, Kleijn RJ, Sauer U, Sonenshein AL. 2010. Regulation of CodY activity through modulation of intracellular branched-chain amino acid pools. *J. Bacteriol.* 192:6357–68.
16. Brodowski S, Amelung W, Lobe I, Du Preez CC. 2004. Losses and biogeochemical cycling of soil organic nitrogen with prolonged arable cropping in the South African Highveld – evidence from D- and L-amino acids. *Biogeochemistry* 71:17–42.
17. Brückner H, Becker D, Lüpke M. 1993. Chirality of amino acids of microorganisms used in food biotechnology. *Chirality* 5:385–92.
18. Brückner H, Schieber A. 2001. Ascertainment of D-amino acids in germ-free, gnotobiotic and normal laboratory rats. *Biomed. Chromatogr.* 15:257–62.
19. Brückner H, Westhauser T. 2003. Chromatographic determination of L- and D-amino acids in plants. *Amino Acids* 24:43–55.
20. Brückner H, Hausch M. 1989. Gas chromatographic detection of D-amino acids as common constituents of fermented foods. *Chromatographia* 28:487–92.
21. Buschiazzi A, Goytia M, Schaeffer F, Degrave W, Shepard W, Grégoire C, Chamond N, Cosson A, Berneman A, Coatnoan N, Alzari PM, Minoprio P. 2006. Crystal structure, catalytic mechanism, and mitogenic properties of *Trypanosoma cruzi* proline racemase. *Proc. Natl. Acad. Sci. U. S. A.* 103:1705–10.
22. Caboche S, Pupin M, Leclère V, Fontaine A, Jacques P, Kucherov G. 2008. NORINE: a database of nonribosomal peptides. *Nucleic Acids Res.* 36:D326–31.
23. Candela T, Fouet A. 2006. Poly-gamma-glutamate in bacteria. *Mol. Microbiol.* 60:1091–8.

24. Cassab GI. 1998. Plant cell wall proteins. *Annu. Rev. Plant Physiol. Plant Mol. Biol.* 49:281–309.
25. Cava F, De Pedro MA, Lam H, Davis BM, Waldor MK. 2011. Distinct pathways for modification of the bacterial cell wall by non-canonical D-amino acids. *EMBO J.* 30:3442–53.
26. Chang YF, Adams E. 1974. D-Lysine catabolic pathway in *Pseudomonas putida*: interrelations with L-lysine catabolism. *J. Bacteriol.* 117:753–64.
27. Chen I-C, Lin W-D, Hsu S-K, Thiruvengadam V, Hsu W-H. 2009. Isolation and characterization of a novel lysine racemase from a soil metagenomic library. *Appl. Environ. Microbiol.* 75:5161–6.
28. Chen WM, Moulin L, Bontemps C, Vandamme P, Béna G, Boivin-masson C. 2003. Legume symbiotic nitrogen fixation by β -Proteobacteria is widespread in nature. *J. Bacteriol.* 185:7266–72.
29. Choi K-H, Schweizer HP. 2005. An improved method for rapid generation of unmarked *Pseudomonas aeruginosa* deletion mutants. *BMC Microbiol.* 5:30.
30. Collins LV, Kristian SA, Weidenmaier C, Faigle M, Van Kessel KPM, Van Strijp JAG, Götz F, Neumeister B, Peschel A. 2002. *Staphylococcus aureus* strains lacking D-alanine modifications of teichoic acids are highly susceptible to human neutrophil killing and are virulence attenuated in mice. *J. Infect. Dis.* 186:214–9.
31. Collmer A, Badel JL, Charkowski AO, Deng WL, Fouts DE, Ramos AR, Rehm A, Anderson DM, Schneewind O, Van Dijk K, Alfano JR. 2000. *Pseudomonas syringae* Hrp type III secretion system and effector proteins. *Proc. Natl. Acad. Sci. U. S. A.* 97:8770–7.
32. Conti P, Tamborini L, Pinto A, Blondel A, Minoprio P, Mozzarelli A, De Micheli C. 2011. Drug discovery targeting amino acid racemases. *Chem. Rev.* 111:6919–46.
33. Dereeper A, Guignon V, Blanc G, Audic S, Buffet S, Chevenet F, Dufayard J-F, Guindon S, Lefort V, Lescot M, Claverie J-M, Gascuel O. 2008. Phylogeny.fr: robust phylogenetic analysis for the non-specialist. *Nucleic Acids Res.* 36:W465–9.
34. Duque E, de la Torre J, Bernal P, Molina-Henares MA, Alaminos M, Espinosa-Urgel M, Roca A, Fernández M, de Bentzmann S, Ramos JL. 2013. Identification of reciprocal adhesion genes in pathogenic and non-pathogenic *Pseudomonas*. *Environ. Microbiol.* 15:36–48.

35. Errington J. 1993. *Bacillus subtilis* sporulation: regulation of gene expression and control of morphogenesis. *Microbiol. Rev.* 57:1–33.
36. Esaki N, Walsh CT. 1986. Biosynthetic alanine racemase of *Salmonella typhimurium*: purification and characterization of the enzyme encoded by the *alr* gene. *Biochemistry* 25:3261–67.
37. Espaillat A, Carrasco-López C, Bernardo-García N, Pietrosevoli N, Otero LH, Álvarez L, de Pedro MA, Pazos F, Davis BM, Waldor MK, Hermoso JA, Cava F. 2014. Structural basis for the broad specificity of a new family of amino acid racemases. *Acta Crystallogr. D. Biol. Crystallogr.* 70:79–90.
38. Falke JJ, Bass RB, Butler SL, Chervitz SA, Danielson MA. 1997. The two-component signaling pathway of bacterial chemotaxis: a molecular view of signal transduction by receptors, kinases, and adaptation enzymes. *Annu. Rev. Cell Dev. Biol.* 13:457–512.
39. Fernández M, Conde S, Duque E, Ramos J-L. 2013. *In vivo* gene expression of *Pseudomonas putida* KT2440 in the rhizosphere of different plants. *Microb. Biotechnol.* 6:307–13.
40. Finlay T, Adams E. 1970. Kinetic and structural studies of Hydroxyproline-2-epimerase. *J. Biol. Chem.* 245:5248–60.
41. Friedman M. 2010. Origin, microbiology, nutrition, and pharmacology of D-amino acids. *Chem. Biodivers.* 7:1491–530.
42. Geueke B, Weckbecker A, Hummel W. 2007. Overproduction and characterization of a recombinant D-amino acid oxidase from *Arthrobacter protophormiae*. *Appl. Microbiol. Biotechnol.* 74:1240–47.
43. Glavas S, Tanner ME. 1999. Catalytic acid/base residues of glutamate racemase. *Biochemistry* 38:4106–13.
44. Goodlett DR, Abuaf PA, Savage PA, Kowalski KA, Mukherjee TK, Tolan JW, Corkum N, Goldstein G, Crowther JB. 1995. Peptide chiral purity determination: hydrolysis in deuterated acid, derivatization with Marfey's reagent and analysis using high performance liquid chromatography-electrospray ionization-mass spectrometry. *J. Chromatogr. A* 707:233–44.
45. Goodman JL, Wang S, Alam S, Ruzicka FJ, Frey PA, Wedekind JE. 2004. Ornithine cyclodeaminase: structure, mechanism of action, and implications for the μ -crystallin family. *Biochemistry* 43:13883–91.

46. Gryder R, Adams E. 1969. Inducible degradation of hydroxyproline in *Pseudomonas putida*: pathway regulation and hydroxyproline uptake. *J. Bacteriol.* 97:292–306.
47. Hamer R, Chen P-Y, Armitage JP, Reinert G, Deane CM. 2010. Deciphering chemotaxis pathways using cross species comparisons. *BMC Syst. Biol.* 4:3.
48. Hancock R. 1960. The amino acid composition of the protein and cell wall of *Staphylococcus aureus*. *Biochim. Biophys. Acta* 37:42–46.
49. He W, Li C, Lu C-D. 2011. Regulation and characterization of the *dadRAX* locus for D-amino acid catabolism in *Pseudomonas aeruginosa* PAO1. *J. Bacteriol.* 193:2107–15.
50. He W, Li G, Yang C-K, Lu C-D. 2014. Functional characterization of the *dguRABC* locus for D-glutamate and D-glutamine utilization in *Pseudomonas aeruginosa* PAO1. *Microbiology* 404–13.
51. Hills GM. 1949. Chemical factors in the germination of spore-bearing aerobes. The effect of yeast extract on the germination of *Bacillus anthracis* and its replacement by adenosine. *Biochem. J.* 45:353–62.
52. Hu H, Emerson J, Aronson AI. 2007. Factors involved in the germination and inactivation of *Bacillus anthracis* spores in murine primary macrophages. *FEMS Microbiol. Lett.* 272:245–50.
53. Hunt A. 2015. A Rapid, simple, and inexpensive method for the preparation of strand-specific RNA-seq libraries. *Methods Mol. Biol.* 1255:195–207.
54. Hurst C, Crawford R, Knudsen G, McInerney M, Stetzenbach L. 2002. Cultivation of bacteria and fungi, p. 62–71. *In* Hurst, CJ (ed.), *Manual of Environmental Microbiology* 2nd edition.
55. Itoh Y, Nakada Y. 2004. Arginine and polyamine metabolism, p. 243–72. *In* Ramos, J-L (ed.), *Pseudomonas: biosynthesis of macromolecules and molecular metabolism*.
56. Janssen PH, Yates PS, Grinton BE, Taylor PM, Sait M. 2002. Improved culturability of soil bacteria and isolation in pure culture of novel members of the divisions *Acidobacteria*, *Actinobacteria*, *Proteobacteria*, and *Verrucomicrobia*. *Appl. Environ. Microbiol.* 68:2391–96.
57. Jensen JVK, Wendisch VF. 2013. Ornithine cyclodeaminase-based proline production by *Corynebacterium glutamicum*. *Microb. Cell Fact.* 12:63.

58. Jones D, Keddie R. 2006. The genus *Arthrobacter*, p. 945–60. *In* Prokaryotes.
59. Ju J, Misono H, Ohnishi K. 2005. Directed evolution of bacterial alanine racemases with higher expression level. *J. Biosci. Bioeng.* 100:246–54.
60. Ju J, Xu S, Furukawa Y, Zhang Y, Misono H, Minamino T, Namba K, Zhao B, Ohnishi K. 2011. Correlation between catalytic activity and monomer-dimer equilibrium of bacterial alanine racemases. *J. Biochem.* 149:83–9.
61. Ju J, Yokoigawa K, Misono H, Ohnishi K. 2005. Cloning of alanine racemase genes from *Pseudomonas fluorescens* strains and oligomerization states of gene products expressed in *Escherichia coli*. *J. Biosci. Bioeng.* 100:409–17.
62. Junker F, Ramos J. 1999. Involvement of the *cis/trans* Isomerase Cti in solvent resistance of *Pseudomonas putida* DOT-T1E. *J. Bacteriol.* 181:5693.
63. Kato S, Ishihara T, Hemmi H, Kobayashi H, Yoshimura T. 2011. Alterations in D-amino acid concentrations and microbial community structures during the fermentation of red and white wines. *J. Biosci. Bioeng.* 111:104–08.
64. Kato S, Hemmi H, Yoshimura T. 2012. Lysine racemase from a lactic acid bacterium, *Oenococcus oeni*: structural basis of substrate specificity. *J. Biochem.* 152:505–08.
65. Kim OS, Cho YJ, Lee K, Yoon SH, Kim M, Na H, Park SC, Jeon YS, Lee JH, Yi H, Won S, Chun J. 2012. Introducing EzTaxon-e: A prokaryotic 16S rRNA gene sequence database with phylotypes that represent uncultured species. *Int. J. Syst. Evol. Microbiol.* 62:716–21.
66. Kobayashi J, Shimizu Y, Mutaguchi Y, Doi K, Ohshima T. 2013. Characterization of D-amino acid aminotransferase from *Lactobacillus salivarius*. *J. Mol. Catal. B Enzym.* 94:15–22.
67. Kolodkin-Gal I, Romero D, Cao S, Clardy J, Kolter R, Losick R. 2010. D-Amino acids trigger biofilm disassembly. *Science* 328:627–9.
68. Kristian S, Datta V, Weidenmaier C, Kansal R, Fedtke I, Peschel A, Gallo R, Nizet V. 2005. D-Alanylation of teichoic acids promotes group A *Streptococcus* antimicrobial peptide resistance, neutrophil survival, and epithelial cell invasion. *J. Bacteriol.* 187:6719.

69. Kuan Y-C, Kao C-H, Chen C-H, Chen C-C, Hu H-Y, Hsu W-H. 2011. Biochemical characterization of a novel lysine racemase from *Proteus mirabilis* BCRC10725. *Process Biochem.* 46:1914–20.
70. Lam H, Oh D-C, Cava F, Takacs CN, Clardy J, De Pedro MA, Waldor MK. 2009. D-Amino acids govern stationary phase cell wall remodeling in bacteria. *Science* 325:1552–5.
71. Lederberg J. 1950. The beta-D-galactosidase of *Escherichia coli*, strain K-12. *J. Bacteriol.* 60:381.
72. Leiman SA, May JM, Lebar MD, Kahne D, Kolter R, Losick R. 2013. D-Amino acids indirectly inhibit biofilm formation in *Bacillus subtilis* by interfering with protein synthesis. *J. Bacteriol.* 195:5391–5.
73. Li C, Lu C-D. 2009. Arginine racemization by coupled catabolic and anabolic dehydrogenases. *Proc. Natl. Acad. Sci. U. S. A.* 106:906–11.
74. Li C, Yao X, Lu C-D. 2010. Regulation of the *dauBAR* operon and characterization of D-amino acid dehydrogenase DauA in arginine and lysine catabolism of *Pseudomonas aeruginosa* PAO1. *Microbiology* 156:60–71.
75. Lim YH, Yokoigawa K, Esaki N, Soda K. 1993. A new amino acid racemase with threonine α -epimerase activity from *Pseudomonas putida*: purification and characterization. *J. Bacteriol.* 175:4213–7.
76. Liu L, Iwata K, Kita A, Kawarabayasi Y, Yohda M, Miki K. 2002. Crystal structure of aspartate racemase from *Pyrococcus horikoshii* OT3 and its implications for molecular mechanism of PLP-independent racemization. *J. Mol. Biol.* 319:479–89.
77. Liu X, Wood PL, Parales JV., Parales RE. 2009. Chemotaxis to pyrimidines and identification of a cytosine chemoreceptor in *Pseudomonas putida*. *J. Bacteriol.* 191:2909–16.
78. Lobočka M, Hennig J, Wild J, Klopotoski T. 1994. Organization and expression of the *Escherichia coli* K-12 *dad* operon encoding the smaller subunit of D-amino acid dehydrogenase and the catabolic alanine racemase. *J. Bacteriol.* 176:1500.
79. Loper JE, Hassan KA, Mavrodi DV, Davis EW, Lim CK, Shaffer BT, Elbourne LDH, Stockwell VO, Hartney SL, Breakwell K, Henkels MD, Tetu SG, Rangel LI, Kidarsa TA, Wilson NL, Van de Mortel JE, Song C, Blumhagen R, Radune D, Hostetler JB, Brinkac LM, Durkin AS, Kluepfel DA, Wechter WP, Anderson AJ, Kim YC, Pierson LS, Pierson EA, Lindow

- SE, Kobayashi DY, Raaijmakers JM, Weller DM, Thomashow LS, Allen AE, Paulsen IT. 2012. Comparative genomics of plant-associated *Pseudomonas* spp.: insights into diversity and inheritance of traits involved in multitrophic interactions. *PLoS Genet.* 8:e1002784.
80. Maclean AM, White CE, Fowler JE, Finan TM. 2009. Identification of a Hydroxyproline Transport System in the Legume Endosymbiont *Sinorhizobium meliloti*. *Mol. Plant-Microbe In.* 22:1116–27.
 81. Espinosa-Urgel M, Ramos JL. 2001. Expression of a *Pseudomonas putida* aminotransferase involved in lysine catabolism is induced in the rhizosphere. *Appl. Environ. Microbiol.* 67:5219–5224.
 82. Marfey P. 1984. Determination of D-amino acids. II. Use of bifunctional reagent 1,5-difluoro-2,4-dinitrobenzene. *Carlsb. Res. Commun.* 49:591–96.
 83. Martins dos Santos VAP, Heim S, Moore ERB, Strätz M, Timmis KN. 2004. Insights into the genomic basis of niche specificity of *Pseudomonas putida* KT2440. *Environ. Microbiol.* 6:1264–86.
 84. Massey LK, Sokatch JR, Conrad RS. 1976. Branched-chain amino acid catabolism in bacteria. *Bacteriol. Rev.* 40:42–54.
 85. Matilla MA, Espinosa-Urgel M, Rodríguez-Herva JJ, Ramos JL, Ramos-González MI. 2007. Genomic analysis reveals the major driving forces of bacterial life in the rhizosphere. *Genome Biol.* 8:R179.
 86. Matilla MA, Ramos JL, Bakker PAHM, Doornbos R, Badri DV, Vivanco JM, Ramos-González MI. 2010. *Pseudomonas putida* KT2440 causes induced systemic resistance and changes in Arabidopsis root exudation. *Environ. Microbiol. Rep.* 2:381–8.
 87. Matsui D, Oikawa T, Arakawa N, Osumi S, Lausberg F, Stähler N, Freudl R, Eggeling L. 2009. A periplasmic, pyridoxal-5'-phosphate-dependent amino acid racemase in *Pseudomonas taetrolens*. *Appl. Microbiol. Biotechnol.* 83:1045–54.
 88. McKellar JLO, Minnell JJ, Gerth ML. 2015. A high-throughput screen for ligand binding reveals the specificities of three amino acid chemoreceptors from *Pseudomonas syringae* pv. *actinidiae*. *Mol. Microbiol.* 96:694-707.
 89. Moe LA. 2013. Amino acids in the rhizosphere: from plants to microbes. *Am. J. Bot.* 100:1692–705.
 90. Molina L, Ramos C, Duque E, Ronchel MC, García JM, Wyke L, Ramos JL. 2000. Survival of *Pseudomonas putida* KT2440 in soil and in the

rhizosphere of plants under greenhouse and environmental conditions. *Soil Biol. Biochem.* 32:315–21.

91. Molina-Henares MA, De la Torre J, García-Salamanca A, Molina-Henares AJ, Herrera MC, Ramos JL, Duque E. 2010. Identification of conditionally essential genes for growth of *Pseudomonas putida* KT2440 on minimal medium through the screening of a genome-wide mutant library. *Environ. Microbiol.* 12:1468–85.
92. Mongodin EF, Shapir N, Daugherty SC, DeBoy RT, Emerson JB, Shvartzbeyn A, Radune D, Vamathevan J, Riggs F, Grinberg V, Khouri H, Wackett LP, Nelson KE, Sadowsky MJ. 2006. Secrets of soil survival revealed by the genome sequence of *Arthrobacter aureescens* TC1. *PLoS Genet.* 2:2094–106.
93. Moreno R, Martínez-Gomariz M, Yuste L, Gil C, Rojo F. 2009. The *Pseudomonas putida* Crc global regulator controls the hierarchical assimilation of amino acids in a complete medium: evidence from proteomic and genomic analyses. *Proteomics* 9:2910–28.
94. Moulin L, Munive A, Dreyfus B, Boivin-Masson C. 2001. Nodulation of legumes by members of the β -subclass of Proteobacteria. *Nature* 411:948–50.
95. Muramatsu H, Mihara H, Kakutani R, Yasuda M, Ueda M, Kurihara T, Esaki N. 2005. The putative malate/lactate dehydrogenase from *Pseudomonas putida* is an NADPH-dependent Δ^1 -piperidine-2-carboxylate/ Δ^1 -pyrroline-2-carboxylate reductase involved in the catabolism of D-lysine and D-proline. *J. Biol. Chem.* 280:5329–35.
96. Nelson KE, Weinel C, Paulsen IT, Dodson RJ, Hilbert H, Martins dos Santos VAP, Fouts DE, Gill SR, Pop M, Holmes M, Brinkac L, Beanan M, DeBoy RT, Daugherty S, Kolonay J, Madupu R, Nelson W, White O, Peterson J, Khouri H, Hance I, Chris Lee P, Holtzapple E, Scanlan D, Tran K, Moazzez A, Utterback T, Rizzo M, Lee K, Kosack D, Moestl D, Wedler H, Lauber J, Stjepandic D, Hoheisel J, Straetz M, Heim S, Kiewitz C, Eisen JA, Timmis KN, Dusterhöft A, Tümmler B, Fraser CM. 2002. Complete genome sequence and comparative analysis of the metabolically versatile *Pseudomonas putida* KT2440. *Environ. Microbiol.* 4:799–808.
97. Neuhaus F, Baddiley J. 2003. A continuum of anionic charge: structures and functions of D-alanyl-teichoic acids in Gram-positive bacteria. *Microbiol. Mol. Biol. Rev.* 67:686.

98. Nishikawa M, Ogawa K. 2004. Occurrence of D-histidine residues in antimicrobial poly(arginyl-histidine), conferring resistance to enzymatic hydrolysis. *FEMS Microbiol. Lett.* 239:255–9.
99. Nishizawa T, Asayama M, Shirai M. 2001. Cyclic heptapeptide microcystin biosynthesis requires the glutamate racemase gene. *Microbiology* 147:1235–41.
100. Oku S, Komatsu A, Tajima T, Nakashimada Y, Kato J. 2012. Identification of chemotaxis sensory proteins for amino acids in *Pseudomonas fluorescens* Pf0-1 and their involvement in chemotaxis to tomato root exudate and root colonization. *Microbes Environ.* 27:462–469.
101. Parales RE, Ferrández A, Harwood CS. 2004. Chemotaxis in *Pseudomonas aeruginosa*, p. 793–815. *In* Ramos, J-L (ed.), *Pseudomonas: Genomics, life style, and molecular architecture*.
102. Radkov AD, Moe LA. 2014. Bacterial synthesis of D-amino acids. *Appl. Microbiol. Biotechnol.* 98:5363–74.
103. Radkov AD, Moe LA. 2013. Amino acid racemization in *Pseudomonas putida* KT2440. *J. Bacteriol.* 195:5016–24.
104. Radkov AD, Moe LA. 2014. Amino acid racemase enzyme assays. Bio-protocol.org.
105. Ramos- González MI, Campos MJ Ramos JL. 2005. Analysis of *Pseudomonas putida* KT2440 gene expression in the maize rhizosphere: *in vitro* expression technology capture and identification of root-activated promoters. *J. Bacteriol.* 187:4033–41.
106. Reichmann NT, Cassona CP, Gründling A. 2013. Revised mechanism of D-alanine incorporation into cell wall polymers in Gram-positive bacteria. *Microbiology* 159:1868–77.
107. Revelles O, Espinosa-Urgel M. 2004. Proline and lysine metabolism, p. 273–292. *In* Ramos, J-L (ed.), *Pseudomonas: biosynthesis of macromolecules and molecular metabolism*.
108. Revelles O, Espinosa-Urgel M, Fuhrer T, Sauer U, Ramos JL. 2005. Multiple and interconnected pathways for L-lysine catabolism in *Pseudomonas putida* KT2440. *J. Bacteriol.* 187:7500–10.
109. Revelles O, Wittich R-M, Ramos JL. 2007. Identification of the initial steps in D-lysine catabolism in *Pseudomonas putida*. *J. Bacteriol.* 189:2787–92.

110. Reynolds PE. 1989. Structure, biochemistry and mechanism of action of glycopeptide antibiotics. *Eur. J. Clin. Microbiol. Infect. Dis.* 8:943–50.
111. Sampedro I, Parales RE, Krell T, Hill JE. 2014. *Pseudomonas* chemotaxis. *FEMS Microbiol. Rev.* 39:17-46.
112. Scaletti ER, Luckner SR, Krause KL. 2012. Structural features and kinetic characterization of alanine racemase from *Staphylococcus aureus* (Mu50). *Acta Crystallogr. D. Biol. Crystallogr.* 68:82–92.
113. Schieber A, Brückner H, Ling JR. 1999. GC-MS analysis of diaminopimelic acid stereoisomers and amino acid enantiomers in rumen bacteria. *Biomed. Chromatogr.* 13:46–50.
114. Siranosian KJ, Ireton K, Grossman AD. 1993. Alanine dehydrogenase (*ald*) is required for normal sporulation in *Bacillus subtilis*. *J. Bacteriol.* 175:6789–96.
115. Smith EA, Macfarlane GT. 1997. Dissimilatory amino acid metabolism in human colonic bacteria. *Anaerobe* 3:327–37.
116. Stein DB, Linne U, Marahiel MA. 2005. Utility of epimerization domains for the redesign of nonribosomal peptide synthetases. *FEBS J.* 272:4506–20.
117. Stover CK, Pham XQ, Erwin AL, Mizoguchi SD, Warrener P, Hickey MJ, Brinkman FS, Hufnagle WO, Kowalik DJ, Lagrou M, Garber RL, Goltry L, Tolentino E, Westbrook-Wadman S, Yuan Y, Brody LL, Coulter SN, Folger KR, Kas A, Larbig K, Lim R, Smith K, Spencer D, Wong GK, Wu Z, Paulsen IT, Reizer J, Saier MH, Hancock RE, Lory S, Olson MV. 2000. Complete genome sequence of *Pseudomonas aeruginosa* PAO1, an opportunistic pathogen. *Nature* 406:959–64.
118. Strych U, Huang H-C, Krause KL, Benedik MJ. 2000. Characterization of the alanine racemases from *Pseudomonas aeruginosa* PAO1. *Curr. Microbiol.* 41:290–94.
119. Studier FW. 2005. Protein production by auto-induction in high-density shaking cultures. *Protein Expr. Purif.* 41:207–34.
120. Sullivan MJ, Petty NK, Beatson SA. 2011. Easyfig: a genome comparison visualizer. *Bioinformatics* 27:1009–10.
121. Sutthiwong N, Fouillaud M, Valla A, Caro Y, Dufossé L. 2014. Bacteria belonging to the extremely versatile genus *Arthrobacter* as novel source of natural pigments with extended hue range. *Food Res. Int.* 65:156–62.

122. Tang G-L, Cheng Y-Q, Shen B. 2007. Chain initiation in the leinamycin-producing hybrid nonribosomal peptide/polyketide synthetase from *Streptomyces atroolivaceus* S-140. Discrete, monofunctional adenylation enzyme and peptidyl carrier protein that directly load D-alanine. *J. Biol. Chem.* 282:20273–82.
123. Tanner M. 2002. Understanding nature's strategies for enzyme-catalyzed racemization and epimerization. *Acc. Chem. Res.* 35:237–46.
124. Toney MD. 2011. Controlling reaction specificity in pyridoxal phosphate enzymes. *Biochim. Biophys. Acta* 1814:1407–18.
125. Tricot C, Stalon V, Legrain C. 1991. Isolation and characterization of *Pseudomonas putida* mutants affected in arginine, ornithine, and citrulline catabolism: function of the arginine oxidase and arginine succinyltransferase pathways. *J. Gen. Microbiol.* 137:2911–18.
126. Uchiyama T, Watanabe K. 2008. Substrate-induced gene expression (SIGEX) screening of metagenome libraries. *Nat. Protoc.* 3:1202–12.
127. Umbarger H. 1978. Amino acid biosynthesis and its regulation. *Annu. Rev. Biochem.* 47:533–606.
128. Vilchez S, Molina L, Ramos C, Ramos JL. 2000. Proline catabolism by *Pseudomonas putida*: cloning, characterization, and expression of the *put* genes in the presence of root exudates. *J. Bacteriol.* 182:91–9.
129. Volkman BF, Zhang Q, Debabov DV, Rivera E, Kresheck GC, Neuhaus FC. 2001. Biosynthesis of D-alanyl-lipoteichoic acid: the tertiary structure of apo-D-alanyl carrier protein. *Biochemistry* 40:7964–72.
130. Vollmer W, Blanot D, De Pedro MA. 2008. Peptidoglycan structure and architecture. *FEMS Microbiol. Rev.* 32:149–67.
131. Vranova V, Zahradnickova H, Janous D, Skene KR, Matharu AS, Rejsek K, Formanek P. 2012. The significance of D-amino acids in soil, fate and utilization by microbes and plants: review and identification of knowledge gaps. *Plant Soil* 354:21–39.
132. Walsh CT. 1989. Enzymes in the D-alanine branch of bacterial cell wall peptidoglycan assembly. *J. Biol. Chem.* 264:2393–6.
133. Walton CJW, Chica RA. 2013. A high-throughput assay for screening L- or D-amino acid specific aminotransferase mutant libraries. *Anal. Biochem.* 441:190–8.

134. Wasserman SA, Daub E, Grisafi P, Botstein D, Walsh CT. 1984. Catabolic alanine racemase from *Salmonella typhimurium*: DNA sequence, enzyme purification, and characterization. *Biochemistry* 23:5182–7.
135. Wasserman SA, Walsh CT, Botstein D. 1983. Two alanine racemase genes in *Salmonella typhimurium* that differ in structure and function. *J. Bacteriol.* 153:1439–50.
136. Watanabe S, Morimoto D, Fukumori F, Shinomiya H, Nishiwaki H, Kawano-Kawada M, Sasai Y, Tozawa Y, Watanabe Y. 2012. Identification and characterization of D-hydroxyproline dehydrogenase and Δ^1 -pyrroline-4-hydroxy-2-carboxylate deaminase involved in novel L-hydroxyproline metabolism of bacteria. *J. Biol. Chem.* 287:32674–88.
137. Winsor GL, Lam DKW, Fleming L, Lo R, Whiteside MD, Yu NY, Hancock REW, Brinkman FSL. 2011. Pseudomonas Genome Database: improved comparative analysis and population genomics capability for *Pseudomonas* genomes. *Nucleic Acids Res.* 39:D596–600.
138. Wu X, Monchy S, Taghavi S, Zhu W, Ramos J, Van der Lelie D. 2011. Comparative genomics and functional analysis of niche-specific adaptation in *Pseudomonas putida*. *FEMS Microbiol. Rev.* 35:299–323.
139. Xu Y, Labedan B, Glansdorff N. 2007. Surprising arginine biosynthesis: a reappraisal of the enzymology and evolution of the pathway in microorganisms. *Microbiol. Mol. Biol. Rev.* 71:36–47.
140. Yang Z, Lu C-D. 2007. Characterization of an arginine:pyruvate transaminase in arginine catabolism of *Pseudomonas aeruginosa* PAO1. *J. Bacteriol.* 189:3954–9.
141. Yang Z, Lu C-D. 2007. Functional genomics enables identification of genes of the arginine transaminase pathway in *Pseudomonas aeruginosa*. *J. Bacteriol.* 189:3945–53.
142. Yoshimura T, Esaki N. 2003. Amino acid racemases: functions and mechanisms. *J. Biosci. Bioeng.* 96:103–9.

Vita

1. Place of birth: Pazardzhik, Bulgaria
2. Education: Bachelor of Arts in Molecular Biology at the University of Wisconsin – Oshkosh, May, 2010
3. Professional positions: None held
4. Scholastic honors: 2014 Doyle Peaslee award, University of Kentucky; 2013 Graduate student mini-symposium presentation award, University of Kentucky
5. Publications:

Seagren, J; Radkov, A D; David, S. 2009. "The total synthesis of (S)-2,4-dihydroxy-1-butyl (4-hydroxyl) benzoate". *Tetrahedron Letters*. 50(27):3827.

Radkov, A D and Moe, L A. 2013. "Amino acid racemization in *Pseudomonas putida* KT2440". *Journal of Bacteriology*. 195(22):5016.

Radkov, A D and Moe, L A. 2014. "Amino acid racemase enzyme assays". *Bio-protocol*. 4(9):e1112. <http://www.bio-protocol.org/e1112>.

Radkov, A D and Moe, L A. 2014. "Bacterial synthesis of D-amino acids". *Applied Microbiology and Biotechnology*. 98(12):5363-74.

Radkov, A D and Moe, L A. 2015. "D-Amino acid catabolism is common among soil- and rhizosphere-dwelling bacteria". *Microbes and Environments*. Submitted.

Uda, K; Abe, K; Dehara, Y; Mizobata, K; Sogawa, N; Akagi, Y; Saigan, M; Radkov, A D; Moe, L A. "Distribution and evolution of the serine/aspartate racemase family in invertebrates". *Amino Acids*. Submitted.

6. Atanas D Radkov